

Metal-Binding Polymers as Chelating Agents

By

Zahra Mohammadi

Submitted to the graduate degree program in Chemical and Petroleum Engineering
and the Graduate Faculty of the University of Kansas School of Engineering in
partial fulfillment of the requirements for the degree of Doctor of Philosophy

.....
Chairperson: Dr. Cory J. Berkland

.....
Dr. Stevin H. Gehrke

.....
Dr. Marylee Z. Southard

.....
Dr. Michael Detamore

.....
Dr. Laird Forrest

Date defended:

The Dissertation Committee for Zahra Mohammadi certifies that this is the approved version of the following dissertation:

Metal-Binding Polymers as Chelating Agents

Committee:

.....
Chairperson: Dr. Cory J. Berkland

.....
Dr. Stevin H. Gehrke

.....
Dr. Marylee Z. Southard

.....
Dr. Michael Detamore

.....
Dr. Laird Forrest

Date approved:

Abstract

Metal chelating polymers are functional polymers that bear specified chemical groups capable of selectively binding metals. Heavy metal contamination is considered a serious problem because these metals, even at relatively low concentration, could accumulate in the human body and cause damage to vital organs. Although, some of these metals like iron, zinc, and manganese participate in controlling various metabolic and signaling pathways, an excess amount of these metals could still lead to toxicity and detrimental side effects.

Metal chelating polymers are frequently used as chelating agents when treating metal toxicity such as iron overload diseases. Siderophores are small, high-affinity iron chelators secreted by microorganisms such as bacteria. The objective of this thesis was to emulate the high affinity, siderophore-mediated iron uptake system of bacteria by mimicking the structure of naturally occurring siderophores, such as enterobactin. First, polyallylamine (PAAm) hydrogels containing 2,3 dihydroxybenzoic acid (2,3 DHBA), a portion of the metal chelating domain of enterobactin, were synthesized as a potential non-absorbed chelator for iron in the gastrointestinal tract. Next, a series of polymeric chelators with various hydrogel:DHBA ratios were prepared. PAAm hydrogels were also synthesized and further modified by conjugating thioglycolic acid (TGA) and DHBA. These hydrogels were utilized for the removal of toxic metal ions such as Pb, Cd and As from aqueous environments. The rapid, high affinity binding of toxic metals by these functionalized hydrogels offers potential applications in waste water treatment and

may enable applications in acute metal poisoning. Finally, a unique synthetic methodology using similar metal chelating polymers for synthesizing magnetic nanoparticles offered potential for contrast-enhanced magnetic resonance imaging or drug delivery. In summary, polymers offer an attractive platform for mimicking siderophore structure which provides new approach for applications in medicine explored here.

**Dedicated to my parents, SeyedMohammad Mohammadi and Sedighe Shami
Moghaddam, whom I owe everything in my life.**

Acknowledgment

I would like to sincerely thank my advisor, Professor Cory Berkland, for his guidance, support, and patience, and the opportunity for me to work constructively in a forward-looking research group. Over the past five years, I have enjoyed independent research project motivated by creative ideas, the opportunity to participate in interdisciplinary collaborations, and the intensive training in writing manuscripts for publication in peer-reviewed journals. Professor Berklands' instructions, not only limited to the academic knowledge, have enabled me to grow as a young scientist, to speculate in a "skeptical" way, and to use a scientific approach to face the challenges in my future research career.

I would also like to thank members of my dissertation committee: Dr. Steven Gehrke, Dr. Marylee Southard, Dr. Liard Forrest and Dr. Micheal Detamor. They were always ready to provide me with generous support and insightful suggestions.

Many thanks to my friends and fellow graduate students in Dr. Berkland's group, for their friendship during my years at University of Kansas, which made the research group an enjoyable and creative environment to work in.

None of this would have been possible without the love and support of my family. My special thanks to my husband, Hosein, for his love, faith, understanding and support, without which this work would not have been accomplished. My sincere thank to my parents who always have had faith and confidence in me. I owe them everything I have today and will have in future. I am also grateful to have my son, Ali, whose smile always encourages me to proceed.

Table of Contents:

Chapter 1: Metal Chelating Polymers

- 1.1 Background
- 1.2 Application of Metal Chelating Polymers in Medicine
 - 1.2.1 Chelating Polymers for Selective Recognition of Dietary Phosphate
 - 1.2.2 Chelating Polymers as Cholesterol-lowering Agents
 - 1.2.3 Chelating Polymers as Iron Sequestering Agents
 - 1.2.4 Chelating Polymers as Toxic Metal Sequestrants
- 1.3 Metal Chelating Polymers in Imaging
- 1.4 Conclusion

Chapter 2: Siderophore-mimetic Hydrogel for Iron Chelation Therapy

- 2.1 Introduction
- 2.2 Materials and Methods
- 2.3 Results and Discussions
- 2.4 Conclusions

Chapter 3: Enhancing the Selectivity of an Iron Binding Hydrogel

- 3.1 Introduction
- 3.2 Materials and Methods
- 3.3. Results and Discussions
- 3.4 Conclusion

Chapter 4: PLL/DHBA: A Potential Alternative for DFO Chelation Therapy

- 4.1 Introduction
- 4.2 Materials and Methods
- 4.3 Results and Discussions
- 4.4 Conclusion

Chapter 5: Thiol Modified Hydrogels: Potential Chelators for Toxic Metals

5.1 Introduction

5.2 Materials and Methods

5.3 Results and Discussion

5.4 Conclusions

Chapter 6: Magnetic Polyvinylamine Nanoparticles by In Situ Manganese Substitution

6.1 Introduction

6.2 Materials and Methods

6.3 Results and Discussions

6.4 Conclusions

Chapter 7: Conclusion and Future work

References

List of Figures:

Figure 1-1: The copper site in plastocyanin, with the four amino acids that bind the metal labeled.

Figure 1-2: A: The Fe site in hemoglobin and B: Mg site in chlorophyll.

Figure 1-3: Binding of phosphate anions to ammonium and guanidinium hosts. Reprinted permission from Elsevier.

Figure 1-4: Binding interactions between polymeric ammonium compounds and phosphate anions. Reprinted with permission from Elsevier.

Figure 1-5: Structure of a polymeric bile acid sequestrant.

Figure 1-6: Structure of current iron chelators.

Figure 2-1: A structural diagram of enterobactin with one arm of the ligand emphasized (A). Structure of the hydrogel synthesized in this study (B).

Figure 2-2: Kinetic swelling data for PAAm (A) and PAAm/DHBA (B) hydrogels at pH=6, PAAm:DHBA= 5.68.

Figure 2-3: Swelling index of PAAm hydrogels with different cross-linker: polymer ratios at different pH values (A), swelling index of PAAm/DHBA with a 2.7 cross-linker: polymer at different pH values (B) (ionic strength=0.5 M).

Figure 2-4: PAAm equilibrated in DI water (A), PAAm equilibrated in 2 mg/mL ferric solution (B), PAA/DHBA equilibrated in DI water (C) and PAAm/DHBA equilibrated in 2 mg/mL ferric solution (D). All hydrogels had equal masses.

Figure 2-5: Ion binding by PAAm/DHBA hydrogels. Gels were equilibrated in 2 mg/mL ferric solution (pH= 2, ionic strength=0.5 M).

Figure 2-6: Kinetic models fitted for PAAm/DHBA hydrogel. Gel was equilibrated in 2 mg/mL ferric solution (pH= 2, ionic strength=0.5 M).

Figure 2-7: Binding isotherms for ferric ions at pH 2-3 (A) and 5-6 (B)

Figure 2-8: Binding isotherms for ferrous ions at pH 2-3 (A), 5-6 (B), and 7.4 (C).

Figure 2-9: Selectivity study for PAAm/DHBA and PAAm hydrogels toward ferric ion in the presence of Mn^{2+} , Cu^{2+} , Ni^{2+} , K^+ , and Ca^{2+} at different pH ranges. A: pH=2.5, B: pH=4, C: pH=5 and D: pH=7.

Figure 3-1: A: PAAm equilibrated in DI water, B: PAAm equilibrated in 2 mg/mL $FeCl_3$ solution C: PAAm-DHBA (~0.3 Molar ratio) equilibrated in 2 mg/mL $FeCl_3$ solution, D: PAAm-DHBA (0.01 Molar ratio) equilibrated in 2 mg/mL $FeCl_3$ solution. All samples are single pieces and have equal masses, pH~2).

Figure 3-2: Kinetic studies of PAAm-DHBA hydrogels. Gels were equilibrated in 2 mg/mL ferric solution (pH= 2, ionic strength=0.5 M).

Figure 4-1: Kinetic data (read from dialysate).

Figure 4-2: Selectivity study (read from dialysate).

Figure 4-3: Cytotoxicity study conducted on (A) A549 cells and (B) HUVEC cells.

Figure 4-4: Hemolytic activities of PLL and PLL/DHBA.

Figure 5-1: Titration data collected for PAAm/TGA and PAAm/TGA/DHBA. pH values represent the values of 3 readings differing by < 5%.

Figure 5-2: Ion binding by functionalized hydrogels, A) Pb, B) Cd, and C) As. Gels were equilibrated in 2 mg/mL metal solution (pH= 2.5). Ionic strength values ranged from 0.02 M to 0.04 M.

Figure 5-3: Selectivity study of functionalized hydrogels toward toxic metal ions A) in the presence of competing toxic metals and B) in the presence of competing essential metals (pH=2.5).

Figure 6-1: Freundlich (A) and Langmuir (B) isotherm plots for Fe and Mn absorption by PVAm.

Figure 6-2: TEM images of PVAm/MnFe₂O₄ aged 45 min (A,B) and 90 min (C,D).

Figure 6-3: XRD spectra of PVAm/MnFe₂O₄ nanoparticles (3A) and EDX spectra of PVAm/MnFe₂O₄ nanoparticles (3B) aged at 90 °C for 45 min.

List of Tables:

Table 1-1: Properties of FDA-approved iron chelators.

Table 2-1: Reaction conditions and swelling behavior of hydrogel at pH=6.

Table 2-2: Kinetic parameters for ferric binding by PAAm/DHBA at pH=2.

Table 2-3: Isotherm parameters for ferric and ferrous binding by PAAm/DHBA. Gels were equilibrated in 2 mg/mL iron solutions.

Table 3-1: Reaction conditions, conjugation reaction efficiency and conditional stability constants (Log k) of hydrogels.

Table 3-2: Selectivity of PAAm-DHBA hydrogel with different PAAm:DHBA molar ratio, pH~2.

Table 4-1: Percent absorption of Fe by PLL/DHBA polymer. Dialysis was conducted until equilibrium.

Table 5-1: Maximum binding capacity of hydrogels at pH=2.5 when ionic strength varied between 0.02 M and 0.04 M.

Table 5-2: Kinetic parameters for metal binding by functionalized hydrogels at pH=2.5. Ionic strength values ranged from 0.02 M to 0.04 M.

Table 5-3: Isotherm parameters for metal binding by functionalized hydrogels at pH=2.5. Ionic strength values ranged from 0.02 M to 0.04 M.

Table 6-1: Fitted affinity parameters using Langmuir and Freundlich models.

Chapter 1

Metal Chelating Polymers

1.1 Background

Metal chelating polymers are functional polymers that bear specified chemical groups capable of selectively binding metals. A metal chelating polymer contains coordination sites (e.g. nitrogen, oxygen or sulphur) obtained either by the polymerization of monomers possessing the desired site or by grafting a low molecular weight compound having high affinity for target ions.¹ These coordination sites or ligands are usually symmetrically oriented or flexible enough to interact with metal ions through coordinate or coordinate-covalent bonds.²

Environmental contamination with heavy metal ions is a serious problem. It is mostly because of the tendency of these metals to accumulate in living organisms, which can lead to toxicity and side effects at relatively low concentration. Although, many studies have reported the toxic and carcinogenic effects of metals in humans and in animals, it is also well known that many metals participate in normal biological functions of cells.³ Several essential transition metals like copper, zinc, iron and manganese participate in controlling various metabolic and signaling pathways. However, the excess amounts of these metals have reportedly caused toxicity in humans. In most cases the excess or free metal could escape the control mechanism such as transport, homeostasis, compartmentalization and binding to designated cell constituents. This may result in disturbing protein function by displacing other metals from their natural binding sites. Such events do not occur normally, but such misplacement of metals can lead to malfunctioning of cells and lead to side effects or toxicity.³

Oxidative stress is one of the major mechanisms behind heavy metal. Metals are capable of interacting with nuclear proteins and DNA causing oxidative deterioration of biological macromolecules. Metals like iron, copper, cadmium, mercury, nickel, lead and arsenic possess the ability to generate reactive radicals, resulting in cellular damage. These reactive radical species include a wide variety of oxygen-, carbon-, sulfur- and nitrogen- radicals, originating not only from superoxide radical, hydrogen peroxide, and lipid peroxides but also from chelates of amino-acids, peptides, and proteins complexed with the toxic metals.³ These metals generate reactive species which may cause neurotoxicity, hepatotoxicity and nephrotoxicity in humans and animals.³

Metal chelating polymers play important roles in the function of some living organisms. Metalloenzymes are polymer-metal complexes present in nature, where metal ions are surrounded by a “chelating polymer”, a large protein molecule with three-dimensional structure. A typical example of such a metalloenzyme whose structure has been determined is plastocyanin, an important copper-containing protein involved in electron-transfer (Figure 1-1). Metal binding polymers are vital for human life. For example, they mediate oxygen transport throughout the body within hemoglobin, the iron-containing oxygen-transport metalloprotein in the red blood cells of vertebrates. Moreover, metal chelates play an essential role in the chemistry of chlorophyll, a vital organ for photosynthesis which allows plants to obtain energy from light (Figure 1-2).

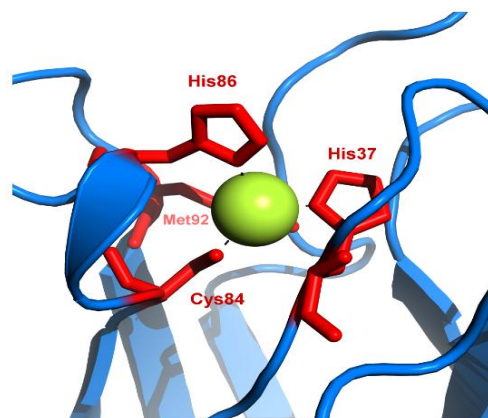


Figure 1-1: The copper site in plastocyanin, with the four amino acids that bind the metal labeled.⁴

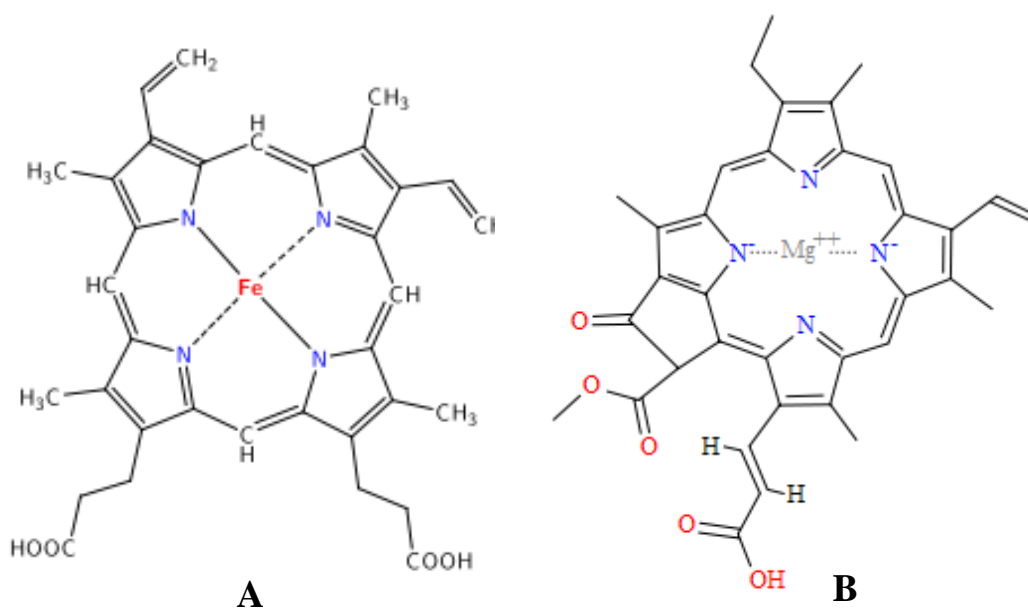


Figure 1-2: A: The Fe site in hemoglobin and B: Mg site in chlorophyll.⁵⁻⁶

Biomimetic polymers are designed to mimic the structure of a desired biological substance. Such polymers can be exploited in various materials, which have the potential to enable unique applications in industry including biomedical implants,

robotic elements, adaptive protective clothing, and orthopedic devices with controllable characteristics.⁷ Many metal chelating polymers have been biologically inspired and are being investigated in medicine. Apart from the biomedical field, metal chelating polymers also play an increasingly important role in chemical industries.⁸⁻⁹

1.2 Application of Metal Chelating Polymers in Medicine

Appealing physical and chemical properties of polymers make them promising materials for use in medical devices and drug delivery systems. Polymer-based biomaterials have been successfully used in artificial organs, in tissue engineering, and as components of medical devices. Moreover, polymers have been utilized in drug delivery for small molecule, proteins, and plasmid DNA and siRNA.¹⁰⁻¹¹ Chelating polymers have garnered significant attention for pharmaceutical application in recent years.¹²⁻¹³

Polymers are not usually considered active pharmaceutical ingredients. It is obvious that polymers generally do not fit to the traditional definition of “drug-like” substances. A unique characteristic of functional or biomimetic polymers suggests that polymers might offer a number of beneficial features that are not present in traditional small molecule therapies. One of these important features is their high molecular weight which makes them interesting for oral drug delivery because of the limit of absorption through the gastrointestinal (GI) tract.

1.2.1 Chelating Polymers for Selective Recognition of Dietary Phosphate

The kidney is the primary route for removal of excess phosphate from the body. As a result, patients with impaired kidney function accumulate phosphate systemically leading to elevated plasma phosphate. This may lead to disease conditions like soft tissue calcification (leading to cardiac complications), renal bone disease leading to reduced bone density, and secondary hyperparathyroidism.¹⁴⁻¹⁵

Phosphate binding therapy has been the primary treatment to manage elevated phosphorous in these hyperphosphataemic patients. Traditional phosphate binders include metal salts, such as those based on calcium, aluminum, lanthanum and iron.¹⁶ These metal salts remove phosphate from the human body through the formation of insoluble phosphate salts. However, due to their propensity for systemic absorption, long-term use of metal salt derived phosphate binders can lead to undesirable toxic side effects leading to neurological disorders (with aluminum) and soft tissue calcification (with calcium).

Researchers then introduced non-absorbed phosphate sequestrants which provided safer treatment for managing elevated serum phosphorous in patients experiencing renal failure. These polymers are typically cationic hydrogels, containing amines and/or guanidinium functional groups that exhibit affinity towards phosphate ions derived from dietary sources.¹⁷⁻¹⁸ Being non-absorbed, they act as effective local therapeutic agents (free from the side effects associated with calcium and related phosphate binders based on metal salts) for the treatment of hyperphosphatemia. The

divalent (and possibly trivalent) nature of phosphate anions requires accessible ammonium groups to provide strong binding of the free phosphate through chelation (Figure 1-3).

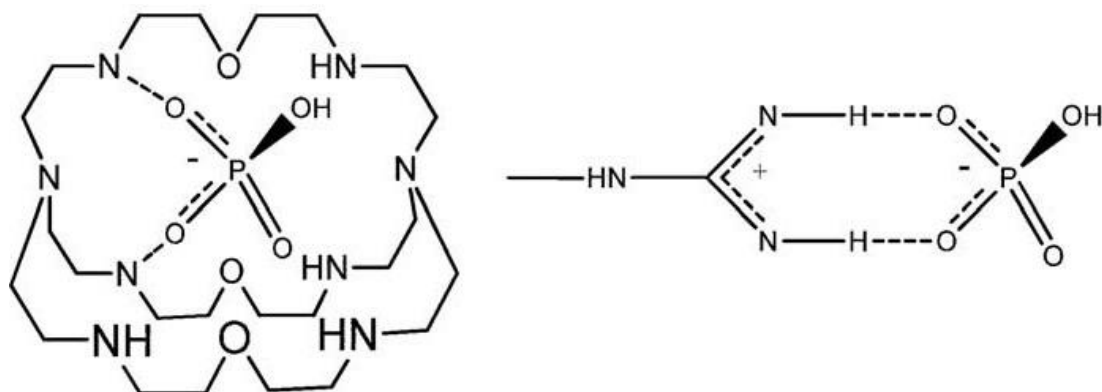


Figure 1-3: Binding of phosphate anions to ammonium and guanidinium hosts. Reprinted permission from Elsevier.¹⁹

Cross-linked, metabolically stable polyamines were introduced later as phosphate binders. These hydrogels offer inherent safety advantages because they are confined to the GI tract. The amino functional polymers bind phosphate anions through electrostatic and possibly through hydrogen bonding interactions (Figure 1-4). In 1998, cross-linked polyallylamine was introduced as a candidate for subsequent preclinical and clinical development.²⁰

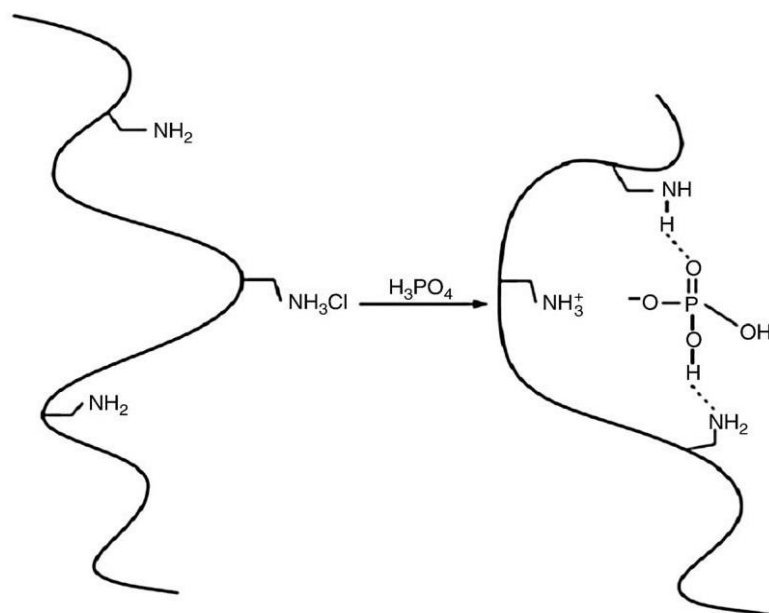


Figure 1-4: Binding interactions between polymeric ammonium compounds and phosphate anions. Reprinted with permission from Elsevier.¹⁹

Cross-linked polyallylamine was approved in the United States by the FDA under the generic name of sevelamer hydrochloride, which was then marketed under the brand name Renagel®. Since its approval, Renagel® has demonstrated effective and long-term control of serum phosphate levels in patients with renal failure.

1.2.2 Chelating Polymers as Cholesterol-lowering Agents

Elevated levels of serum total cholesterol and low-density lipoprotein cholesterol (LDLc) are the primary underlying causes for the development of cardiovascular diseases. The most common treatments for this aim to reduce and control elevated LDLc in the serum.²¹ The most widely used cholesterol lowering drugs belong to the class of compounds called statins; however, the long-term use of these drugs may

cause detrimental side effects. Another approach to reduce the plasma cholesterol level is to maintain bile acid homeostasis in the GI tract. Bile acids are part of the cholesterol metabolism pathway, so effective sequestration and removal of bile offers an alternative therapeutic approach to treat cardiovascular diseases.

One type of bile acid sequestrant is cationically charged cross-linked polymeric gel that binds anionic bile acids in the GI tract to produce non-absorbable complexes. These polymeric complexes restrain bile acids from being systemically absorbed and are eliminated from the body through fecal excretion. The common features of these polymers include the presence of amine/ ammonium groups in adequate densities along polymer chains and the presence of hydrophobic chains. A novel polyammonium salt containing hydrophobically modified hydrogel was introduced as a candidate for clinical development (Figure 1-5). The novel polymer has been approved as cholesterol lowering therapy under the generic name of colesevelam hydrochloride. It is being marketed under the trade name WelChol™ in the USA and Cholestagel® in Europe for the treatment of hypercholesterolemia.

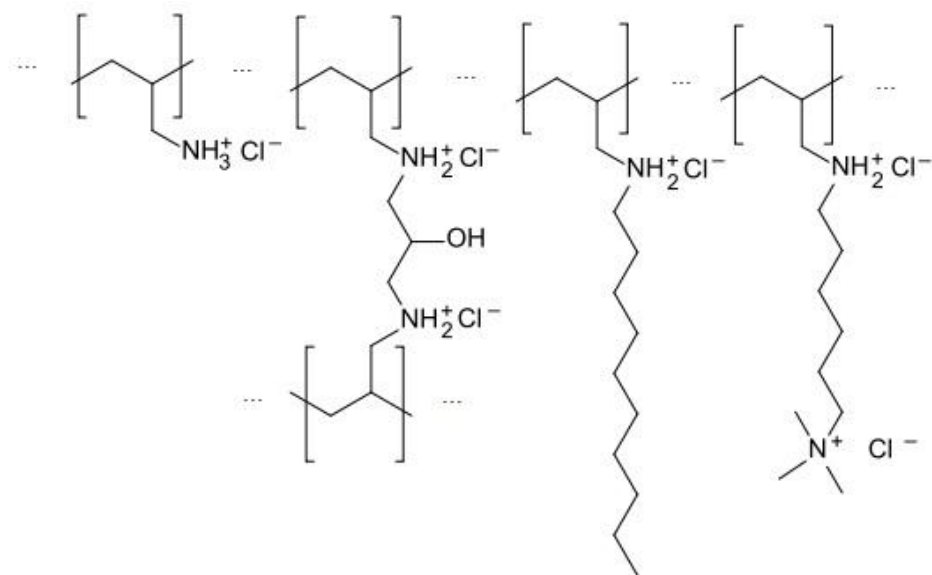


Figure 1-5: Structure of a polymeric bile acid sequestrant.²²

1.2.3 Chelating Polymers as Iron Sequestering Agents

Iron is an essential element in biological systems and it is needed for many critical human biological processes. Yet, the presence of excess iron in the body leads to toxic effects. The pathologic effects of iron accumulation in tissue are recognized in diseases of systemic iron overload, in which the liver, heart, and endocrine glands are the principal affected organs.²³ At the cellular level, labile iron begins to rise once the intracellular capacity for iron storage is surpassed, leading to catalytic formation of reactive oxygen species (ROS) that ultimately overwhelm the cellular antioxidant defense mechanisms and lead to cell damage. Under normal physiological conditions, iron metabolism is tightly conserved with the majority of the iron being recycled within the body. Unsequestered “free” iron can act as a bacterial virulence enhancing

factor.¹⁹ Normal physiology does not provide a mechanism for iron loss through the processes of excretion in urine, feces, or bile.

“Iron overload disorders” refers to a class of diseases caused by the accumulation of iron in the body due to any cause. The causes can be distinguished between primary/hereditary and, less frequently, secondary iron overload. Hemochromatosis is an inherited iron storage disease. It is usually due to mutations in the high Fe (HFE) gene. Secondary iron overload is acquired as a result of another disease. The main causes of secondary iron overload are haemolytic anaemias, β thalassaemia and chronic liver disease. Untreated hereditary hemochromatosis leads to severe iron overload, whereas in secondary iron overload (e.g. resulting from liver diseases) minimal to modest iron overload is usually observed.

Current treatments for iron overload diseases center on chelation therapy. The principal goal of chelation therapy is to decrease tissue iron to concentrations where iron-mediated toxicity cannot occur. Only a small fraction of body iron is available for chelation at any given time and the majority of stored iron is not effectively chelated at clinically achievable chelator concentrations. Return to safe tissue iron levels therefore takes many months or years with current chelation regimens.²⁴

Siderophores are relatively low molecular weight, ferric ion specific chelating agents elaborated by bacteria and fungi growing under low iron stress.²⁵ The role of these compounds is to scavenge iron from the environment and to make the metal, which is almost always essential, available to the microorganism. Siderophores have been related to virulence mechanisms in microorganisms pathogenic to both animals

and plants.²⁵ As naturally occurring chelating agents for iron, siderophores might be expected to be somewhat less harmful for deferrization of patients suffering from transfusion-induced siderosis. A siderophore from *Streptomyces pilosus*, desferrioxamine B, is marketed under the trade name Desferal[®], and is advocated for removal of excess iron resulting from the supportive therapy for thalassaemia.

Deferoxamine B (DFO), which is administered by subcutaneous infusion has shown clear advantages; however, concern has arisen over its use due to numerous, significant toxicities.²⁶ Two other orally administered drugs, Deferiprone (Ferriprox[®]) and Deferasirox (Exjade[®]), are also known to have an effective impact in treatment of iron overload disorders (Figure 1-6). However, several studies have reported serious side effects following the administration of these drugs.²⁷ These side effects have included bone dysplasia, auditory toxicity, hearing loss and ocular toxicity. Serious adverse events such as neutropenia, agranulocytosis, hypersensitivity reactions and blood vessel inflammation have also been reported upon the oral application of Deferiprone and Deferasirox (Table 1-1).²⁸ Enterobactin is another high affinity siderophore that acquires iron for microbial systems. It is the strongest siderophore known, binding to the ferric ion (Fe^{3+}) with an affinity of $K = 10^{52} \text{ M}^{-1}$. The objective of this thesis was to copy the high affinity, siderophore-mediated iron uptake system of bacteria by using polymers to mimic the structure of naturally occurring siderophores, i.e. enterobactin.

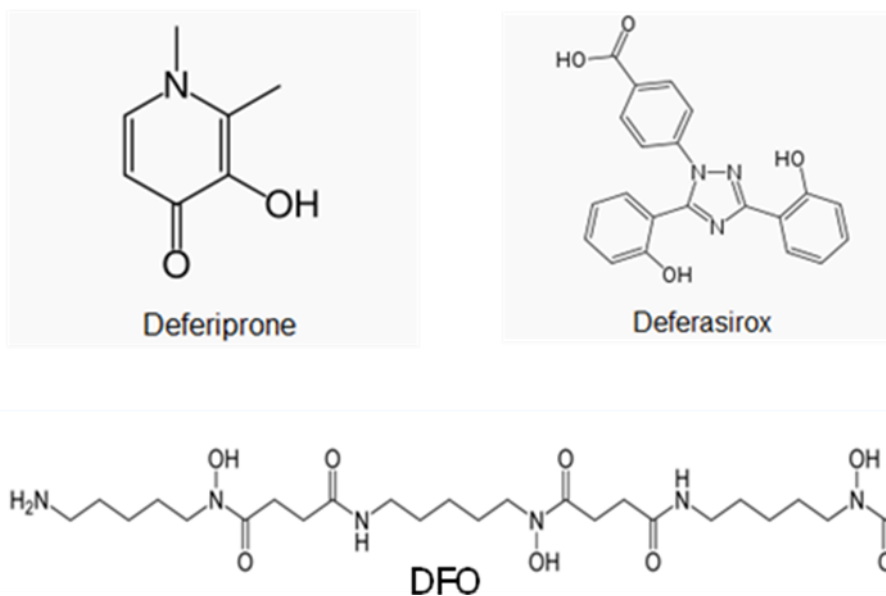


Figure 1-6: Structure of current iron chelators.

Table 1-1: Properties of FDA-approved iron chelators.

	Deferoxamine; DFO	Deferiprone; DFP	Deferasirox; DFX
Chelator molecule: iron atom	1:1	3:1	2:1
Usual dose	25-50 mg/Kg	75-90 mg/Kg	10-30 mg/Kg
Administration	Subcutaneous, intravenous (8-12 hrs), 5 days per week	Oral, twice daily- three times daily	Oral, once daily
Side effects	Local inflammatory reaction, visual and auditory disturbances, disturbances of bone growth, allergic reactions, pulmonary, renal and neurological manifestations	Gastrointestinal manifestation, agranulocytosis /neutropenia, arthralgia elevated liver enzymes	Gastrointestinal manifestation skin exanthem, rise in serum creatinine level, visual and auditory disturbances

Non-absorbed polymeric ligands that selectively sequester and remove dietary iron from the GI tract appear to be attractive therapeutic agents for the treatment of

certain iron overload conditions. Restriction of these functional polymers to the GI tract or other areas of human body for elimination offers a unique medical benefit, when it is desirable to confine a therapeutic agent from systemic exposure. Furthermore, these polymers are capable of selectively recognizing and binding iron in intestinal fluids which makes them a new class of therapeutic agents that block absorption of these potentially detrimental species from the GI tract. Moreover, the ability to incorporate a variety of binding sites as well as high density of such groups along a polymer chain can lead to “polyvalent” interaction with target ligands yielding much higher binding constants than what one would observe with smaller molecular weight drugs.

Crosslinked polymeric hydrogels containing hydroxamic acid and catechol moieties as well as crosslinked polymeric amines have been reported as iron chelators.²⁹⁻³⁰ Under *in vitro* conditions, all of these polymers sequester iron at pH values greater than 7.0. Evaluation of the iron chelating properties of these polymers suggests that they are comparable to current low molecular weight chelators and have potential application in iron overload therapy. One goal of this dissertation was to introduce new polymeric hydrogels that exhibited higher affinity and selectivity toward Fe at relatively low pH when compared to existing polymers.

1.2.4 Chelating Polymers as Toxic Metal Sequestrants

Heavy metals can be substantial pollutants in source and treated water, and are becoming a severe public health problem. Heavy metal ions are reported as priority pollutants, due to their mobility in natural water ecosystems and due to their

toxicity.³¹ The presence of copper, zinc, cadmium, lead, mercury, iron, nickel and others metals, can have a damaging effect on human physiology and other biological systems when tolerance levels are exceeded. The heavy metal ions are stable and persistent environmental contaminants since they cannot be easily degraded and destroyed. Several methods exist to remove detrimental metal ions from aqueous solutions; however, heavy metal toxicity still remains an issue even for treated water.³²

Toxic effects of metals depend on nutritional status, age and gender, as well as the amount and route of exposure, tissue distribution, concentration achieved, and excretion rate. Mechanisms of toxicity include inhibition of enzyme activity and protein synthesis, alterations in nucleic acid function, and changes in cell membrane permeability.³³ These detrimental effects are likely to have long-lasting consequences such as damaging the developing brain.³⁴

Chelating agents have been used as antidotes for metal intoxication in humans. One of the first applied chelators was British Anti-Lewisite (BAL).³⁵ BAL was developed during the Second World War in England as an antidote for the arsenic-containing warfare agent lewisite. After the war, BAL was used as a chelating agent to sequester arsenic, gold, and mercury. Calcium disodium ethylenediaminetetraacetate (CaNa_2EDTA), deferoxamine, and D-penicillamine were also introduced as metal chelators around the same time. Today, these drugs, together with a wide array of newly synthesized chelating agents, are in clinical use or under

preclinical or clinical investigations for treatment of intoxication or overload caused by various transition metals.³⁶

Lead is a ubiquitous metal that has been used by humans for more than three thousand years. It appears in the environment both from natural sources and released by human activities (industrial emission, car exhaust from leaded gasoline, burning coal or oil, and burning solid waste). The general population is exposed to lead mostly by lead-contaminated food or drinking water.³⁷ Cigarette smoke also contains lead. Despite efforts to control lead exposure and despite apparent success in decreasing the incidence, serious cases of lead poisoning still appear in both developed and developing countries all over the world.³⁶

Lead perturbs multiple enzyme systems. As with most heavy metals, any ligand with sulfhydryl groups is vulnerable. The main targets for lead toxicity are the nervous system, especially in children, the hematopoietic system, sperm production, kidney, and possibly the blood pressure regulation system. BAL is an efficient chelator in acute intoxication with inorganic lead. This drug is commercially available but is known to be very toxic. Succimer, *meso*-2,3-dimercaptosuccinic acid (*meso*-DMSA), 2,3- dimercaptopropane-1-sulphonic acid (DMPS), and D-penicillamine (DPA), are other options for the treatment which are orally active and less toxic compared to BAL.³⁸

Exposure to cadmium occurs mostly in the workplace from cadmium fumes and dust in industries where cadmium products are made. The general population is exposed from breathing cigarette smoke or eating cadmium-contaminated food

(cereal products, grains, sea food, potatoes, leafy vegetables).³⁶ Cadmium can cause kidney disease; it damages the lungs, and may irritate the digestive tract. Long-term exposure to low levels of cadmium in air, food or water leads to an accumulation of cadmium in the kidneys and possible kidney disease. Improved regimens and choices of chelation therapy in cadmium-exposed individuals are needed. To date no efficient chelating treatment has been recommended for human usage.³⁶

Arsenic has a long history as a human poison. Arsenic is found in certain water supplies, seafood, glues, pigments, and cigarette smoke. Today, arsenic poisoning occurs through industrial exposure, from contaminated wine or illegally distilled alcohol beverages or because of malicious intent. Very few organ systems escape the toxic effects of arsenic. It is also listed as a confirmed human carcinogen, based on the increased prevalence of lung and skin cancer observed in human populations with chronic exposure, primarily through industrial inhalation.³⁹ Chelation therapy is imperative in all symptomatic patients; however, the use of chelators in patients exposed to arsine gas is controversial.³⁶ It was found that the most efficacious chelators in arsenic poisonings are *meso*-DMSA and DMPS, although less efficient chelators, BAL and DPA, are still in use.³⁶

1.3 Metal Chelating Polymers in Imaging

Radio imaging (RI) and magnetic resonance imaging (MRI) are important tools in the non-invasive diagnosis of diseases. The main goal of developing contrast agents is to improve the contrast for target organs which eventually would lead to more sensitive and more accurate detection. Radio isotopes of iodine have been used in thyroid

metabolism studies and in *in vitro* radioimmunoassays.⁴⁰ Iodine is not efficient for improving the contrast in MRI and none of the iodine isotopes have both ideal nuclear properties and availability for large scale use for *in vivo* diagnostics.

Most widely used contrast agents for MRI were selected from transition metals and rare earth metals. Some of these are normally present in the body as trace elements (Mn, Fe, Cr) and are considered less toxic for this reason. Nevertheless, as pointed out earlier even trace elements may induce adverse toxic effects when the regulation of absorption is bypassed by parenteral administration. To reduce metal ion toxicity, the concepts of covalent binding, chelation, coupling to proteins or peptides, inclusion into dextrans, liposomes or cells, and weakly dissociated salts have been investigated.⁴¹ Formation of weakly dissociated salts, chelation and other methods are of general applicability and are widely used for the preparation of contrast agents based on metallic ions. The chelating method is of particular interest in that acute and long term toxicity of both the metal and the chelating agents are dramatically reduced owing to the complexation.

To differentiate the area of interest from surrounding tissues, sufficient contrast enhancement must be achieved. Contrast agents aim to attenuate or enhance certain signal to a great extent than surrounding tissues, thus providing a clear contrast between healthy and diseased tissue. Nanoparticles have been fabricated and employed to further increase the local concentration of a contrast agent. This can improve delivery of contrast agents to areas of interest, thus enhancing signal from these areas⁴². In most cases, metals have been incorporated within the nanoparticles

through metal chelation. Liposomes and micelles have received attention over the past years because of their controllable properties and good pharmacological characteristics.

Several approaches are used to incorporate the metal within these carriers. One approach is to chelate the reporter metal into a soluble chelate and then include it into the interior of a liposome. For some diagnostic applications, the administration of diagnostic particulates of a very small size (<50 nm) is required. Emerging needs for an increased liposome load with diagnostic moieties while decreasing the size of particles lead to the development of amphiphilic polychelating polymers (PAP). The main chain of the fabricated polymers included multiple side chelating groups capable of firmly binding many reporter metal atoms.⁴¹ In MR imaging, metal atoms chelated by polymer side groups are directly exposed to the water environment that enhances the relaxivity of the paramagnetic ions and leads to the corresponding enhancement of the vesicle contrast properties.

Transition metals are often used as imaging probes. The low molecular weight metals, manganese and iron, are two of most common metals used as MRI probes. These metal ions contain unpaired electrons which facilitate *T1* relaxation by interacting with water protons. Iron contrast agents can be prepared as small or large particles. The larger ones are ferromagnetic and contain multiple alignable magnetic domains, whereas the small particles of a few nanometers in diameter have a single alignable magnetic domain and are highly paramagnetic (superparamagnetic). Iron is a transition metal whose wholebody content is approximately three magnitudes higher

than that of manganese and its use as a contrast agent leads neither to a higher level of free iron ions nor to toxicity. The iron released from this contrast agent may become incorporated into the body's iron store. Manganese is administered in complexed forms to diminish the toxicity of the free metal ions and to improve urinary elimination without significant loss of the paramagnetic properties. The normal manganese whole-body content in humans is 12–20 mg while the MRI doses are usually ranging from 15 to 45 mg of metal.

Other elements from the first transition metal group such as copper, chromium or nickel can also be used as contrast agents. Chromium has been used either as radioactive chromium for cell radiolabelling or in a non-radioactive form for killer lymphocyte labeling.⁴³ Nickel–Diethylene triamine pentaacetic acid (Ni-DTPA) doped agarose gel is a phantom material for Gd–DTPA enhancement of contrast.⁴⁴ Nevertheless, this element has been used very little compared to manganese and iron.

1.4 Conclusion

Because of the unique properties of metal binding polymers, these materials are being utilized in a variety of biomedical applications. Biologically inspired metal chelating polymers have been used as sequestering agents for bile acid and phosphate in patients with elevated cholesterol levels and chronic kidney disease, respectively. Similar polymers are also interesting candidates for use as an iron sequestering agent in patients suffering from hemochromatosis. The overall goal of this work was to develop biologically inspired polymers capable of binding iron or toxic metals. Iron binding polymers can have application in treatment of hemochromatosis where

patients absorb excess iron from the GI tract. The selective and effective binding of iron by these polymers within the GI tract prevents the absorption of excess iron from the intestine.

In this thesis, 2,3 dihydroxybenzoic acid was used to mimic the structure of enterobactin, a naturally occurring, high affinity siderophore that acquires iron for microbial systems. Further, the iron chelating properties of biomimetic polymer were improved to achieve optimized iron absorption within the GI tract.

Polymers containing thioglycolic acid explored to mimic the structure of those enzymes that are functionally perturbed following poisoning with toxic metals. In most cases, a toxic metal replaces zinc, which already has been chelated by thiol groups within the enzyme. Biomimetic polymers offer potential applications for chelation therapy and detoxification.

Finally, nanoparticles are of great interest as contrast agents in MR imaging. The last goal of this work was to develop a magnetic nanoparticle with enhanced magnetization. The chelating property of functional polymers was utilized to facilitate the magnetic property within polymeric network.

Chapter 2

Siderophore-mimetic Hydrogel for Iron Chelation Therapy

2.1 Introduction

Chelate-forming hydrogels have found widespread application in the selective extraction of trace heavy metal ions from aqueous solutions.⁴⁵⁻⁴⁶ More recently, studies have shown that hydrogels have been successfully used as non-absorbable drugs for sequestering phosphate and cholesterol.⁴⁷ Desirable chelating hydrogels have a higher selectivity than ion-exchange resins in sorption processes. Chemical modification of hydrogels is a well-established technique for the fabrication of selective chelate-forming polymers.⁴⁸⁻⁴⁹ Functional monomer(s) or grafted side groups may be introduced to the hydrogel to form covalent or non-covalently bonds.⁵⁰ The chelation characteristics of the modified hydrogel are largely dependent on the density and composition of the ligands incorporated into the polymeric matrix as well as the type of linker used for conjugation in the case of grafted polymer.

Fe(III) chelators are currently desired because of the toxic effects of iron overload and the biological implications of excess iron in all living organisms.⁵¹ As a specific approach for the removal of Fe (III), immobilization of Fe (III) chelators onto Sepharose hydrogels has been investigated. This method was found to be useful in the treatment of Fe(III) overload and wastewater treatment.⁵²⁻⁵³ The Fe(III) chelating resins and polymeric Fe(III) chelating agents reported so far are based on immobilized desferrioxamine or hydroxamic acid polymers.⁵⁴⁻⁵⁵ Desferrioxamine (DFO), a naturally occurring Fe (III) chelator, has a strong affinity and selectivity for Fe (III). DFO is one of drugs approved by FDA in clinical use for the treatment of iron overload in patients⁵⁶.

Microorganisms have developed a sophisticated Fe (III) acquisition and transport systems involving siderophores. Siderophores are low molecular weight chelating agents that bind Fe (III) ion with high specificity. These potent and specific chelators usually include either catecholate or hydroxamate functional groups for iron coordination.⁵⁷ Enterobactin, a naturally occurring tris-catechol siderophore, is the most powerful Fe(III) chelator known with an overall stability constant of 10^{49} (Scheme 1). More recently researchers have been trying to mimic the structure of this siderophore to design iron chelators with relatively high affinity and selectivity toward iron.⁵⁸⁻⁵⁹

Here, we report the synthesis and characterization of a highly effective iron chelator that mimics the enterobactin structure (Figure 2-7). Polyallylamine (PAAm) is a polycation hydrogel consisting of reactive primary amine side groups which can be conjugated to 2,3 dihydroxybenzoic acid (2,3 DHBA), the iron chelating domain of the enterobactin.⁶⁰⁻⁶¹ PAAm hydrogel was synthesized by cross-linking the precursor PAAm chains. Conjugation of 2,3 dihydroxybenzoic acid dramatically improved the iron binding affinity and iron selectivity of the final hydrogel. The selective and rapid, high affinity binding of iron by this siderophore-mimetic hydrogel offers potential for applications in iron chelation therapy in patients suffering from iron overload diseases.

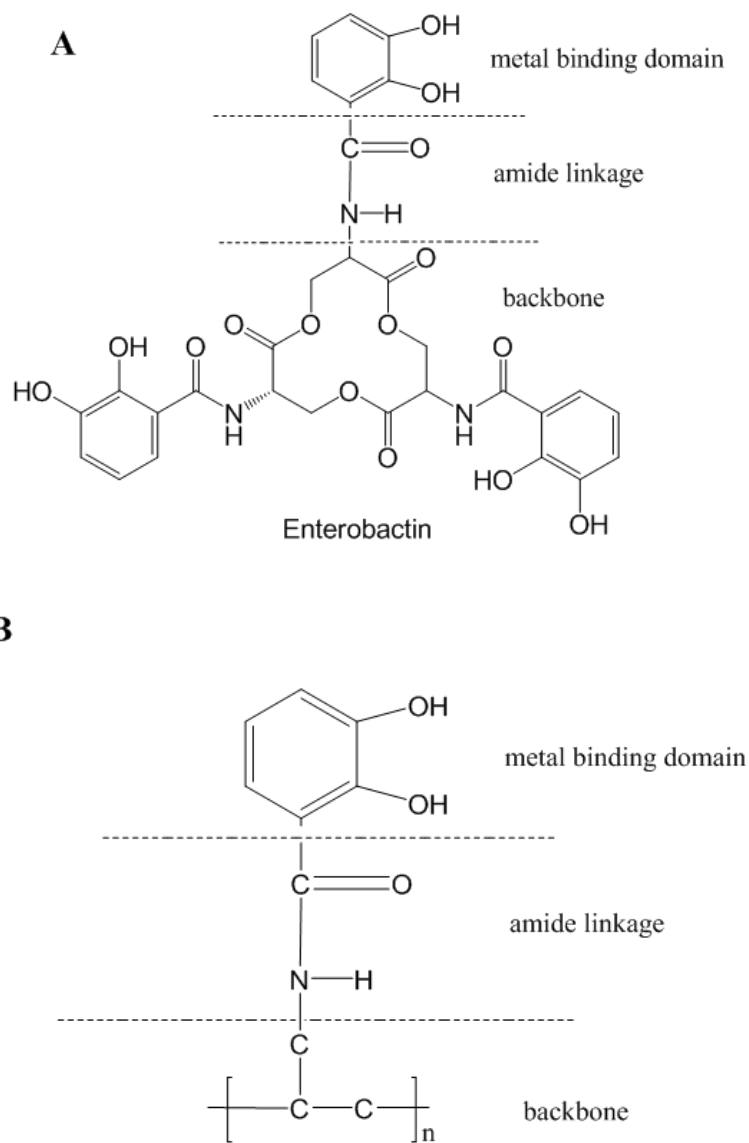


Figure 2-7: A structural diagram of enterobactin with one arm of the ligand emphasized (A). Structure of the hydrogel synthesized in this study (B).

2.2 Materials and Methods

Material: Poly(allylamine hydrochloride) (PAAm) with an average molecular weight of 56 kDa and analytical grade reagent *N,N'*-methylenebisacrylamide (MBA) were

obtained from Sigma-Aldrich and used without further modification. 2,3-dihydroxybenzoic acid, *N,N,N*-triethylamine, dimethylformamide (DMF), citric acid, potassium phosphate and all metal chlorides were purchased from Fisher Scientific and used as received. Dicyclohexylcarbodiimide (DCC) and *N*-hydroxysuccinimide (NHS) were purchased from Thermo Scientific and used without further modification. Deionized water (DI) was obtained from a Barnstead EasyPure water purifier.

Preparation of PAAm Hydrogel: PAAm was cross-linked with MBA by a Michael-type addition reaction. This cross-linking procedure was developed by Oliveira et al. to synthesize PAAm and poly(α -L-lysine hydrobromide) hydrogels.⁶² Briefly, a 20% w/v polymer solution containing a predetermined amount of MBA was prepared. The cross-linker was dissolved in deionized water (flushed with nitrogen for 5 min) and then added to the polyallylamine polymer. Several different molar ratios of cross-linking agent to PAAm were investigated. TEA, the cross-linking catalyst (300 μ L), was then added to the solutions and mixed thoroughly. Next, the precursors were transferred by micropipet into small plastic cuvetts and subsequently covered with parafilm. The cuvettes were held at ambient temperature for 1 h and then cooled to ca. 3 °C and held there for an additional 24 h. After this time, hydrogels were removed from the cuvettes and washed with 0.05 M sodium chloride for several days. Multiple synthesis conditions were employed to prepare the hydrogel investigated in this study (Table 2-2).

Swelling studies: The swelling behavior of hydrogels was studied using buffered solutions with fixed ionic strength (0.5 M). An historic protocol by Elving et al. was used for making buffer solution with a known ionic strength.⁶³ Dried samples with known weights (irregular dimensions) were placed in a solution of defined pH at room temperature. Samples were taken from the solution after reaching equilibrium. The swelling indexes (SI) were calculated using the following equation:

$$SI = \frac{W_s - W_d}{W_d} \quad (1-2)$$

where W_s is the weight of the swollen hydrogel at an equilibrium state, and W_d is the weight of the dried hydrogel.

2,3 Dihydroxybenzoic acid modification of hydrogel: A solution of 2,3 DHBA (100 mg, 0.65 mmol) and NHS (74 mg, 0.65 mmol) in 5 mL of DMF was mixed with a solution of DCC (67 mg, 0.325 mmol) in 5 mL of DMF. The mixture was stirred at low temperature for 6 h to give a white precipitate. The precipitate was filtered, and the filtrate was added directly to a dry gel with known weight (25 mg). PAAm hydrogels were ground to ~0.5-1 mm particles. The reaction mixture was held at room temperature for 3 days. PAAm conjugate hydrogel was then washed with water for several days.

Quantification of Amine Functional Group: Primary amine groups were quantified by potentiometric titration. After grinding to a powder, 40 mg of PAAm and PAAm/DHBA polymer were suspended in 35 mL of 0.2 M aqueous KCl solution. Next, 140 μ L of 8 M KOH aqueous solution was added to polymer suspensions to

raise the pH to ~12. Standard 0.1 M HCl was used to titrate the suspension. HCl was added until the pH was about 2.5 in both polymer suspensions. Free amine groups were quantified from potentiometric data.

Binding Kinetics Study: Ferric chloride solution (2 mg/mL) was adjusted to pH 6.5 and kept at room temperature for kinetic studies. Samples were taken from the media at different time intervals to determine the rate of iron binding by PAAm/DHBA.

Binding Experiments: Known concentrations of ferric chloride and ferrous chloride solutions (0.25, 0.5, 1, 2, and 2.5) mg/mL were prepared. Binding experiments were carried out by taking 20 mL of metal solutions in 125 mL volumetric flasks, solutions were adjusted to the desired pH while maintaining iron concentration. Next, a known mass of PAAm/DHBA particles with a size of about 0.5-1 mm was added to the mixture and was held at room temperature for 2 h or until equilibrium was reached. The solutions were then filtered and the filtrates were analyzed for metal concentration.

Selectivity Study: The selectivity for Fe by PAAm/DHBA in the presence of several heavy metals such as copper, zinc, manganese, calcium, and potassium was studied. Metal solutions (10 mL) containing a 1:1 (wt) mixture of iron and heavy metals were prepared (2 mg/mL). The solution mixtures were then adjusted to pH 2.5, 4, 5, and 7 and held at room temperature for 2 h after adding a known mass of PAAm/DHBA.

Metal analysis: Mono- and multi-elemental analysis of samples was quantified by Inductively Coupled Plasma Optical Emission Spectrometry (ICP-OES) (Optima

2000 DV, PerkinElmer, USA) fitted with an AS 93plus autosampler (PerkinElmer, USA). A Cross-Flow nebulizer and a Scott spray chamber were used. The RF Power was 1300 W and nebulizer and auxiliary flows were 0.8 and 0.2 L/min, respectively. Sample flow was set at 1.5 mL/min. ICP-OES data was processed using Winlab 32 (Ver. 3.0, PerkinElmer, USA). The analytical curves used for samples analysis had coefficients of correlation >0.999.

Adsorption isotherms: Different isotherm models were employed to determine how the metal molecules distributed between the liquid phase and the solid hydrogel phase when the adsorption process reached equilibrium state. Langmuir, Freundlich, and Temkin isotherm models were applied to the data. Adsorption parameters of ferric and ferrous ions were calculated at different pH values. The accuracy of the isotherm models was evaluated by linear correlation coefficient (R^2) values.

Langmuir isotherm: Langmuir isotherms assume monolayer adsorption onto a surface containing a finite number of adsorption sites. The linear form of the Langmuir isotherm equation is given as:

$$\frac{C_e}{q_e} = \frac{1}{q_{\max} K_L} + \frac{C_e}{q_{\max}} \quad (2-2)$$

where C_e is the equilibrium concentration of the metal ion (mg/L), q_e is the amount of metal ion adsorbed per unit mass of hydrogel (mg/g), K_L and q_{\max} are Langmuir constants related to the adsorption/desorption energy and adsorption capacity, respectively. When C_e/q_e was plotted against C_e , a straight line with slope of $1/q_{\max}$

was obtained. The R^2 values are summarized in Table 2. The Langmuir constants K_L and q_{\max} were calculated from Eq. (2) and their values are shown in Table 2-3.

Freundlich isotherm: Freundlich isotherms assume heterogeneous surface energies, in which the energy term in the Langmuir equation varies as a function of the surface coverage. The linear form of the Freundlich isotherm is given by the following equation:

$$\ln q_e = \ln K_F + \frac{1}{n} \ln C_e \quad (3-2)$$

where C_e is the equilibrium concentration of the metal ion (mg/L), q_e is the amount of metal ion adsorbed per unit mass of hydrogel (mg/g), K_F (mg/g (l/mg)^{1/n}) and n are Freundlich constants with n giving an indication of how favorable the absorption process is. The plot of $\ln q_e$ versus $\ln C_e$ gave a straight line with slope of $1/n$. Freundlich constants K_F and n were also calculated and are listed in Table 2-3.

Temkin isotherm: Temkin and Pyzhev considered the effects of indirect adsorbate/adsorbent interactions on adsorption isotherms.⁶⁴ The heat of adsorption of all the molecules in the layer would decrease linearly with coverage due to adsorbate/adsorbent interactions. The Temkin isotherm has been used in the form as follows:

$$q_e = \left(\frac{RT}{b} \right) \ln(AC_e) \quad (4-2)$$

A plot of q_e versus $\ln C_e$ yielded a straight line. The constants A and b together with the R^2 values are shown in Table 2-3.

2.3 Results and Discussions

Synthesis and characterization: Poly(allylamine hydrochloride) was cross-linked with *N,N*-methylenebisacrylamide (MBA) by a Michael-type addition reaction.⁶⁵ The reaction was performed in water using several monomers to cross-linker ratios. An acceptable hydrogel yield was obtained for various reaction conditions (Table 2-2).

Table 2-2: Reaction conditions and swelling behavior of hydrogel at pH=6.

PAAm (mg)	Cross-linker (mg)	A/B*	Swelling index**	Yield (%)
123.6	21.2	0.1	8.0	79.6
124.3	33.9	0.2	7.1	75.7
126.4	45.8	0.3	5.0	76.8
124.9	58.9	0.4	4.6	68.0

* mole ratio of crosslinker double bonds to polymer amines.

** swelling index of PAAm/DHBA hydrogel.

Although cross-linking was done by linking the primary amine groups, there were still a considerable number of reactive amino sites available for further modification of the PAAm hydrogel. 2,3 DHBA was covalently linked to the PAAm hydrogel via DCC/NHC conjugation chemistry.

Swelling studies: The swelling kinetics of PAAm and PAAm/DHBA were studied to determine the time to reach equilibrium. Hydrogel swelling increased with time; however, it eventually plateaued, thus, allowing calculation of the equilibrium

swelling percentage. PAAm hydrogel reached equilibrium in 10 h whereas PAAm/DBHA reached equilibrium in less than 1 hr (Figure 2-8).

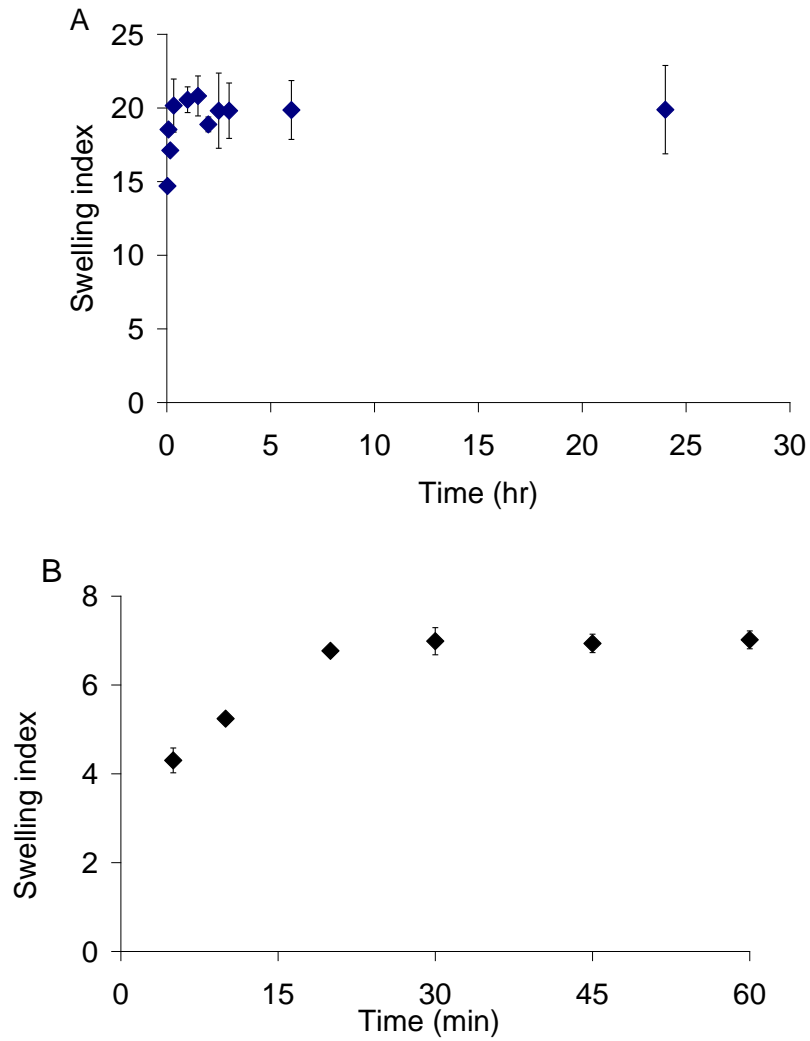


Figure 2-8: Kinetic swelling data for PAAm (A) and PAAm/DHBA (B) hydrogels at pH=6, PAAm:DHBA= 5.68.

The cross-linker concentration was varied and the swelling behavior of the final PAAm hydrogels was determined. Table 2-2 includes swelling indexes of PAAm

hydrogels with different PAAm: cross-linker ratios. A 2.7 ratio was selected because the swelling index for this ratio is within an acceptable range for either chemical or biomedical applications.⁶⁶ Next, The swelling behaviors of the hydrogels

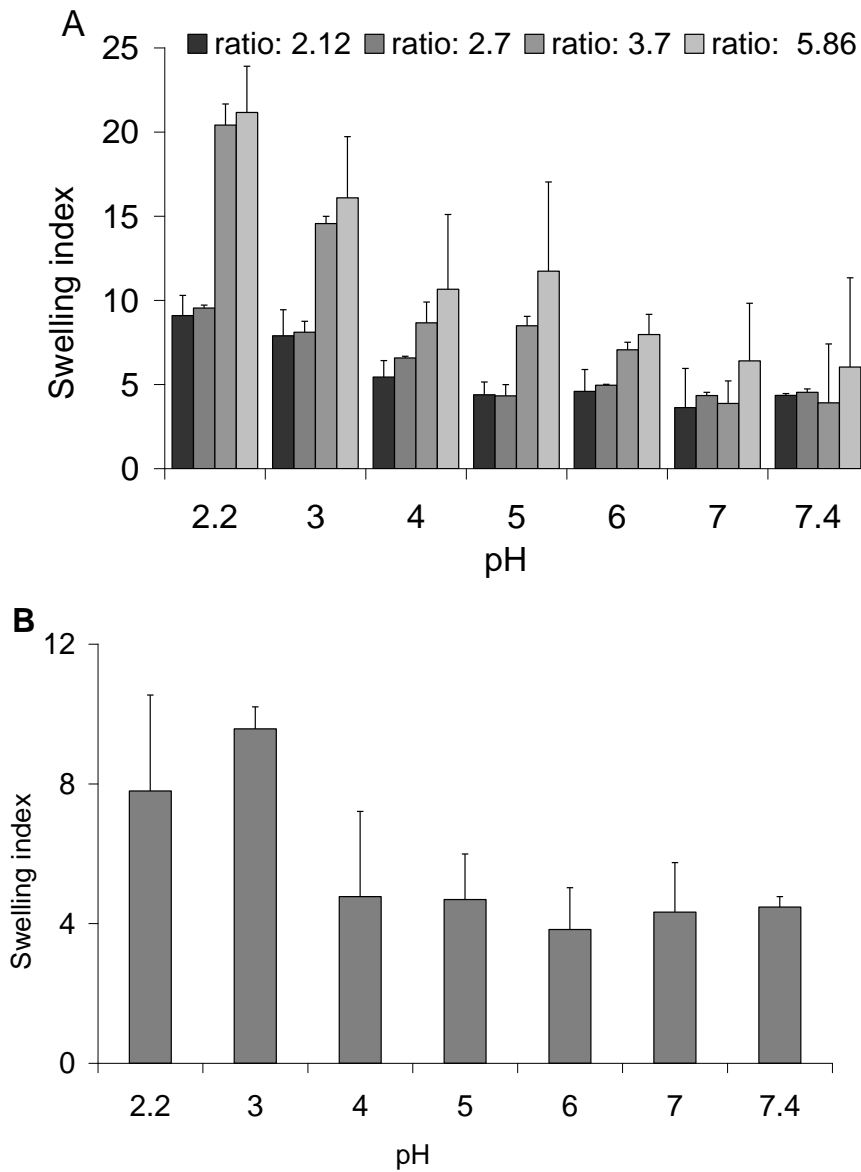


Figure 2-9: Swelling index of PAAm hydrogels with different cross-linker: polymer ratios at different pH values (A), swelling index of PAAm/DHBA with a 2.7 cross-linker: polymer at different pH values (B) (ionic strength=0.5 M).

were further investigated as a function of pH by immersing the gels in buffered solutions at pH 1, 2, 4, 5, and 7.4 at room temperature (~25°C).

The swelling behavior of PAAm was determined after equilibrating at different pH values (Figure 2-9). The swelling of the PAAm hydrogel is higher at low pH values, with the maximum swelling observed at a pH of 2.2. This could be attributed to the complete protonation of the amine groups of PAAm at low pH. The pK_a of primary amines in PAAm is ~ 9.67; therefore, the behavior observed resulted from the ionized amines of the polymer as expected.⁶⁷ Osmotic pressure results from counterions to the protonated primary amines and is a probable cause of swelling. When immersed in electrolyte solutions, ion exchange takes place in these types of hydrogels during the swelling process and can exert a considerable effect on the water absorption.⁶⁸ The same experiment was carried out for PAAm conjugate hydrogels and the swelling behavior of the 2,3 DHBA modified gels was studied at different pH values (Figure 2-9). Because many of the amine groups were occupied via amide linkage, the ionizable groups within the hydrogel were diminished. Almost no significant changes in the swelling behavior were observed for PAAm/DHBA at different pH values. Images of equal weights of the different hydrogels also illustrated the vast difference in swelling. PAAm hydrogels showed a significant reduction in swelling after modification by 2,3 DHBA (Figure 2-10). The occupation of ionizable amine groups after conjugation of DHBA greatly reduced water uptake and presumably reduced the uptake of counterions.

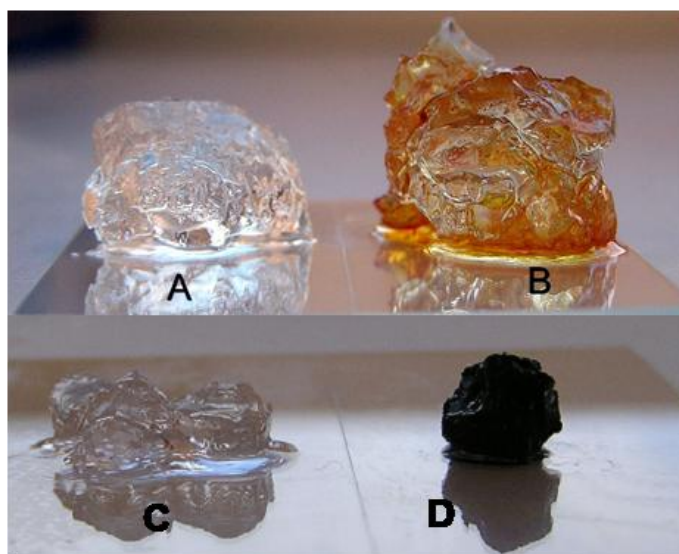


Figure 2-10: PAAm equilibrated in DI water (A), PAAm equilibrated in 2 mg/mL ferric solution (B), PAA/DHBA equilibrated in DI water (C) and PAAm/DHBA equilibrated in 2 mg/mL ferric solution (D). All hydrogels had equal masses.

Moreover, PAAm/DHBA hydrogel further collapsed after immersion in a 2 mg/mL solution of ferric chloride (Figure 2-10). Hydroxyl groups along with oxygen molecules bearing a negative charge (due to the partial double bond characteristic of the amide linkage) provided probable coordination sites for Fe. Moreover, as evident from potentiometric data, some protonated amine groups may also contribute to the coordination of Fe. The potentiometric data obtained for PAAm and PAAm/DHBA indicated that Ca. 23% of amine groups were occupied after conjugation reaction. Further collapse of PAAm/DHBA hydrogel in the ferric solution may be explained by multiple DHBA coordination of Fe.

Binding Kinetics: Determination of the kinetics of metal absorption is critical in elucidating the reactivity of PAAm/DHBA and evaluating its potential for chemical

and biomedical applications. The kinetics of metal binding was monitored using a known initial concentration of metal solution (2 mg/mL, FeCl_3) in the presence of a known mass of dry hydrogels. The equilibrium binding was found to be 1180 and 810 mg Fe/g Gel for PAAm/DHBA and PAAm, respectively (Figure 2-11).

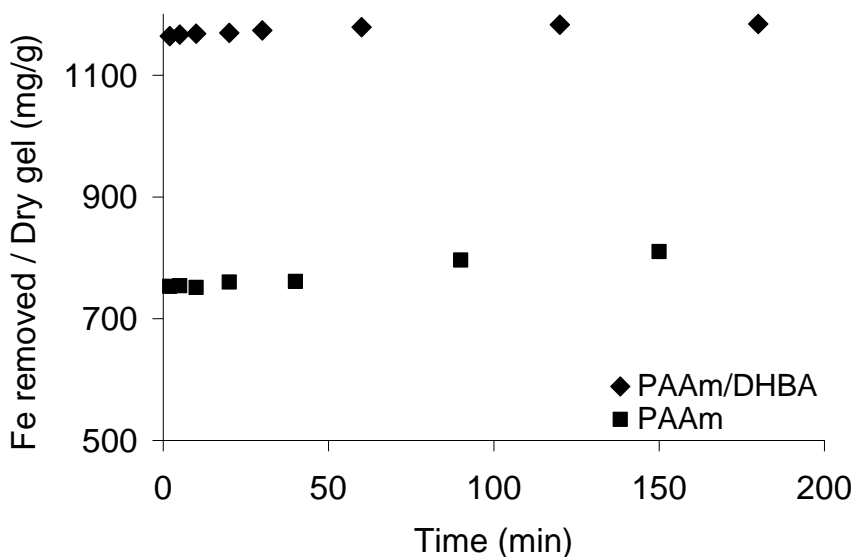


Figure 2-11: Ion binding by PAAm/DHBA hydrogels. Gels were equilibrated in 2 mg/mL ferric solution (pH= 2, ionic strength=0.5 M).

About 80% of the total iron absorption was attained in less than 5 min for the PAAm/DHBA hydrogel. This rapid absorption behavior is important in biomedical application especially for treatment of acute metal poisoning. To derive the rate constant and binding capacity, the kinetic data were modeled with pseudo-first-order (Lagergren model) and pseudo-second-order (Ho model) kinetic models which are expressed in their linear forms as:

$$\log(q_e - q_t) = \log(q_e) - \frac{k_1}{2.303}t \quad (2-5)$$

$$\frac{t}{q_t} = \frac{1}{q_e^2 k_2} + \frac{t}{q_e} \quad (2-6)$$

where k_1 (L/min) and k_2 (g/mg · min) are pseudo-first-order and pseudo-second-order rate constants, respectively. Fitted kinetic models are shown (Figure 2-12), and the model variables obtained by linear regression were compared (Table 2-3). The pseudo-second order reaction model showed the best fit for ferric ions because its R^2 was ~1.

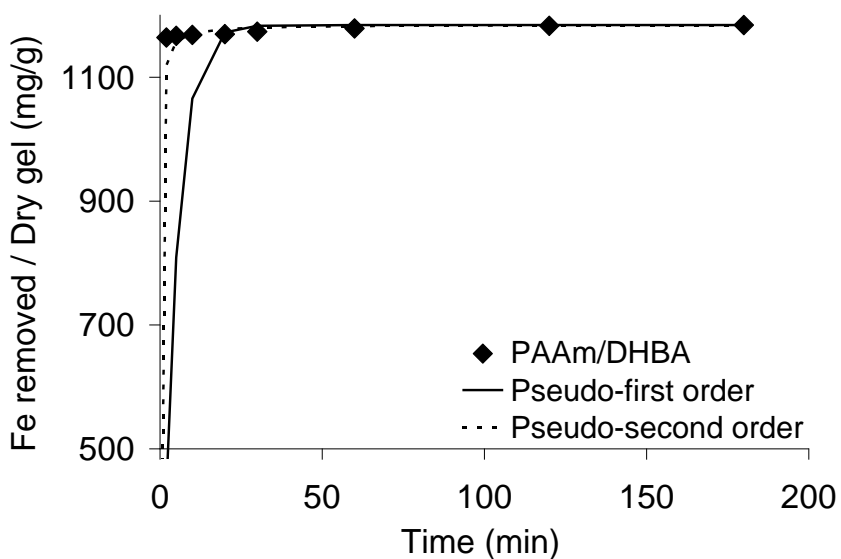


Figure 2-12: Kinetic models fitted for PAAm/DHBA hydrogel. Gel was equilibrated in 2 mg/mL ferric solution (pH= 2, ionic strength=0.5 M).

Table 2-3: Kinetic parameters for ferric binding by PAAm/DHBA at pH=2.

Kinetic model	Rate constant	Ion	R²
Pseudo-first order	0.24	ferric	0.9988
Pseudo-second order	0.23	ferric	1

Binding Isotherms: The metal ion binding capacity was determined at different pH values and different isotherm models were used to fit the data. At low pH, the metal ion uptake was relatively high. This could be due to the presence of protonated primary amine groups along with iron coordination sites, which together may improve the binding capacity of the hydrogel for iron. Increasing the pH decreased the ionization of the remaining primary amine groups, and in turn lower values for the metal ion uptake were observed.

Table 2-4: Isotherm parameters for ferric and ferrous binding by PAAm/DHBA. Gels were equilibrated in 2 mg/mL iron solutions.

pH	2.2	5.4	7.4	2.2	5.4	7.4
Isotherm model	Ferric			Ferrous		
Freundlich						
K_F	$77.53 \cdot 10^{+1}$	$34.55 \cdot 10^{+2}$		$31.33 \cdot 10^{+2}$	$22.29 \cdot 10^{+2}$	$43.84 \cdot 10^{+2}$
n	3.680	1.510		2.770	1.580	2.150
R^2	0.9884	0.9902		0.9927	0.9233	0.9895
sen	$1.826 \cdot 10^{-2}$	$3.289 \cdot 10^{-2}$		$1.545 \cdot 10^{-2}$	$9.546 \cdot 10^{-2}$	$2.395 \cdot 10^{-2}$
sey	$1.610 \cdot 10^{-2}$	$2.821 \cdot 10^{-2}$		$1.504 \cdot 10^{-2}$	$2.928 \cdot 10^{-2}$	$2.573 \cdot 10^{-2}$
Langmuir						
q_{max}	$52.63 \cdot 10^{+1}$	$14.28 \cdot 10^{+2}$		$20.00 \cdot 10^{+2}$	$25.00 \cdot 10^{+2}$	$14.28 \cdot 10^{+2}$
K_L	63.33	17.50		25.00	2.000	87.50
R^2	0.9998	0.9823		0.9581	0.8216	0.9840
sen	$3.100 \cdot 10^{-7}$	$4.431 \cdot 10^{-6}$		$1.901 \cdot 10^{-6}$	$2.135 \cdot 10^{-5}$	$5.699 \cdot 10^{-7}$
sey	$1.126 \cdot 10^{-5}$	$1.713 \cdot 10^{-4}$		$6.645 \cdot 10^{-5}$	$6.150 \cdot 10^{-5}$	$1.253 \cdot 10^{-4}$
Temkin						
A	331.70	1.000		199.3	19.20	635.7
b	21.06	6.190		5.130	4.080	7.770
R^2	0.9637	0.9646		0.9639	0.9380	0.9612
sen	4.691	37.78		$4.669 \cdot 10^{-2}$	$7.805 \cdot 10^{-2}$	$3.054 \cdot 10^{-2}$
sey	9.522	74.62		0.1046	$5.512 \cdot 10^{-2}$	$7.556 \cdot 10^{-2}$

The respective isotherm curves of ferric and ferrous solutions were obtained at different pH values (Figure 2-13&Figure 2-14).

Modeling of isotherm data is vital for deriving meaningful information of binding characteristics, such as maximum binding capacity and binding constant. Therefore, several theoretical isotherm equations, including those of Freundlich, Langmuir, and Temkin, were employed to evaluate which could best describe the experimental data. Generally, the Freundlich and Temkin models are applicable to heterogeneous systems, while the Langmuir model is based on a homogeneous monolayer

adsorption. Among the three models, both Freundlich and Temkin models provided accurate ferric and ferrous isotherms at low implying the heterogeneous nature of adsorption (Figure 2-13& Figure 2-14).

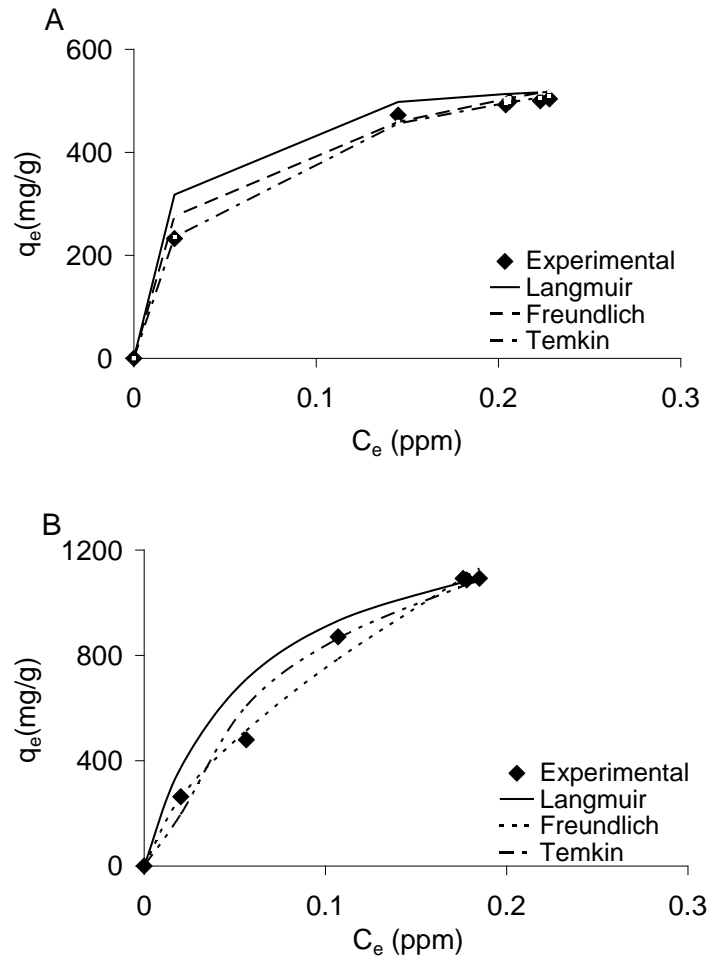
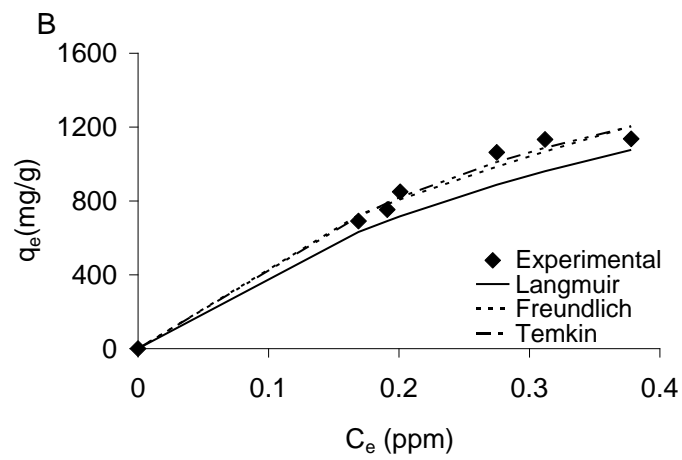
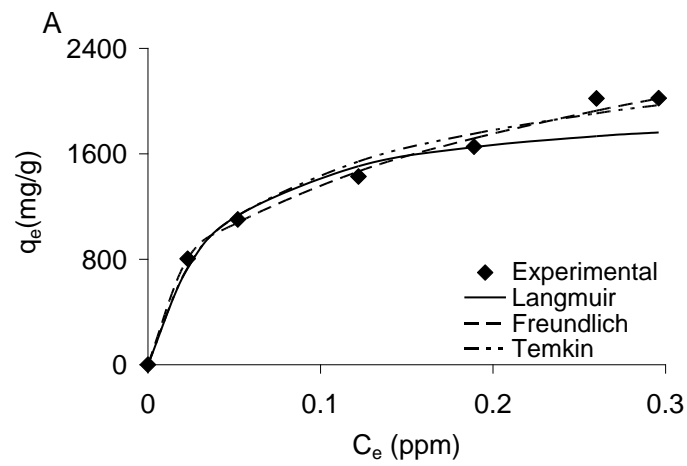


Figure 2-13: Binding isotherms for ferric ions at pH 2-3 (A) and 5-6 (B)

R^2 values obtained for these models were close to unity compared to the Langmuir model (Table 2-4). The data may allow speculation that more than one type

of binding site with different affinities may be involved in iron binding by PAAm/DHBA. This hypothesis will require further studies to confirm or refute.



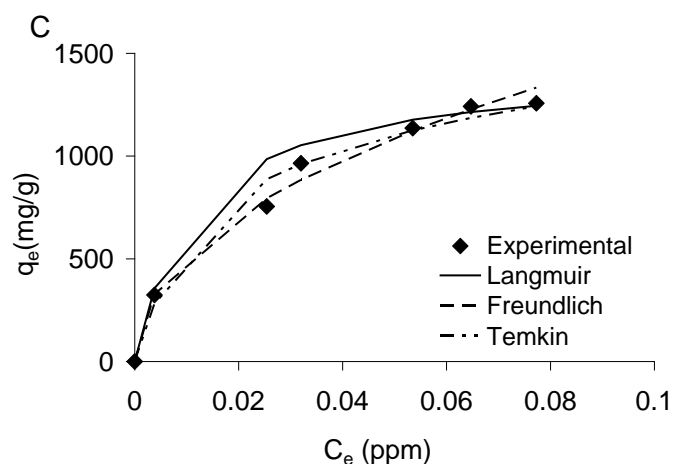
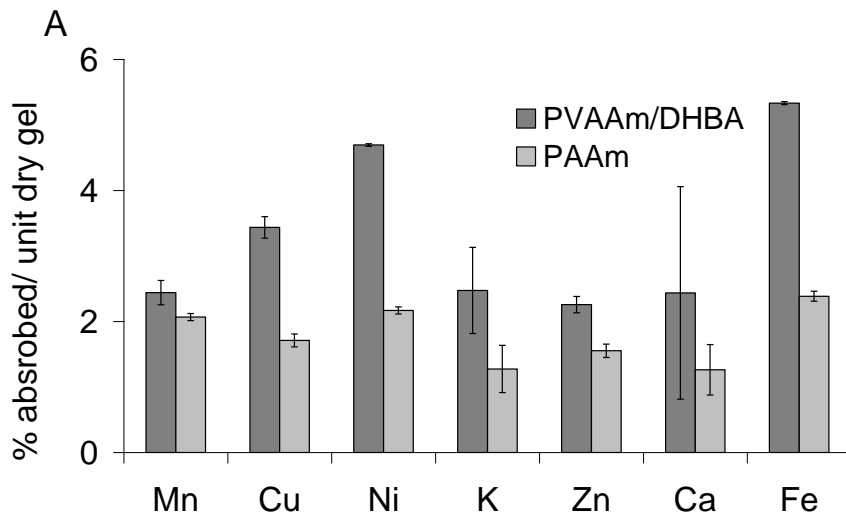
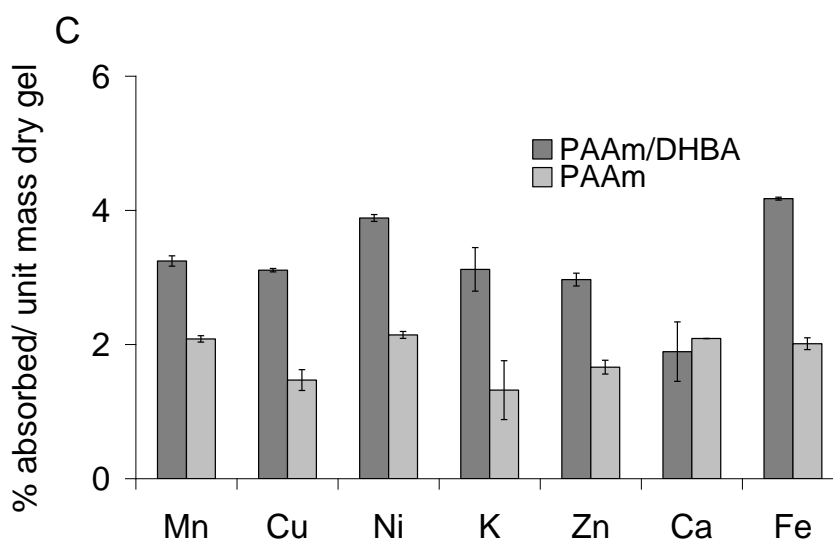
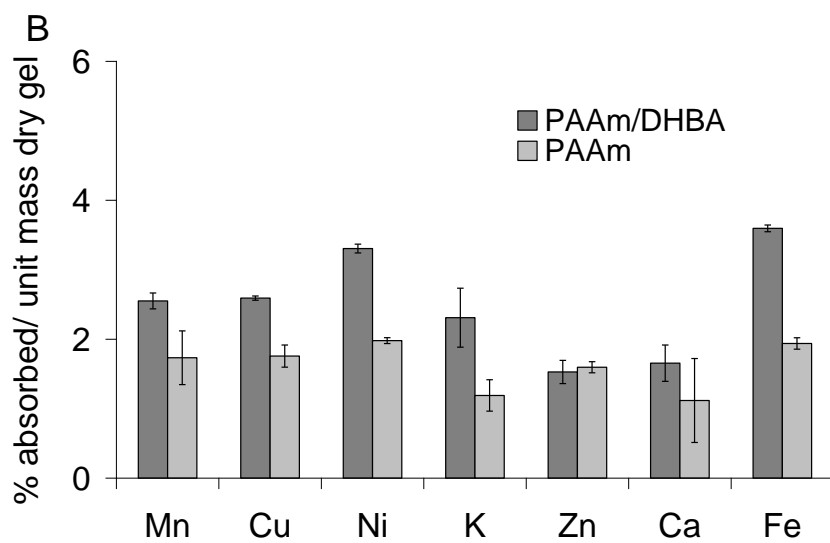


Figure 2-14: Binding isotherms for ferrous ions at pH 2-3 (A), 5-6 (B), and 7.4 (C).

Ment et al. reported the removal of iron from different systems using Sepharose-desferrioxamine B gels.⁵⁰ They also studied the effect of the immobilization of other iron chelators like 1-(*l*-aminoethyl)-3-hydroxy-2-methyl-4-pyridinone (HP) and L-mimosine onto Sepharose.⁶⁹ However, the effectiveness of the immobilized DFO was low. Even though gels had a high affinity for Fe(III) and were used for removing iron from milk, wine, whey and lactoferrin, they were not very stable mainly due to hydrolysis of their isourea bonds.^{50, 69} In another study, Polomoscanik et al. studied the iron binding parameters of hydroxamic acid-containing hydrogels derived from derived from cross-linked polymeric acid chloride precursor and polymeric hydroxyethyl ester precursor. The maximum iron(III) binding capacities of these hydrogels were 0.81 and 0.45 mmol/g respectively.⁷⁰ The maximum iron (III) binding capacity of PAAm/DHBA hydrogel varies between 9.3-25.5 mmol/g depending on the pH of the solution.

Selectivity Studies Effect of Essential Metal: One of the important features of metal chelating hydrogels is their ability to specifically target the metal of interest and remove it from the media. Selectivity is especially important if the desired application of the hydrogel is in the treatment of metal poisoning. The hydrogel selectivity may affect the bioavailability of some other essential metal ions such as Cu^{2+} , Zn^{2+} , Ca^{2+} , Mn^{2+} , Ni^{2+} , or K^+ . Selective absorption of essential metals could cause serious damage to vital organs. The influence of essential metals on the binding of ferric ions was investigated using a multi-solute system to evaluate the metal selectivity of PAAm/DHBA at different pH values. At an equal concentration of all metals (2 mg/mL), PAAm/DHBA absorbed almost 80% of the iron present in the media while typically the absorption for essential metals (e.g. Ca, Zn) was less than 50% (Figure 2-15).





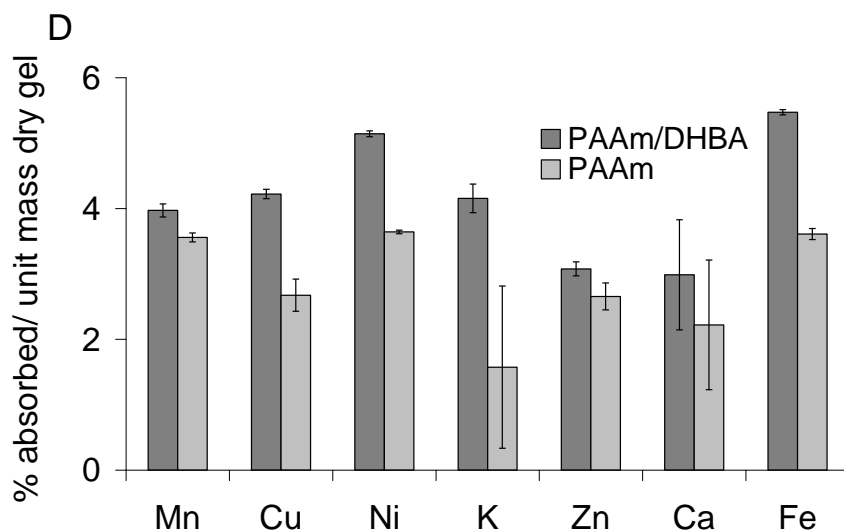


Figure 2-15: Selectivity study for PAAm/DHBA and PAAm hydrogels toward ferric ion in the presence of Mn^{2+} , Cu^{2+} , Ni^{2+} , K^+ , and Ca^{2+} at different pH ranges. A: pH=2.5, B: pH=4, C: pH=5 and D: pH=7.

The ratio was similar across a wide range of pH values. Zhou et al. has studied the selectivity of 3-hydroxypyridin-4-one hexadentate ligand-containing copolymers (DMAA) for iron in the presence of some essential metals. Even though the DMAA hydrogel showed high affinity for iron it still bound Cu^{2+} efficiently (more than 53%). Comparatively, PAAm/DHBA showed a higher selectivity toward Fe in the presence of other metals, implying the greater stability of the Fe-PAAm/DHBA complex.

2.4 Conclusions

2,3 dihydroxybenzoic acid was immobilized on polyallylamine hydrogel to mimic the structure of the enterobactin, a potent, naturally occurring Fe (III) chelator. The final hydrogel was able to remove and accumulate ferric and ferrous ions from aqueous solutions at relatively low concentrations. PAAm/DHBA demonstrated an almost

instant iron absorbance when equilibrated in ferric solution. The pseudo-second order H_0 kinetic model was found to be an excellent fit with the experimental results. These siderophore-mimetic hydrogels also exhibited a high affinity and selectivity for iron at different pH values. Freundlich and Temkin adsorption models adequately described the relationship between metal concentration in solution and the amount retained by the hydrogel. The high affinity and selectivity of PAAm/DHBA hydrogel for iron provides important features for this hydrogel in biomedical and chemical applications.

Chapter 3

Enhancing the Selectivity of an Iron Binding Hydrogel

3.1 Introduction

Iron is an essential and ubiquitous element in all forms of life involved in a multitude of biological processes and essential for many critical human biological processes.⁷¹⁻⁷³ Yet, the presence of excess iron in the body leads to toxic effects.⁷⁴ Iron is absorbed from the mammalian gastrointestinal tract by protein-mediated mechanisms.⁷⁵ Body iron levels are tightly controlled by the absorption process. Excess iron is extremely toxic due to its ability to generate relatively high levels of the hydroxyl radical.⁷⁶ Moreover, un-sequestered iron can also act as a bacterial virulence enhancing factor.⁷¹ Under normal physiological conditions, iron metabolism is tightly conserved with the majority of the iron being recycled within the body.⁷⁷ Normal physiology does not provide a mechanism for iron excretion in urine, feces, or bile.⁷⁸ Certain genetic disorders like hemochromatosis can lead to an increased systemic absorption of dietary iron.⁷⁹ Iron overload also results from blood transfusions in the case of β -thalassaemia and sickle cell anemia patients.⁸⁰

The current standard of care for iron overload diseases is iron chelation therapy with desferrioxamine.⁷³ Desferrioxamine (DFO) therapy has reportedly been associated with several drawbacks including a narrow therapeutic window and lack of oral bioavailability.⁷⁰ As a result, it requires administration for 8–12 h per day by infusion.⁷¹ DFO cannot be readily absorbed through the intestine and must be injected intravenously thus, is not an ideal chelator since systemic side effects are inevitable.⁸¹ One possible method of avoiding the use of systemic iron chelators is to inhibit iron

absorption from the gastrointestinal tract by orally available, non-absorbed iron chelators that selectively sequester and remove excess dietary iron from the GI tract. Non-absorbed polymer therapeutics that act by sequestering a number of undesired ionic species in the gastrointestinal tract have been successful clinically.^{77, 82-83} This method is particularly relevant to thalassaemia intermedia and hemochromatosis. Iron binding polymers have considerable potential in this therapeutic approach as they can effectively bind iron irreversibly to form nontoxic, inert complexes that are not absorbed by the gastrointestinal tract, thereby reducing the absorption of iron from the intestine.

Because of the importance of other metal ions for normal human physiology, clinically acceptable polymeric ligands must possess high affinity, capacity, and selectivity towards iron. Furthermore, such polymers should be biocompatible and preferably non-absorbed. These considerations prompted further improvement of the binding affinity and selectivity of previously reported siderophore-mimetic iron chelators. Polyallylamine (PAAm) hydrogels with conjugated 2,3 dihydroxybenzoic acid (2,3 DHBA) have been introduced as potential iron-specific chelating agents. Here the effect of the PAAm:DHBA ratio on the binding constant and the selectivity of the hydrogel was investigated. Several concentrations of DHBA were grafted within the gel and the stability constant of each corresponding concentration was calculated. PAAm-DHBA hydrogel with ~ %15 grafted DHBA with the gel network seemed to have an optimum affinity ($\text{Log } K = 27.01$), selectivity (its selectivity toward

Fe is ~ 3-14 times more than its selectivity toward other competing metals) and binding capacity (~600 mg/g dry gel) for Fe(III).

3.2 Materials and Methods

Material: Poly(allylamine hydrochloride) (PAAm) with an average molecular weight of 56 kDa and analytical grade reagent *N,N'*-methylenebisacrylamide (MBA) were obtained from Sigma-Aldrich and used without further modification. 2,3-dihydroxybenzoic acid, *N,N,N*-triethylamine (TEA), dimethylformamide (DMF), and all metal chlorides were purchased from Fisher Scientific and used as received. Dicyclohexylcarbodiimide (DCC) and *N*-hydroxysuccinimide (NHS) were purchased from Thermo Scientific and used without further modification. Deionized water (DI) was obtained from a Barnstead EasyPure water purifier.

Preparation of PAAm Hydrogel: PAAm hydrogel was synthesized following the procedure reported in the literature.⁸⁴ Briefly, a 20% w/v polymer solution containing a predetermined amount of MBA was prepared. The cross-linker was dissolved in deionized water (flushed with nitrogen for 5 min) and then added to the polyallylamine polymer. TEA, the cross-linking catalyst (300 μ L), was then added to the solutions and mixed thoroughly. Next, the precursors were transferred by micropipet into a small plastic cuvette and subsequently covered with parafilm. The cuvettes were held at ambient temperature for 1 h and then cooled to ca. 3 °C and held there for an additional 24 h. After this time, hydrogels were removed from the cuvettes and washed with 0.05 M sodium chloride for several days.

2,3 Dihydroxybenzoic acid Modification of Hydrogel: A solution of 2,3 DHBA and NHS in 5 mL of DMF was mixed with a solution of DCC in 5 mL of DMF. The mixture was stirred at low temperature for 6 h to give a white precipitate. The precipitate was filtered, and the filtrate was added directly to dry gel particles with approximate size of about 0.5-1 mm. several concentrations of DHBA were grafted to the hydrogel network to optimize the selectivity and iron binding affinity of the final hydrogel (Table 1). The reaction mixture was held at room temperature for 3 days. PAAm conjugate hydrogel was then washed with water for several days.

Quantification of Amine Functional Groups: Primary amine groups were quantified by potentiometric titration. After grinding to a powder, 40 mg of PAAm and each PAAm-DHBA hydrogel were suspended in 35 mL of 0.2 M aqueous KCl solution. Next, 140 μ L of 8 M KOH aqueous solution was added to polymer suspensions to raise the pH to \sim 12. Standard 0.1 M HCl was used to titrate the suspension. HCl was added until the pH was about 2.5 in both polymer suspensions. Free amine groups were quantified from potentiometric data following reported procedures.⁸⁵

Polymer-Iron Stability Constant Determination: The stability constant of gel chelators was measured using an historic ligand competition assay.⁸⁶ The competitive chelation of iron by polymeric chelator in equilibrium with a water-soluble chelator (ethylenediaminetetraacetic acid: EDTA) was used to determine the stability constant of iron-ligand complexes of PLL/DHBA hydrogel. Briefly, to a 1.5 ml of 10 mM

EDTA solution was added 2 mL of 5 mM of FeCl₃ solution and 21.5 mL PBS and a known mass of ground gel. The mixture rotated at 20 °C for 3 days and the concentration of the soluble iron complex was determined by inductively coupled plasma mass spectroscopy (ICP-MS). The stability constant of the gel was determined following the procedure reported in literature.⁸⁶ The same procedure was repeated for all the different PAAm:DHBA ratios.

Selectivity Study: The selectivity for Fe by PAAm-DHBA in the presence of several heavy metals such as copper, zinc, manganese, calcium, and potassium was studied. Metal solution (10 mL) containing all metal components was prepared. The upper tolerable intake level of each metal was used as an initial concentration in the solution. These concentrations were chosen on the basis of the U.S. recommended daily allowance (RDA) data on the daily dietary uptake of these metal ions present in a normal meal. The solution mixture was then adjusted to pH 2.5 and held at room temperature for 2 h after adding a known mass of PAAm-DHBA ground gel. The selectivity study was carried out for all different PAAm-DHBA ratios.

Metal Analysis: Mono- and multi-elemental analysis of samples was quantified by Inductively Coupled Plasma Optical Emission Spectrometry (ICP-OES) (Optima 2000 DV, PerkinElmer, USA) fitted with an AS 93plus autosampler (PerkinElmer, USA). A Cross-Flow nebulizer and a Scott spray chamber were used. The RF Power was 1300 W and nebulizer and auxiliary flows were 0.8 and 0.2 L/min, respectively. Sample flow was set at 1.5 mL/min. ICP-OES data was processed using Winlab 32

(Ver. 3.0, PerkinElmer, USA). The analytical curves used for sample analysis had coefficients of correlation >0.999.

3.3. Results and Discussions

Poly(allylamine hydrochloride) was cross-linked with *N,N*-methylenebisacrylamide (MBA) by a Michael-type addition reaction. The ratio of monomer to cross-linker was selected based on recommendations from the literature.⁸⁷ The DCC/NHS coupling chemistry was adopted to react the free amine side chains of the hydrogel with the carboxylic end of the 2,3 DHBA. Since the concentration of 2,3 DHBA hydroxyl groups is critical for enhanced binding of iron, the choice of appropriate PAAm:DHBA ratio was important for obtaining hydrogels with high iron affinity. To optimize the binding affinity and selectivity of the final product, several ratios of PAAm:DHBA were investigated (Table 3-5). Potentiometric titration data were used to calculate the degree of conjugation. The conjugation efficiency varied from 75%-95% depending on the initial concentration of 2,3 DHBA.

Table 3-5: Reaction conditions, conjugation reaction efficiency and conditional stability constants (Log k) of hydrogels.

<u>%DHBA grafted</u>	<u>% conjugation</u>	<u>Log K</u>
86.10	95.71	27.04±0.06
14.97	73.95	27.01±0.24
8.45	83.00	26.6±0.42
1.41	69.50	26.4±0.28
0.00	0.00	25.2±0.28

Conditional Stability Constant of Fe(III)-Hydrogel: The ligand competition method is widely used for the determination of stability constants of both soluble iron(III)-ligand complexes and cross-linked polymeric chelators.^{86, 88} The stability constants (log *K*) of PAAm-DHBA-iron complexes were considerably higher ($\times 10$) than of those similarly synthesized hydrogels (Table 3-5).⁸⁸ A decrease in the concentration of DHBA resulted in a decrease of the conditional stability constant. As the concentration of functional groups incorporated in hydrogels decreased, the binding capacity of the hydrogel decreased as well (Figure 3-16& Figure 3-17). Chelating properties of a polymeric chelator have also been shown to be affected by steric hindrance between the ligand and the polymeric matrix, but in the case of PAAm-DHBA hydrogels there may be little inference by the polymer backbone in the iron chelation process based on the binding capacities observed.⁸⁹⁻⁹⁰

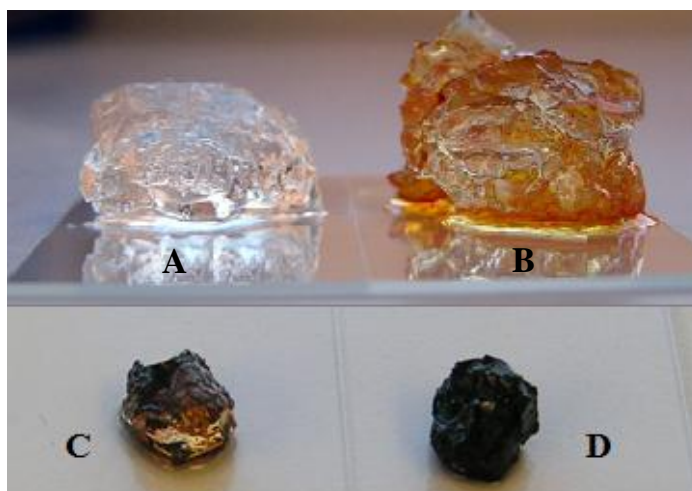


Figure 3-16: A: PAAm equilibrated in DI water, B: PAAm equilibrated in 2 mg/mL FeCl₃ solution C: PAAm-DHBA (~0.3 Molar ratio) equilibrated in 2 mg/mL FeCl₃ solution, D: PAAm-DHBA (0.01 Molar ratio) equilibrated in 2 mg/mL FeCl₃ solution. All samples are single pieces and have equal masses, pH~2).

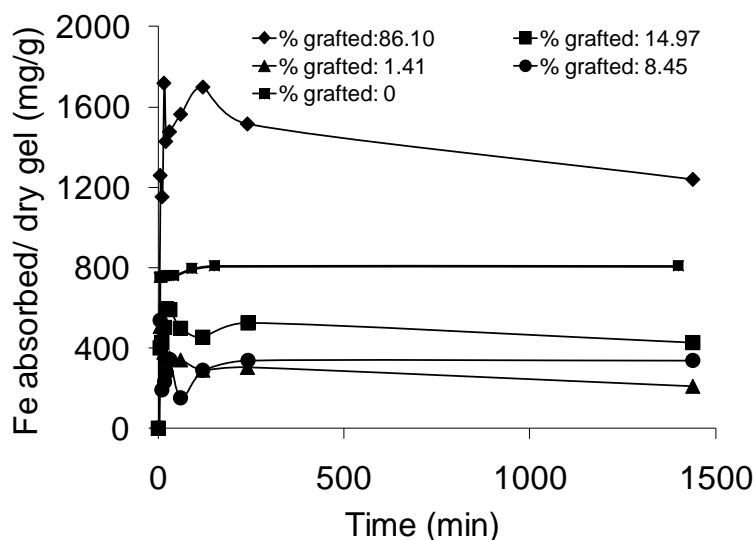


Figure 3-17: Kinetic studies of PAAm-DHBA hydrogels. Gels were equilibrated in 2 mg/mL ferric solution (pH= 2, ionic strength=0.5 M).

Zhou et al. have reported the synthesis of a range of iron binding dendrimers terminated with hexadentate ligands formed from hydroxypyridinone,

hydroxypyranone, and catechol moieties.⁹¹ The stability constant of these dendrimers were similar to those reported in this study. In another study, a series of polymeric iron chelators have been introduced by the synthesis of 3-hydroxypyridin-4-1 hexadentate ligand incorporated into polymers via co-polymerization with *N,N*-dimethylacrylamide, and *N,N'*-ethylene-bis-acrylamide. The Fe(III) chelation capacity of this polymer reached 80% within 1 h, and the stability constant ($\log K'$) for iron(III) was determined to be 26.55, slightly lower than reported here.⁸⁸

Selectivity of the PAAm-DHBA hydrogels: Since PAAm-DHBA hydrogels possessed a high affinity for Fe (III), it was anticipated that these hydrogels may also possess an improved selectivity for Fe (III) over other metal ions. Copper (II), zinc (II), and manganese (II) are all present in biological tissues and in food. As these three metals are essential for life, it is important that the hydrogels designed in this study possess much lower affinities for this group of divalent cations. In competition studies, iron(III) was shown to be selectively bound to the hydrogels in the presence of competing metals, i.e. Zn^{2+} , Mn^{2+} , and Cu^{2+} (Table 3-6). In all these cases, iron concentrations were decreased significantly after incubation with hydrogel, whereas the concentrations of the competing bivalent metals remained almost unchanged.

Table 3-6: Selectivity of PAAm-DHBA hydrogel with different PAAm:DHBA molar ratio, pH~2.

%DHBA grafted	Fe absorbed/ competing metal		
	Fe/Zn	Fe/Mn	Fe/Cu
86.10	3.03	2.70	N/A
14.97	18.63	15.56	10.90
8.54	5.95	3.16	0.92
1.41	1.49	2.96	2.14
0	1.43	1.10	1.42

In comparison, Zhou et al. have reported a Fe(III) hydrogel chelator composed of a relatively high stability constant; however, the selectivity studies revealed that the binding capacity for both Fe(III) and Cu(II) were almost identical, indicating the lack of selectivity toward Fe(III).⁸⁸

3.4 Conclusion

A cross-linked polymer that mimics the structure of enterobactin, a naturally occurring siderophore, was synthesized. 2,3 Dihydroxybenzoic acid, a metal binding domain of enterobactin, was used as a conjugated moiety to simulate the high iron affinity and selectivity of enterobactin. Several ratios of PAAm:DHBA were used to optimize the stability constant, selectivity and binding capacity of these iron chelating hydrogels. Hydrogels with ~ 15% DHBA grafted demonstrated high stability constant while maintaining selectivity and a high binding capacity for Fe (III). The high affinity and selectivity of PAAm-DHBA hydrogel for iron provides important features for this hydrogel in the treatment of iron overload disease such as

hemochromatosis. When administered orally, these siderophore-mimetic hydrogels may effectively absorb iron from the GI tract for excretion.

Chapter 4

PLL/DHBA: A Potential Alternative for DFO Chelation Therapy

4.1 Introduction

Under normal physiological conditions, iron metabolism and bioavailability are tightly controlled through dietary absorption, trafficking, and recycling of iron within the body. The human body does not have an active mechanism for iron excretion and therefore excess iron is usually stored in the body. Free iron is primarily stored in the liver, spleen, and bone marrow in the form of bound ferritin molecules. Several studies have been done on patients suffering from iron overload diseases. The results of these studies have demonstrated that an excess accumulation of free iron in the body occurs as a consequence of enhanced dietary uptake (hemochromatosis), medical treatment (chronic blood transfusions), destabilized hemoglobin (sickle cell disease), reduced hemoglobin (β thalassemia), or as a result of conditions such as cardiomyopathies, hepatic fibrosis and diabetes mellitus.⁹² To treat iron overload conditions such as these, iron chelation therapy is often employed.⁹³

The naturally occurring siderophore, deferoxamine (DFO), is one of the most effective chelators that has been approved for therapeutic use to remove the excessive accumulation of tissue iron.⁹⁴ Although DFO may be clinically effective, it is beset by many disadvantages, the most significant of which are the high toxicity and very short plasma half-life (~5.5 min).⁹⁵ Moreover, administration occurs via subcutaneous infusion over a long period of time. This poses some difficulties with compliance as well as the high cost of patient care.⁹⁶ In addition, DFO has serious side effects that require limiting the daily dose to a tolerable amount. Side effects include but are not

limited to local inflammatory reactions, visual and auditory disturbance, disturbances of bone growth, allergic reactions, and pulmonary, renal and neurological manifestations.⁹⁶ Therefore, there is an urgent need for iron chelators that have fewer side effects while exhibiting excellent iron chelating efficacy.

For the development of such molecules, attempts have been made to correlate the chemical structure as well as certain physical parameters with their biological activity. Controlled polymerization methods such as reversible addition fragment chain transfer and atom transfer radical polymerization developed over the last decade afforded the synthesis of polymer conjugates with predetermined molecular weight, composition, stability, and immunological and pharmacological properties.⁹⁷ One of the important features of an alternative chelator is that the resulting iron complex formed should be non-toxic and the coordinated iron should be protected from interaction with either hydrogen peroxide or oxygen. Here, the *in vitro* evaluation of siderophore-mimetic polymer, poly-L-lysine (PLL) conjugated to 2,3 dihydroxybenzoic (2,3 DHBA) acid is reported as a new iron chelator. The rapid, selective absorption of iron and non-cytotoxic behavior of this compound make it suitable for iron chelation therapy. Moreover, the ability to predetermine the molecular weight of the polymer offers the potential to extend the plasma half-life of the chelator.

4.2 Materials and Methods

Materials: Poly-L-lysine hydrobromide (PLL) with an average molecular weight of 15-30 kDa was obtained from Sigma-Aldrich and used without further modification. 2,3 dihydroxybenzoic acid (2,3 DHBA), *N,N,N*-triethylamine (TEA), dimethylformamide (DMF), potassium phosphate and all metal chlorides were purchased from Fisher Scientific and used as received. Dicyclohexylcarbodiimide (DCC) and *N*-hydroxysuccinimide (NHS) were purchased from Thermo Scientific and used without further modification. Deionized water (DI) was obtained from a Barnstead EasyPure water purifier.

Blood: Blood plasma was collected from a male Wistar Rat (566 grams) following an IACUC-approved procedure.

2,3 Dihydroxybenzoic acid modification of polymer: A solution of 2,3 DHBA (64 mg, 0.42 mmol) and NHS (47.48 mg, 0.4 mmol) in 5 mL of DMF was mixed with a solution of DCC (42.5 mg, 0.2 mmol) in 5 mL of DMF. The mixture was stirred at room temperature (~ 23 °C) for 6 hr to yield a white precipitate. The precipitate was filtered, and the filtrate was added directly to a solution of PLL (15mg/mL, 2 mL). The reaction mixture was held at room temperature for 6 hr. Next, DMF was evaporated using a rotovap and sample was kept in a vacuum oven overnight to ensure the complete evaporation of DMF. The PLL conjugate polymer product was dissolved in water and was dialyzed against water for several days.

Binding Kinetics Study: Ferric chloride solution (2 mg/mL) was adjusted to pH 6.5 and kept at room temperature for kinetic studies. The polymer solution was kept within a dialysis bag while immersed in a media containing FeCl₃ solution. Iron concentration was read both from retentate and dialysate. Samples were taken from the media at different time intervals to determine the rate of iron binding by PLL/DHBA.

Selectivity Study: The selectivity for Fe by PLL/DHBA in the presence of several heavy metals such as copper, zinc, manganese, calcium, and potassium was studied. Metal solutions (10 mL) containing a 1:1 (wt) mixture of iron and heavy metals were prepared (2 mg/mL). The solution mixtures were then adjusted to pH 2.5 and held at room temperature. PLL/DHBA (6 mg/mL, 10 mL) was transferred to the dialysis bag and immersed into the above solution. Samples were taken from the solution after 2 hrs to study the metal concentration.

Cytotoxicity of polymeric iron chelator: The cytotoxicity of polymers was determined by the CellTiter 96® Aqueous Cell Proliferation Assay (Promega). Human umbilical vein endothelial (HUVEC) cells and human lung adenocarcinoma epithelial (A549) cells were cultured and incubated with polymers for ~24 h. Next, the media was removed and replaced with a mixture of 100 µL of fresh culture media and 20 µL of MTS reagent solution and cells were incubated for 3 h at 37°C in a 5% CO₂ incubator. The absorbance of each well was then measured at 490 nm using a

microtiter plate reader (SpectraMax, M25, Molecular Devices Corp.) to determine relative cell viability.

In vitro hemolysis assay of the polymer: To determine the effect of polymer solution on red blood cell (RBC) aggregation, a hemolysis assay was performed using blood from mice. The erythrocytes were collected by centrifugation at 1500 rpm for 15 min, and then washed three times with 35 mL of phosphate buffered saline (PBS) buffer at pH 7.4. The stock solution was prepared by mixing 2 mL of centrifuged erythrocytes into 45 mL of PBS. The PLL/DHBA solutions were prepared in PBS buffer with four different concentrations (1 mg/mL, 100 µg/mL, 10 µg/mL, and 1 µg/mL). One hundred microliter of sample solution was added to 1 mL of the stock solution in a 96-well plate. The solutions were incubated for 1 hr at 37 °C. The percentage of hemolysis was measured by UV-vis analysis of the supernatant at 570 nm absorbance after centrifugation at 3000 rpm for 1 hr. One milliliter of saline was used as the negative control.

4.3 Results and Discussions

The kinetics of metal binding was monitored in a 2 mg/mL FeCl₃ solution. The equilibrium binding was found to be 1303.7 mg/g for the PLL/DHBA iron chelating polymer. The safe dose of DFO for adults and children is 15 mg/kg/h. This does chelates only 1.275 mg/kg/h. This means that the maximum Fe binding of DFO is ~85 mg/g.⁹⁸ The high equilibrium binding of Fe by PLL/DHBA can offer a potential alternative for DFO.

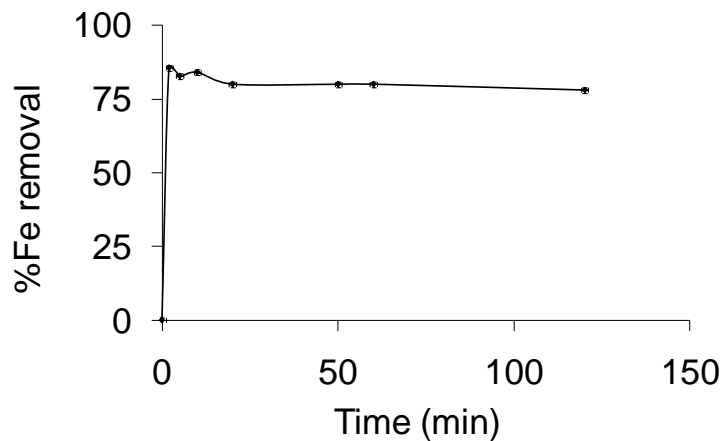


Figure 4-18: Kinetic data (read from dialysate).

More importantly, about 80% of the total absorption was attained in <5 min (Figure 4-18, Table 4-7). The rate and duration of the response of non-transferrin-bound iron to chelation therapy are largely unknown and have important implications for the design of optimal chelation regimens. One problem with DFO is the slow rate at which it removes iron from transferrin, which is probably the most readily available pool of iron in the body.⁹⁹ Such slow kinetics may limit the performance of DFO since it exhibits such a short half-life. This might become an important issue when using DFO as a chelator in patients with acute iron poisoning. The high affinity and rapid binding of iron by PLL/DHBA polymers may offer improvement in iron chelation therapy. This near instantaneous iron absorption behavior may be highly desired for treatment of acute iron overload.

Table 4-7: Percent absorption of Fe by PLL/DHBA polymer. Dialysis was conducted until equilibrium.

Measured from	% absorbed
Retentate	85.85±0.025
Dialysate	76.98±0.076

A multi-solute system was used to evaluate the metal selectivity of PLL/DHBA polymer. At an equal concentration of all metals (2 mg/mL), PLL/DHBA absorbed almost 75% of the iron in the media, the highest of any metal present except for Ni, which may not be a concern since Ni normally has a lower concentration in blood ((0.46±0.26)*10⁻⁶ mg/mL) (Figure 2).¹⁰⁰ PLL/DHBA polymers were highly selective for iron and nickel over other essential elements present in the blood, (i.e. zinc and calcium), as desired.

The application of DFO in iron overload diseases has been limited by its toxic properties. Its inherent hypotensive effect limits the amount of drug that may be administered in acute iron overload, with the intravenous infusion not to exceed 15 mg/kg/hr or a total of 6.0 g in 24 hours.¹⁰¹ The chronic use of DFO results in some difficulties due to its short circulation half-life. Consequently DFO, which is not absorbed orally, must be administered by frequent intramuscular injection, continuous subcutaneous infusion, or more rarely by slow intravenous infusion.

The use of PLL/DHBA may provide benefits by optimizing vascular retention. A relatively large molecular weight PLL will likely prolong plasma retention of PLL/DHBA. This may alter the dosage and frequency required for the treatment of acute and chronic iron overload disorders.

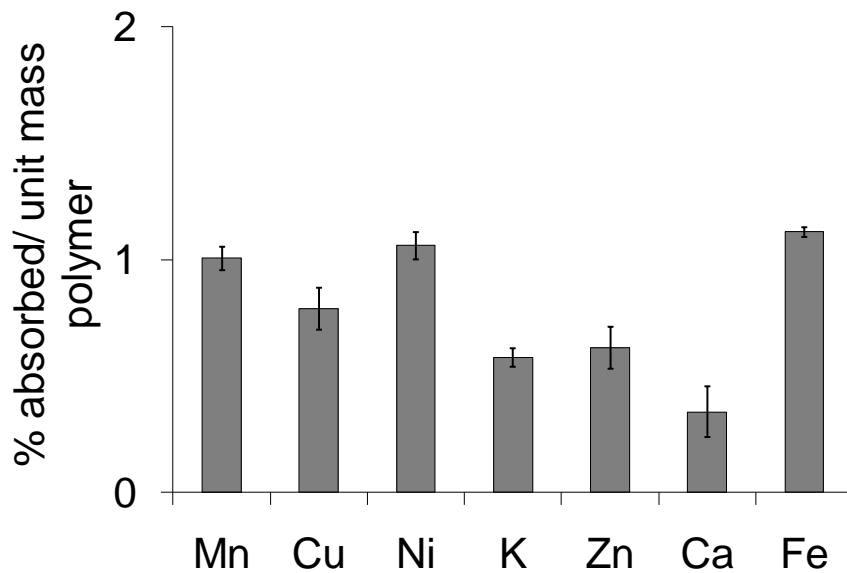


Figure 4-19: Selectivity study (read from dialysate).

A cytotoxicity assay was used to study the effect of PLL/DHBA on HUVEC and A549 cells. DFO, an FDA-approved drug which is currently used for the treatment of iron overload disease, was used as a control. PLL/DHBA showed almost no cytotoxicity on HUVEC cells at low to moderate concentrations while DFO was considerably cytotoxic even at concentrations as low as 10 $\mu\text{g}/\text{mL}$ (Figure 4-20). Both PLL/DHBA and DFO had a negligible effect on A549 cells. Cell viability data exceeding 100% that was observed in this study is likely an indication of an increased cellular metabolic rate in the presence of low concentrations of polycations.

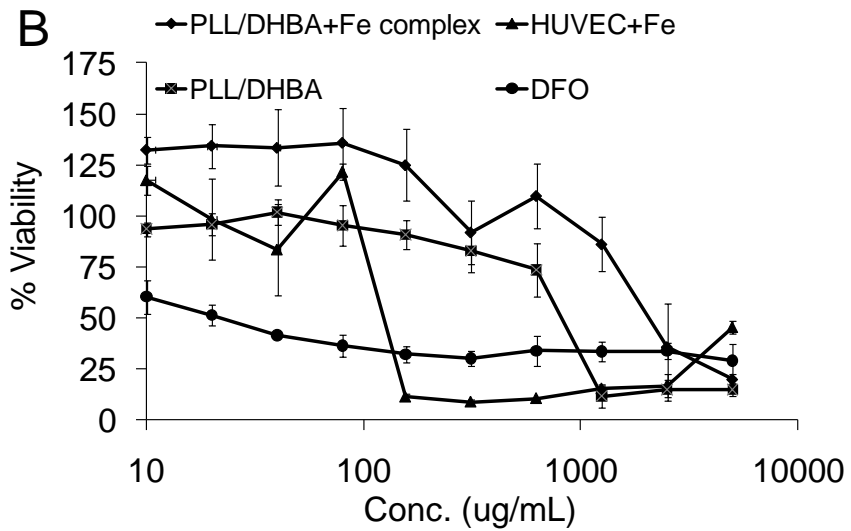
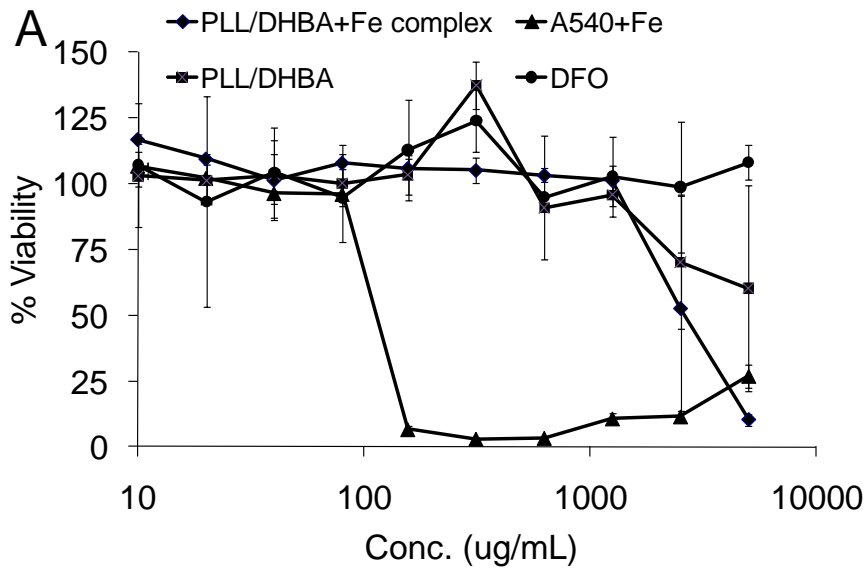


Figure 4-20: Cytotoxicity study conducted on (A) A549 cells and (B) HUVEC cells.

When charged or membrane-permeable polymers are injected into the blood, any detrimental interactions with blood constituents must be avoided. The effect of these polymers on red blood cells was studied at relatively high concentrations.

PLL/DHBA samples did not show any evidence of hemolytic activity over the experimental range (Figure 4-21).

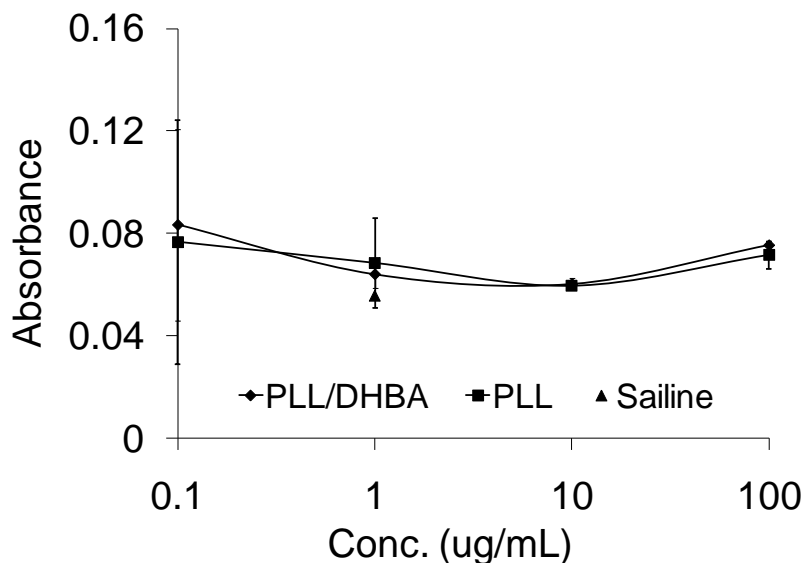


Figure 4-21: Hemolytic activities of PLL and PLL/DHBA.

4.4 Conclusion

A water soluble polymer that mimics the structure of enterobactin was synthesized. DHBA was conjugated to poly-L-lysine and the binding affinity and selectivity of the conjugate polymer was studied. Fe removal by this siderophore-mimetic polymer was nearly instantaneous. Moreover, this bio-inspired polymer exhibited relatively high selectivity toward iron in the presence of other competing metals. PLL/DHBA and its conjugate with Fe also showed relatively low cytotoxicity and was not hemolytic, thus further studies *in vivo* are justified.

Chapter 5

Thiol Modified Hydrogels: Potential Chelators for Toxic Metals

5.1 Introduction

Heavy metals such as cadmium, lead and arsenic are highly toxic to living organisms.¹⁰² Wastewater discharge is a primary source of heavy metal release into the environment.¹⁰³ The removal of heavy metal ions from industrial wastewater has been given much attention in the last decade, because such components can accumulate in living organisms.¹⁰⁴⁻¹⁰⁵ Upon their accumulation in the human body, these toxic metals may cause kidney failure, nerve system and bone damage, and other serious diseases.¹⁰⁶ The necessity to reduce the amount of heavy metal ions from the environment has led to an increasing interest in technologies that selectively remove such toxic metals.

Solvent extraction techniques are frequently employed for removal of selected metal species from aqueous solutions; however, this technology is not always desirable as it requires a large inventory of an organic solvent that is often flammable, toxic or otherwise hazardous.¹⁰⁷ Membrane filtration is another method to remove toxic metals from waste water.¹⁰⁸ Aside from their application in areas such as drug delivery and immobilization of enzymes, hydrogels have received attention in the last decade because of applications in the recovery of metals and metal pre-concentration for environmental analysis.¹⁰⁹ Metal-coordinating resins and selectively absorbent polymers or copolymers have been extensively studied.¹¹⁰⁻¹¹¹

Because of the serious damage toxic metals may cause to the human body and to the environment, desirable polymeric ligands must possess high affinity, capacity, and selectivity towards the toxic metal of interest. Furthermore, such polymeric

ligands may have potential use in biomedicine if the polymers are non-toxic, well tolerated, and exhibit high capacity and selectivity for the toxic metal.

This work reports the synthesis of functionalized hydrogels capable of selectively removing toxic metals (i.e. Pb, Cd, As) from an aqueous solution. Functionalized polyallylamine (PAAm) hydrogels have been introduced previously as potential iron-specific chelating agents. Here, thioglycolic acids (TGA) in combination with the siderophore moiety dihydroxybenzoic acid (DHBA) were introduced onto PAAm and the binding capacity and selectivity of the hydrogels were investigated. Conjugation of the thiol groups dramatically improved the binding affinity and selectivity of the hydrogels for toxic metals. The rapid, high affinity binding of toxic metals by these functionalized hydrogels offers potential applications in waste water treatment and chelation therapy in patients suffering from acute poisoning.

5.2 Materials and Methods

Materials: Poly(allylamine hydrochloride) (PAAm) with an average molecular weight of 56 kDa and analytical grade reagent N,N'-methylenebisacrylamide (MBA) were obtained from Sigma-Aldrich and used without further modification. 2,3-dihydroxybenzoic acid, thioglycolic acid (TGA), N,N,N'-triethylamine (TEA), dimethylformamide (DMF), and all metal chlorides were purchased from Fisher Scientific and used as received. Dicyclohexylcarbodiimide (DCC) and N-hydroxysuccinimide (NHS) were purchased from Thermo Scientific and used without further modification. Deionized water (DI) was obtained from a Barnstead EasyPure water purifier.

Preparation of PAAm Hydrogel PAAm hydrogel was synthesized following the procedure reported in the literature.¹¹² Briefly, a 20% w/v polymer solution containing a predetermined amount of MBA was prepared. The cross-linker was dissolved in deionized water (flushed with nitrogen for 5 min) and then added to the polyallylamine polymer. TEA, the cross-linking catalyst (300 μ L), was then added to the solutions and mixed thoroughly. Next, the precursors were transferred by pipet into small vials. The vials were held at ambient temperature for 1 h and then cooled to ca. 3 °C and held there for an additional 24 h. After this time, hydrogels were removed from the vial and washed with 0.05 M sodium chloride for several days.

Functionalization of Hydrogel: A solution of TGA and NHS in 5 mL of DMF was mixed with a solution of DCC in 5 mL of DMF. The mixture was stirred at low temperature for 6 h to give a white precipitate. The precipitate was filtered, and the filtrate was added directly to a known mass of ground hydrogel. The reaction mixture was held at room temperature for 3 days. PAAm conjugate hydrogel was then washed with water for several days. The same procedure was done for the conjugation of 1:1 molar ratio of TGA/DHBA.

Quantification of Amine Functional Groups: Primary amine groups were quantified by potentiometric titration. After grinding to a powder, 40 mg of functionalized hydrogels were suspended in 35 mL of 0.2 M aqueous KCl solution. Next, 140 μ L of 8 M KOH aqueous solution was added to polymer suspensions to raise the pH to ~12. Standard 0.1 M HCl was used to titrate the suspension. HCl was added until the pH

was about 2.5 in all polymer suspensions. Free amine groups were quantified from potentiometric data following reported procedures.¹¹³

Binding Kinetics Study: Metal chloride solutions (2 mg/mL) were adjusted to pH 2.5 with ionic strength in the range of 0.02 M to 0.04 M and kept at room temperature for kinetic studies. Samples were taken from the media at different time intervals to determine the rate of metal binding by functionalized hydrogel.

Binding Experiments: Known concentrations of metal chloride solutions (0.25, 0.5, 1, 2, 2.5) mg/mL were prepared. Binding experiments were carried out by taking 20 mL of metal solution in 125 mL volumetric flasks. Solutions were adjusted to pH=2.5 while maintaining metal concentration. Ionic strength of all solutions was between 0.02 M to 0.04 M. Next, a known mass of functionalized hydrogel was added to the mixture and was held at room temperature for 2 h or until equilibrium was reached. The solutions were then filtered and the filtrates were analyzed for metal concentration.

Adsorption isotherms: Different isotherm models were employed to determine how the metal molecules distributed between the liquid phase and the hydrogel phase when the adsorption process reached equilibrium. Langmuir, Freundlich, and Temkin isotherm models were applied to the data. Adsorption parameters for each metal ion were calculated at a pH value of 2.5. The constants for each isotherm model were calculated and the accuracy of the isotherm models were evaluated using linear correlation coefficient (R^2) values.

Selectivity Study: The selectivity for Pb, Cd, and As by functionalized PAAm in the presence of competing metals was studied. A metal solution (10 mL, 2 mg/mL) containing all metal components was prepared. The solution mixture was then adjusted to pH 2.5 and held at room temperature for 2 h after adding a known mass of functionalized dry gel. Ionic strength of all solutions was between 0.02 M to 0.04 M.

Metal Analysis: Mono- and multi-elemental analysis of samples was quantified by Inductively Coupled Plasma Optical Emission Spectrometry (ICP-OES) (Optima 2000 DV, PerkinElmer, USA) fitted with an AS 93plus autosampler (PerkinElmer, USA). A Cross-Flow nebulizer and a Scott spray chamber were used. The RF Power was 1300 W and nebulizer and auxiliary flows were 0.8 and 0.2 L/min, respectively. Sample flow was set at 1.5 mL/min. ICP-OES data was processed using Winlab 32 (Ver. 3.0, PerkinElmer, USA). The analytical curves used for sample analysis had coefficients of correlation >0.999.

5.3 Results and Discussion

Synthesis and characterization: Poly(allylamine hydrochloride) was cross-linked following a previously reported method.⁸⁴ Here, an optimized reaction yield was chosen from the previously reported data. 2,3 DHBA and TGA were covalently linked to available amino sites of PAAm hydrogel via DCC/NHC conjugation chemistry. Moreover, potentiometric titration data were used to calculate the degree of conjugation using the following equation (Figure 5-22).¹¹³

$$\bar{n} = \frac{C_{HCl} - (H^+) + (OH^-)}{C_H} \quad (5-1)$$

Here, C_H is the concentration of hydrogel. The conjugation efficiency was 47% and 67% for PAAm/TGA and PAAm/TGA/DHBA hydrogels, respectively.

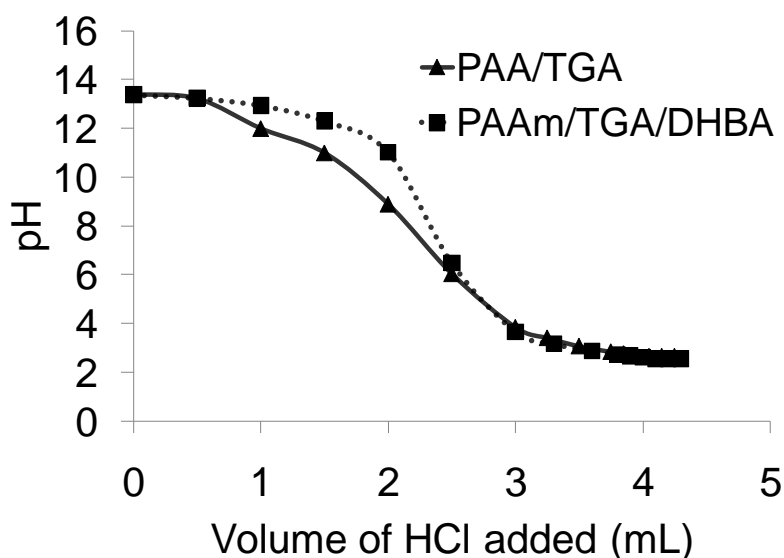
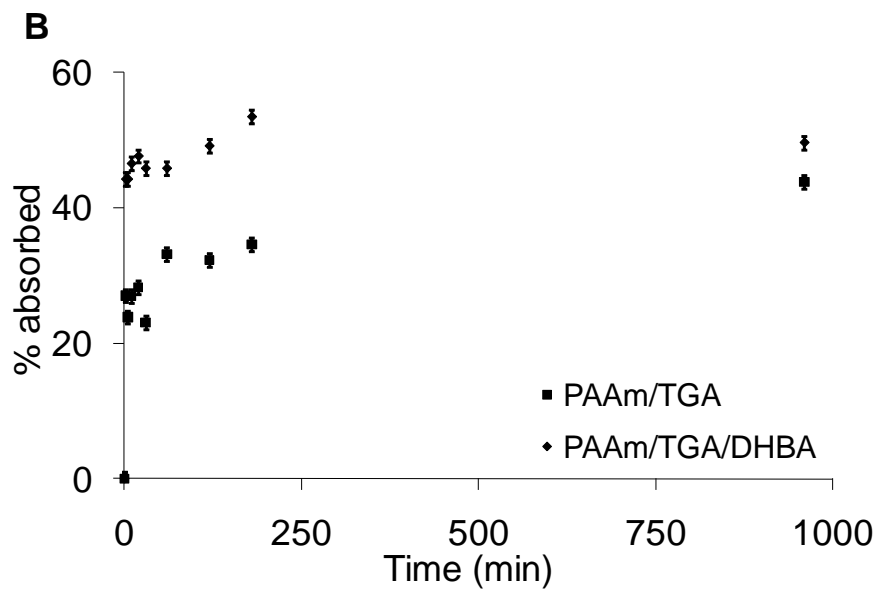
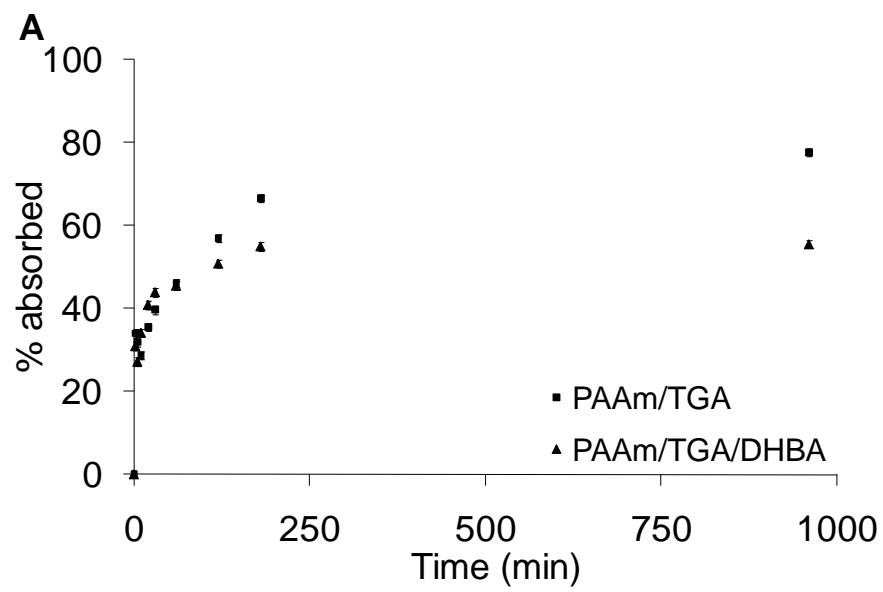


Figure 5-22: Titration data collected for PAAm/TGA and PAAm/TGA/DHBA. pH values represent the values of 3 readings differing by < 5%.

Binding Kinetics: Determination of the kinetics of metal absorption is critical for elucidating the performance of hydrogels and for evaluating the potential for chemical and biomedical applications. The kinetics of metal binding was monitored by adding a known mass of dry hydrogels to a known initial concentration of metal solution (2 mg/mL, metal chloride). The concentration of metal in solution was monitored over time. About 40%-50% of the total metal absorption was attained in less than 5 min for all functionalized hydrogels (Figure 5-23).



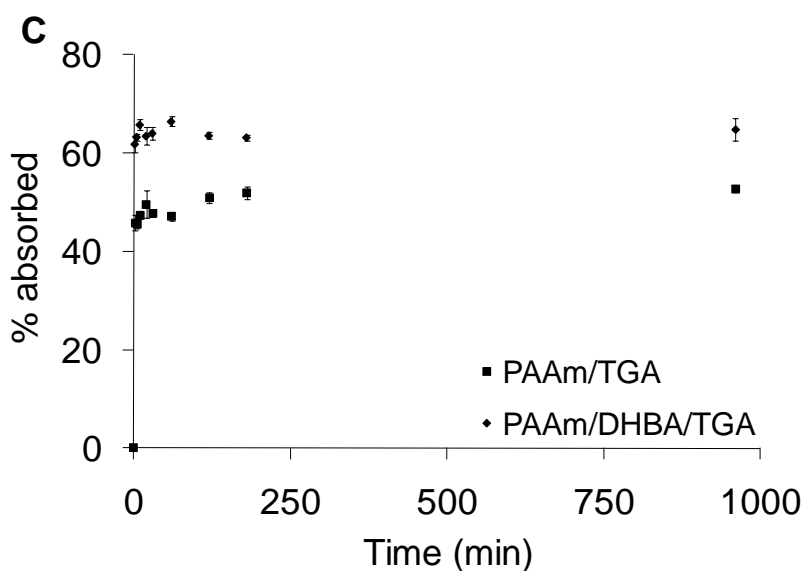


Figure 5-23: Ion binding by functionalized hydrogels, A) Pb, B) Cd, and C) As. Gels were equilibrated in 2 mg/mL metal solution (pH= 2.5). Ionic strength values ranged from 0.02 M to 0.04 M.

The absorption was fastest for As in the presence of the different functionalized hydrogels and slowest for Cd. This might be due to the smaller atomic radius of As compared to Pb and Cd. Previously, Ozay et al. synthesized composite hydrogels with magnetic properties and studied the hydrogels for the removal of toxic metal ions from aqueous environments. In all their case studies, less than 40% of the total metal was absorbed after 2 h. In most studies, the minimum required time to reach ~50% of the total removal was about 15-30 min.¹¹⁴ The rapid absorption behavior of hydrogels reported here may offer an important advantage, especially in biomedical applications such as the treatment of acute metal poisoning.¹¹⁵

The equilibrium binding values were systematically higher for PAAm/TGA hydrogels compared to PAAm/TGA/DHBA (Table 5-8).

Table 5-8: Maximum binding capacity of hydrogels at pH=2.5 when ionic strength varied between 0.02 M and 0.04 M.

Metal ion	PAAm/TGA (mg/g)	PAAm/TGA/DHBA (mg/g)
As	568	520
Pb	345	291
Cd	452	294

This might be because of a high density of thiol groups available for coordinating with toxic metals. Tofan et al. have conducted a systematic study on Cd and Pb absorption kinetics for a metal-binding material produced by introducing sulphhydryl functional groups into natural hemp fibers.¹¹⁶ The absorption capacity of modified hemp was reported to be 14.0 and 23.0 mg/ g of fibers for Cd and Pb ions, respectively at room temperature. In comparison, hydrogels reported here achieved ~ 20 fold and ~ 10 fold higher binding capacity when using PAAm/TGA to bind Cd and when using PAAm/TGA/DHBA gels to bind Pb, respectively.

To derive the rate constant and binding capacity, the kinetic data were modeled with pseudo-first-order (Lagergren model) and pseudo-second-order (Ho model) kinetic models which are expressed in their linear forms as:

$$\ln q_e - \ln q_t = \log q_e - \frac{k_1}{2.303} t \quad (5-2)$$

$$\frac{t}{q_t} = \frac{1}{q_e^2 k_2} - \frac{t}{q_e} \quad (5-3)$$

where k_1 (L/min) and k_2 (g/mg · min) are pseudo-first-order and pseudo-second-order rate constants, respectively. The model variables obtained by linear regression were compared (Table 6-112). The pseudo-second order reaction model showed the best fit since it had a R^2 value close to unity in each of these cases.

Binding Isotherms: The metal ion binding capacity was determined and different isotherm models were used to fit the data. A low pH was selected for these studies because of the potential application of these hydrogels in acute metal poisoning (stomach pH ~2.5). The metal ion uptake was relatively high. This could be due to the presence of protonated primary amine groups along with thiol functional groups which together provided excellent coordination sites for metal binding.

Table 5-9: Kinetic parameters for metal binding by functionalized hydrogels at pH=2.5. Ionic strength values ranged from 0.02 M to 0.04 M.

Chelating hydrogel	Ho model		Lagregern model	
	PAAm/TGA	PAAm/TGA/DHBA	PAAm/TGA	PAAm/TGA/DHBA
Metal ion				
R ²	0.999	1	0.864	0.0466
K	14.7	13.4	0.0100	N/A
As				
R ²	0.997	0.999	0.986	0.939
K	16.0	5.46	0.0100	0.0203
Pb				
R ²	0.996	0.999	0.00360	0.521
K	0.00380	1.079	N/A	N/A
Cd				

Several theoretical isotherm equations, including those of Freundlich, Langmuir, and Temkin, were employed to evaluate which could best describe the experimental data. None of the three adsorption models provided an accurate fit for data reported in this study as low correlation coefficient values were observed (Table 5-10). In most cases, a reciprocal plot of the data gave a straight line fit for Langmuir isotherms but negative intercept values suggested that simple Langmuir adsorption did not occur. The Freundlich model assumes that there are many types of sites acting simultaneously, each with a different free energy of absorption, and that there is a large number of available sites. The negative cooperativity factor (n) below unity in this study is an indicator of heterogeneous absorption due to the negative lateral

interaction between absorbed metal and/or non-uniform binding affinities of hydrogel sites.¹¹⁷⁻¹¹⁸

Table 5-10: Isotherm parameters for metal binding by functionalized hydrogels at pH=2.5. Ionic strength values ranged from 0.02 M to 0.04 M.

Hydrogel	TGA	DHBA/TGA	TGA	DHBA-TGA	TGA	DHBA/TGA
Isotherm model	Pb		Cd		As	
Freundlich						
K _F	NA	1.027	NA	NA	1.060*10 ⁷	16.7*10 ²
n	NA	-2.16	NA	NA	2.40	-0.516
R ²	0.141	0.778	0.455	0.228	0.875	0.926
sen	NA	0.122	NA	NA	0.0784	0.273
sey	NA	0.142	NA	NA	0.216	0.476
Langmuir						
q _{max}	NA	0.890*10 ²	NA	81.7	664.5	-4.51
K _L	NA	-5.10	NA	-2.79	32.2	62.9
R ²	0.0215	0.644	0.321	0.793	0.952	0.863
sen	NA	8.16*10 ⁻⁴	NA	0.00111	5.20*10 ⁻⁶	6.98*10 ⁻⁴
sey	NA	0.00301	NA	0.00215	4.057*10 ⁻⁴	0.00204
Temkin						
A	NA	0.0814	NA	NA	25.3*10 ¹	NA
b	NA	-33.5	NA	NA	16.1	NA
R ²	0.101	0.611	0.176	0.356	0.695	0.365
sen	NA	29.4	NA	NA	50.6	NA
sey	NA	78.7	NA	NA	13.9*10 ¹	NA

The Temkin isotherm assumes that a decrease in the heat of adsorption is linear and that the absorption is characterized by a uniform distribution of binding energies. This model did not fit data either, suggesting that multiple, complex binding mechanisms may be involved in metal absorption.

Selectivity Studies: An important feature of metal chelating hydrogels is the ability to specifically target the metal of interest and remove it from the media. The metal selectivity of PAAm/TGA and PAAm/TGA/DHBA hydrogels was investigated using a multi-solute system. At an equal concentration of all toxic metals (i.e. Pb, Cd, As at 2 mg/mL), PAAm/TGA absorbed almost 100% of the lead present in the media while in the same experiment and in the presence of other competing metals such as Fe and Zn this value decreased to ~70% (Figure 5-24). The tendency of PAAm/TGA hydrogel for absorption of metals followed the order of Pb > As > Cd > Zn > Fe. This trend was similar for PAAm/TGA/DHBA. Previously a high Pb removal capacity using magnetic hydrogels (130 mg/g) has been reported.¹¹⁵ The Pb removal capacity with PAAm/TGA and PAAm/TGA/DHBA was 345.6 and 291.7 mg/g, respectively. All data suggested that these hydrogels may have excellent potential in waste water treatment and probable application in acute metal poisoning.

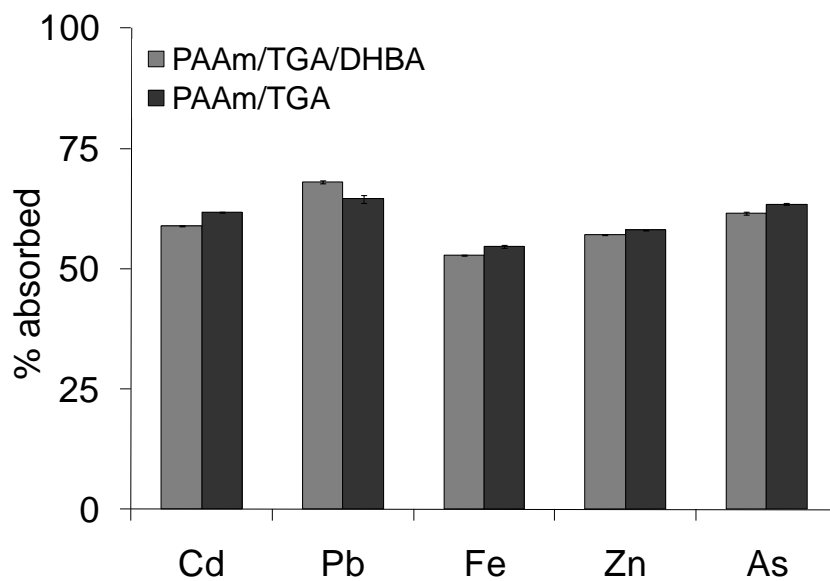
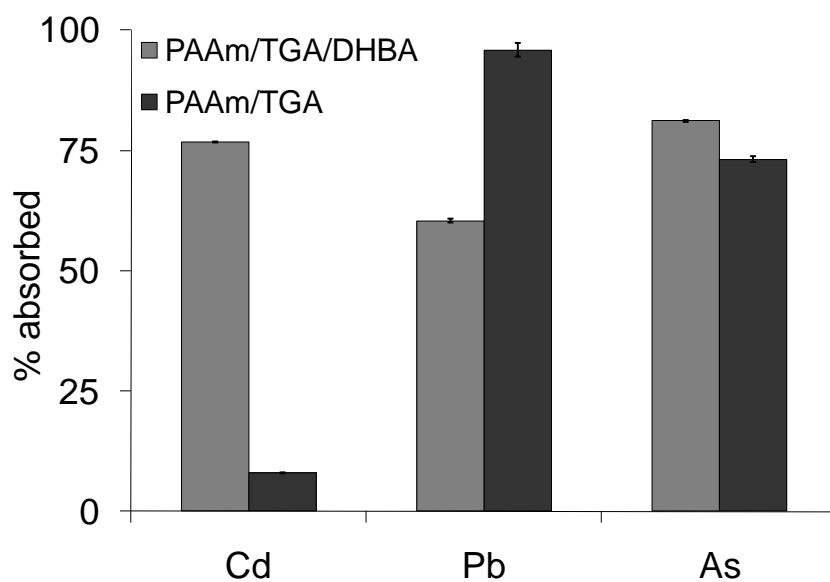


Figure 5-24: Selectivity study of functionalized hydrogels toward toxic metal ions A) in the presence of competing toxic metals and B) in the presence of competing essential metals (pH=2.5).

5.4 Conclusions

Cross-linked polymers with different functional groups were designed for removal of toxic metals. Dihydroxybenzoic acid and thioglycolic acid were used as conjugated moieties to improve the affinity and selectivity of PAAm toward toxic metals. These hydrogels were able to remove and accumulate Pb, Cd and As ions from aqueous solutions at relatively low metal concentrations. PAAm/TGA and PAAm/TGA/DHBA hydrogels demonstrated an almost instant metal absorbance when equilibrated in the metal solution. The pseudo-second order Ho kinetic model offered an excellent fit to absorption data. The inclusion of thiol groups to hydrogels seemed to improve selectivity toward Pb and As. The rapid binding and selectivity of these functionalized hydrogels for toxic metals provides important features for waste water treatment and may enable applications in acute metal poisoning.

Chapter 6

Magnetic Polyvinylamine Nanoparticles by *In Situ* Manganese Substitution

6.1 Introduction

Magnetic nanoparticles with high magnetization saturation have received attention because of exciting new applications in biomedicine as well as more traditional applications such as magnetic data storage.¹¹⁹ Spinel ferrites have been intensively studied in recent years because they show high magnetic permeability and low magnetic losses.¹²⁰⁻¹²¹ There are a variety of transition metal cations that can be incorporated into the lattice of the magnetite structure such as Mn, Co, Ni, Mg, and Zn. Manganese ferrite (MnFe_2O_4), has emerged as an important superparamagnetic material that has been widely studied in magnetothermal therapy, in contrast-enhanced magnetic resonance imaging (MRI) and in sustainable energy research.¹²² A recurrent problem with these metal ferrite nanoparticles, however, is the hydrophobic surface which often leads to agglomeration if stored as a colloid or if introduced *in vivo*.¹²³ Agglomeration is suspected to increase the probability for clearance by macrophages and the risk of unwanted occlusions.¹²⁴⁻¹²⁵ Furthermore, agglomeration of manganese ferrite nanoparticles reduces the superparamagnetic properties.¹²⁶ Other problems commonly occurring during the synthesis of manganese ferrite include the wide particle size distributions and a lack of well-defined crystal structure.¹²⁷

To overcome these difficulties a practical route to monodisperse, stable MnFe_2O_4 nanoparticles is needed. Also, reactive sites for the conjugation of complex biological molecules such as pharmaceuticals or targeting moieties are desirable.¹²⁸⁻¹²⁹ A commonly used procedure for making MnFe_2O_4 particles has been the co-

precipitation of Mn^{2+} and Fe^{3+} ions under basic conditions, usually NaOH in an aqueous solution or in an inverse micelle template.¹³⁰⁻¹³¹ Researchers have been studying different techniques such as engineering the surface of manganese ferrite nanoparticles or applying a size selection process at the end of the synthesis procedure to overcome the mentioned difficulties.¹²³ However, these methods are often ineffective, labor intensive, and can exhibit low yields.

Recently, we reported a convenient procedure for making monodisperse magnetic polyvinylamine nanoparticles through the *in situ* reaction of FeCl_3 and FeCl_2 within cross-linked polyvinylamine nanoreactors.¹³² Results indicated that magnetic PVAm nanoparticles with a size around 100 nm had a saturation magnetization of ~30 emu/g of iron oxide, and narrow size distribution. PVAm nanoparticles had a size ~200 nm. Here, the synthesis and characterization of MnFe_2O_4 incorporated in PVAm nanoparticles is reported as an approach to increase the magnetization of magnetic PVAm. Amine groups within polyvinylamine nanoparticles were utilized to bind manganese and iron ions. Metal ion concentration was adjusted to obtain the stoichiometric ratio within nanoparticles required for the co-precipitation reaction. The final magnetic nanoparticles were ~ 50 nm in diameter, offered colloidal stability, and exhibited a narrow size distribution (polydispersity~ 0.134). Moreover, the magnetization saturation increased by 60% when compared to magnetite containing PVAm nanoparticles.

6.2 Materials and Methods

Materials: N-vinylformamide (NVF; Aldrich) was used as a monomer without further modification, and 2, 2'-Azobis (2,4-dimethylpentanitrile) (Vazo-52, purchased from DuPont) used as an initiator for the polymerization reaction of N-vinylformamide. Deionized water (DI) was obtained from a Barnstead EasyPure water purifier. Ferric chloride, manganese chloride, hexane, Span 80, Tween 80, and sodium hydroxide (purchased from Fisher Scientific) were all used as received. 2-(N-Vinylformamido) ethyl ether (NVEE), a derivative of NVF, was synthesized in our lab and used as a cross-linker.

Synthesis of polyvinylamine Nanoparticles: Cross-linked PVAm nanoparticles were produced following the same procedure reported previously.¹³² Briefly, cross-linked PNVF nanoparticles were fabricated by inverse microemulsion polymerization of monomer (NVF) with cross-linker (NVEE). Subsequently, the PNVF nanoparticles were hydrolyzed using 0.1 M NaOH solution for 2 hrs to produce PVAm nanoparticles.

Fabrication of magnetic polyvinylamine Nanoparticles: To synthesize MnFe₂O₄, the following reaction should be performed in an aqueous solution using a molar ratio of Mn^{II} : Fe^{III} ~ 0.5.¹³³



In a representative experiment, MnCl₂ (3.95 g, 0.02 mol) and FeCl₃ (5.2 g, 0.019 mol) were dissolved in 25 mL of deoxygenated PVAm nanoparticle suspension (5 mg/mL). This mass ratio was determined experimentally to yield roughly a 0.5 ratio of MnCl₂ : FeCl₃ within nanoparticles.¹³⁴ The solution was stirred for 2 h at room temperature. Next, the solution of PVAm nanoparticles containing MnCl₂ and FeCl₃ was transferred to a centrifuge tube and centrifuged for 30 minutes at 15,000 rpm. The pellet was re-dispersed in deoxygenized water. The re-suspended pellet was added drop-wise into 50 mL of 1.5 M NaOH solution with rate of 10 mL/min under vigorous stirring. The last step generated a black/brown suspension of magnetic PVAm nanoparticles almost instantly. Langmuir (1) and Freundlich (2) binding kinetics were observed while saturating PVAm nanoparticles with required concentrations of metal ions,

$$\Gamma = \frac{\Gamma_{\max} KC}{1 + KC} \quad (1-6)$$

$$\frac{x}{m} = KC^{\frac{1}{n}} \quad (2-6)$$

where K and 1/n are constants for a given absorbate and absorbent at a particular temperature, Γ is amount absorbed, C is an equilibrium aqueous concentration, x is mass of absorbate and m is mass of absorbent.

After the co-precipitation reaction was carried out, the suspension was put into a sealed, temperature-controlled reaction vessel for aging. It has been reported that the

pH value, aging temperature and aging time affect the MnFe_2O_4 particle size and morphology.¹³⁵⁻¹³⁶ The suspension was then aged at 90 °C for 45 or 90 min. The particles were isolated using a magnetic field and the supernatant was removed. Deoxygenated water was then added to re-disperse the magnetically collected particles and the solution was centrifuged at 15,000 rpm for 30 min. 20 mL of 0.1 M HCl solution was added to the precipitate under stirring to re-disperse the magnetic pellet in centrifuge tubes. The resulting opaque/brown suspension was then washed with PBS (pH~ 9) and then with PBS (pH 7.4) using similar centrifugation and re-dispersion cycles.

Transmission electron microscopy studies: The size and morphology of magnetic nanoparticles were observed by transmission electron microscopy (JEOL 1200 EXII) at 200 kV. In addition, energy dispersive X-ray spectroscopy (EDX) was used to confirm the manganese and iron presence inside PVAm nanoparticles. The powder was re-suspended in water and drop-cast onto a 300 mesh carbon-coated copper grid that was air dried before imaging.

Iron and Mn content measurement within PVAm Nanoparticles: Parameters of Langmuir and Freundlich equation were determined by calculating the concentration of Mn and Fe absorbed by PVAm particles at various initial concentrations. These concentrations along with the final concentration of MnFe_2O_4 in magnetic PVAm nanoparticles were measured by atomic absorption spectroscopy (AA) using a Perkin Elmer Analyst 300 with a AS90 plus auto sampler. The suspension of magnetic

PVAm was diluted with HNO₃ (0.1% v/v). A regular sensitivity nebulizer without an impact bead was installed as well as a 10 cm single slot burner head. The analysis was conducted using a Perkin Elmer Fe/Mn multi tasker bulb.

Magnetic measurements: The magnetization of PVAm containing manganese ferrite with different Mn:Fe initial ratio were studied at room temperature (magnetic field between -20 and 20 kOe) using a Quantum Design MPMS 5 superconducting quantum interface device (SQUID) magnetometer. Mass magnetization is defined as the magnetic moment per total mass of the sample.

6.3 Results and Discussions

Synthesis of Magnetic PVAm: PVAm is a water-soluble polymer which has stable primary amine functionality along its backbone and may be partially or fully hydrolyzed to impart a low or high density polycation, respectively. This polymer has been employed in industrial applications such as water treatment, adhesives, industrial coatings, ion exchange resins, etc. The high reactivity of amino groups provides important active sites for cross-linking and ion exchanging.¹³⁷ To synthesize magnetic PVAm nanoparticles containing MnFe₂O₄, a co-precipitation reaction was performed within PVAm nanoparticles. As reported previously, this approach utilizes the chelating property of primary amine groups presented in PVAm nanoparticles to bind iron and manganese ions.¹³² The co-precipitation reaction is then carried out to form metal oxides which are retained inside crosslinked PVAm nanoparticles.

The binding affinity of PVAm nanoparticles was determined as a means to calculate concentrations required to maintain the stoichiometric ratio for the co-precipitation reaction. Traditional Langmuir and Freundlich models were used to fit the metal ion concentration data obtained from atomic absorption spectroscopy. Fitting parameters were calculated and applied to isothermal Freundlich and Langmuir models (Figure 6-25 and Table 6-11).

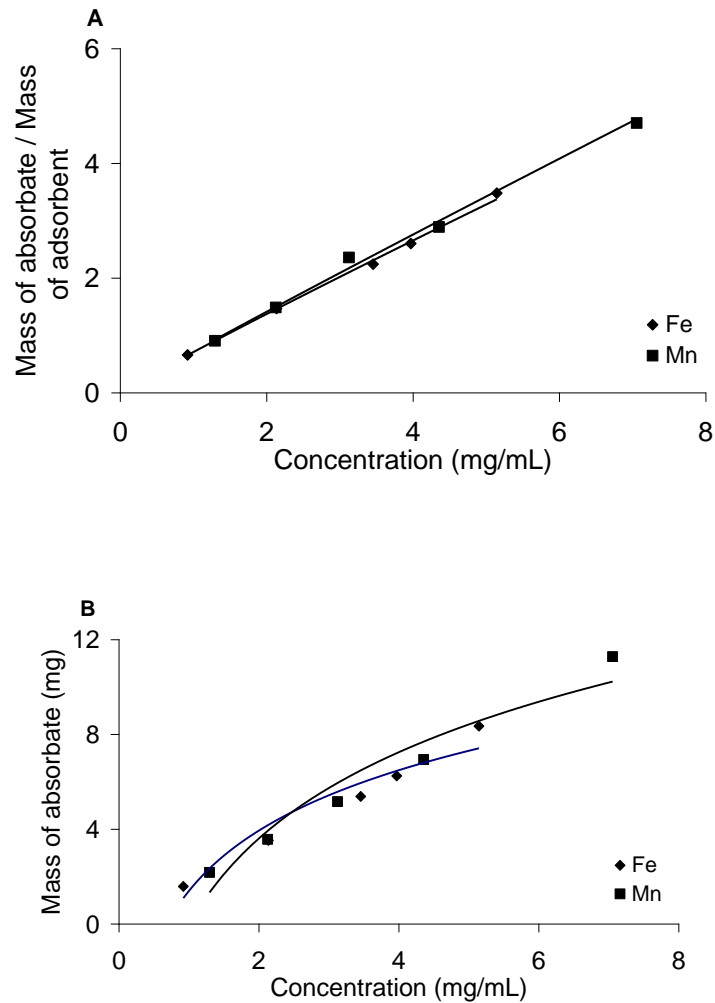


Figure 6-25: Freundlich (A) and Langmuir (B) isotherm plots for Fe and Mn adsorption by PVAm.

Table 6-11: Fitted affinity parameters using Langmuir and Freundlich models.

Model	Parameter	Correlation <i>R</i>
Freundlich	Fe: $K_D = 0.71 \text{ mg}^{-1.05} \text{ mL}^{1.05}$; $n = 1.05$	0.9988
	Mn: $K_D = 0.72 \text{ mg}^{-1.03} \text{ mL}^{1.03}$; $n = 1.03$	0.9945
Langmuir	Fe: $K_D = 0.02 \text{ mg}^{-1} \text{ mL}$; $C_m = 59.88 \text{ mg mL}^{-1}$	0.9995
	Mn: $K_D = 0.01 \text{ mg}^{-1} \text{ mL}$; $C_m = 149.25 \text{ mg mL}^{-1}$	0.9998

The traditional Freundlich model allows for the description of a broad range of affinity interactions. Here, a deviation of the theoretical curve from the experimental data was found. In contrast, the classical Langmuir isotherm model produced a theoretical curve, which was in better agreement with the experimental data. Data from binding studies showed that the binding constant of the PVAm/Fe complex was almost twice that of the PVAm/Mn complex. Values were used to predict the initial concentration of each metal ion required for maintaining the 1:2 molar ratio of Mn: Fe inside nanoparticles. Based on absorption isotherms, a 1:1 molar ratio of metal salts are required in PVAm nanoparticle suspension to obtain the 1:2 ratio of Mn: Fe inside PVAm nanoparticles.

In the next step, a co-precipitation reaction was carried out inside PVAm nanoparticles loaded with metal ions to yield manganese ferrite nanoparticles. The loading efficiency of iron oxide generated within PVAm nanoparticles was previously

found to be 12% (w/w). Here, the loading efficiency of manganese ferrite was >18%; an increase in loading of more than 66%. Studies have shown that the solubility of iron oxide increases as the pH decreases; therefore, the presence of HCl in the nanoparticle purification process may be a reason for the low loading of iron oxide previously.¹³⁸ The improvement in the loading yield of manganese oxide in comparison to iron oxide may be explained by the fact that low pH might not be as effective in dissolving manganese ferrite particles, thus, improving retention of the metal oxide.

Several methods have been reported for the synthesis of a stable manganese ferrite colloid. Keng et al. have reported a high temperature organometallic synthesis procedure of MnFe_2O_4 .¹³⁹ This method was based on thermal decomposition of $\text{Fe}(\text{CO})_5$ and $\text{Mn}_2(\text{CO})_{10}$ in the presence of oleic acid. FeMn alloy nanoparticles were formed followed by oxidation with trimethylamine-N-oxide. The reaction resulted in highly crystalline and nearly monodisperse nanoparticles (less than 10% standard deviation), but very high temperatures were required to perform the reaction. Sun et al. have used a hot injection method to synthesize MnFe_2O_4 nanoparticles.¹⁴⁰ They reported a high-temperature reaction of iron (III) acetylacetonate and manganese (II) acetylacetonate with 1,2-hexadecanediol in the presence of oleic acid and oleyl amine. This high temperature procedure yielded polydisperse nanoparticles and required size selection to achieve the desired particle size. Compared to the reported methods for preparing stabilized colloidal suspensions of manganese ferrite nanoparticles, the synthetic procedure reported here was simple since colloidal

stabilization persisted during the manganese ferrite synthesis and the final product did not require any further size-selection process

Characterization of the particles: The morphology of PVAm/MnFe₂O₄ particles was studied by transmission electron microscopy (TEM). TEM images of PVAm/MnFe₂O₄ nanoparticles at different time intervals were obtained after aging at 90 °C. Image analysis software determined that dry PVAm/MnFe₂O₄ nanoparticles were roughly 50 nm in diameter (Figure 6-26).

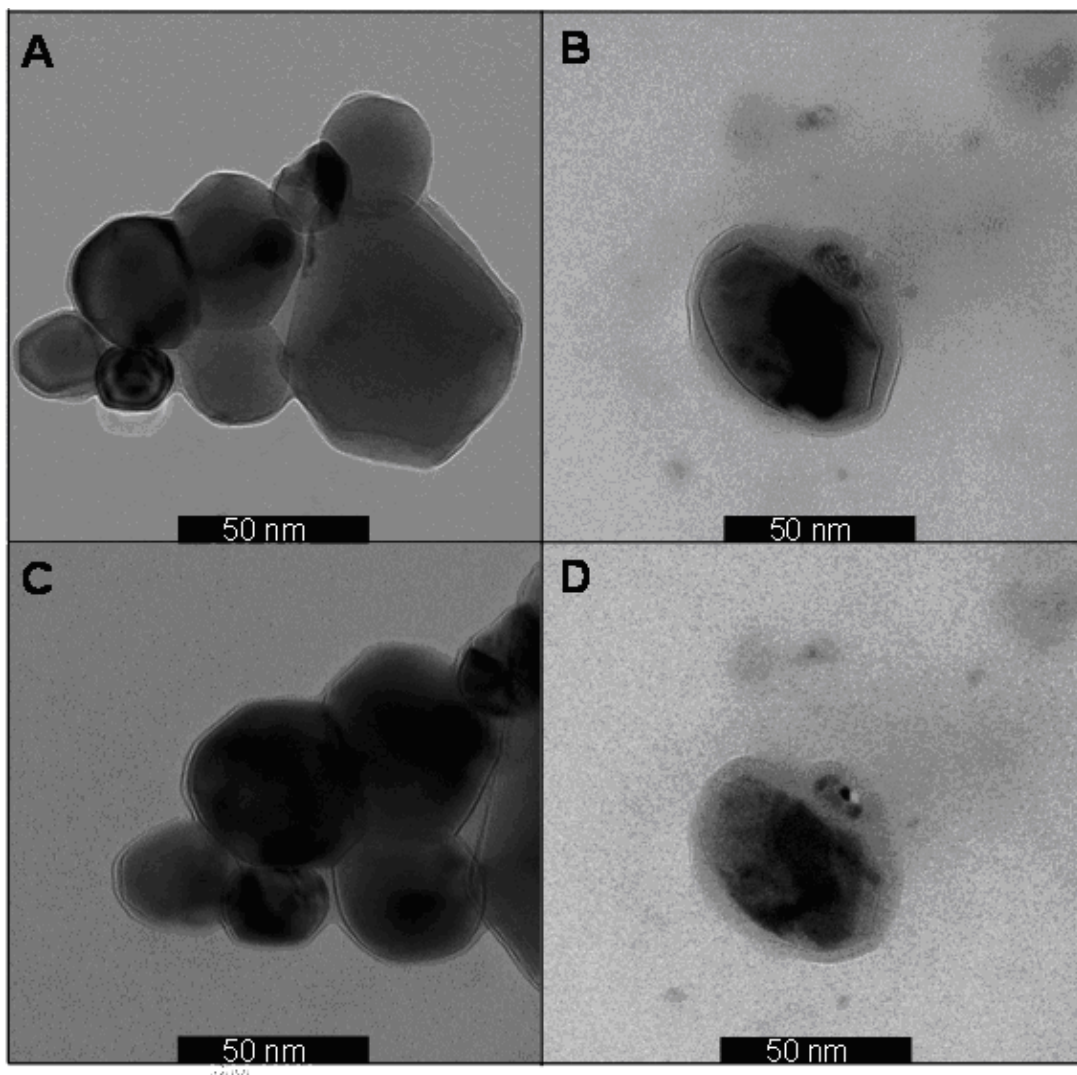


Figure 6-26: TEM images of PVAm/MnFe₂O₄ aged 45 min (A,B) and 90 min (C,D).

Magnetic nanoparticles exhibited a reduction in particle size as a result of the reaction while compared to PVAm nanoparticles. Since many of the primary amine groups presented in PVAm nanoparticles were occupied by iron and manganese ions, the overall particle charge decreased resulting in a corresponding decrease in particle size as well. Dynamic light scattering studies confirmed that PVAm and magnetic

PVAm nanoparticles had low polydispersity, 0.134 and 0.159 respectively. Dark spots were also evident inside PVAm nanoparticles which were fabricated using different aging times (Figure 6-26). Diffuse dark areas were formed after 45 min of aging and punctuate dark spots resulted after 90 min. Dark spots inside the PVAm nanoparticles suggested the presence of small manganese ferrite nanoparticles (<7 nm).

Published reports have shown that non-aged MnFe_2O_4 particles may be amorphous, independent of reaction conditions.¹⁴¹ After aging, particles transition to a cubic crystal structure. Depending on aging time, the size and shape of manganese ferrite nanoparticles might vary. Researchers have reported similar observations for other types of magnetic nanoparticles.¹⁴² X-ray diffraction spectra of the PVAm/ MnFe_2O_4 nanoparticles after 45 minutes of aging revealed several peaks, all of which corresponded to MnFe_2O_4 (Figure 6-27). Conversely, studies have shown that the spectrum for non-aged particles has two broad peaks, with complete crystallization usually not observed until the temperature exceeded 400 °C.¹⁴³⁻¹⁴⁴ The relatively low intensity of the peaks can be explained by the low mass fraction of manganese ferrite present in PVAm nanoparticles (<20%). Energy dispersive X-ray spectroscopy (EDX) also provided direct evidence of the presence of both Mn and Fe within PVAm nanoparticles (Figure 6-27).

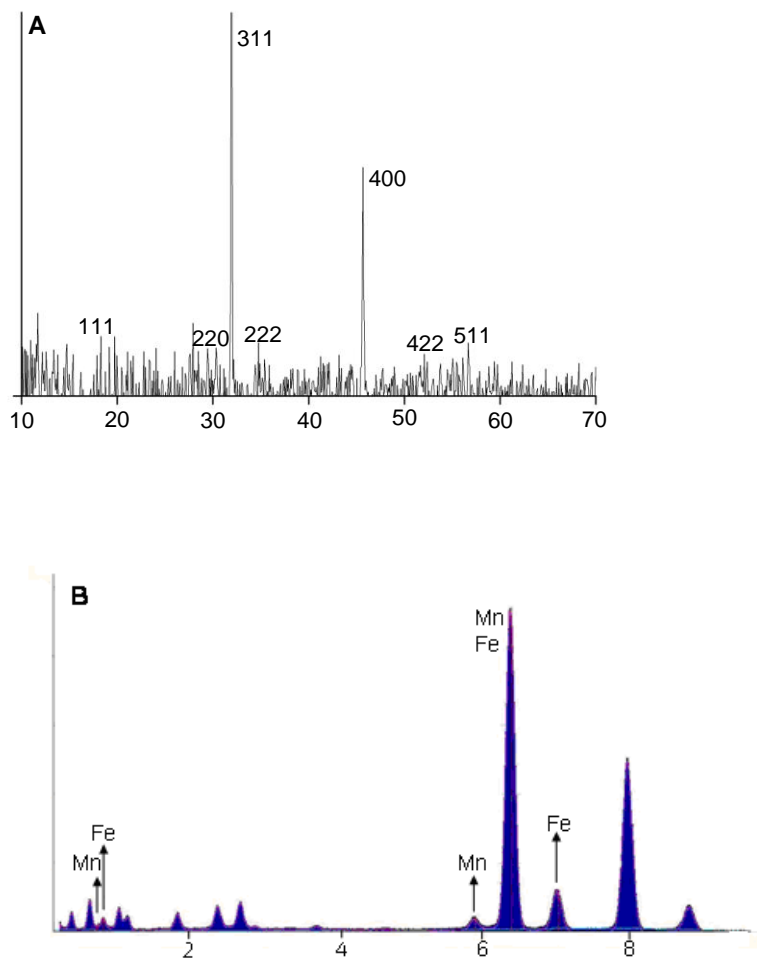


Figure 6-27: XRD spectra of PVAm/MnFe₂O₄ nanoparticles (3A) and EDX spectra of PVAm/MnFe₂O₄ nanoparticles (3B) aged at 90 °C for 45 min.

Magnetization Study: Relative magnetization curves were determined as a function of magnetic field strength for PVAm/MnFe₂O₄ nanoparticles (Figure 6-28). The magnetic PVAm nanoparticles exhibited a high magnetic moment when placed under

a high strength magnetic field. The magnetization curve exhibited zero magnetization upon the removal of magnetic field, which is a characteristic behavior of superparamagnetic particles. The saturation magnetization of PVAm/MnFe₂O₄ particles with a 1:2 Mn:Fe ratio was ~40 emu/g of MnFe₂O₄.

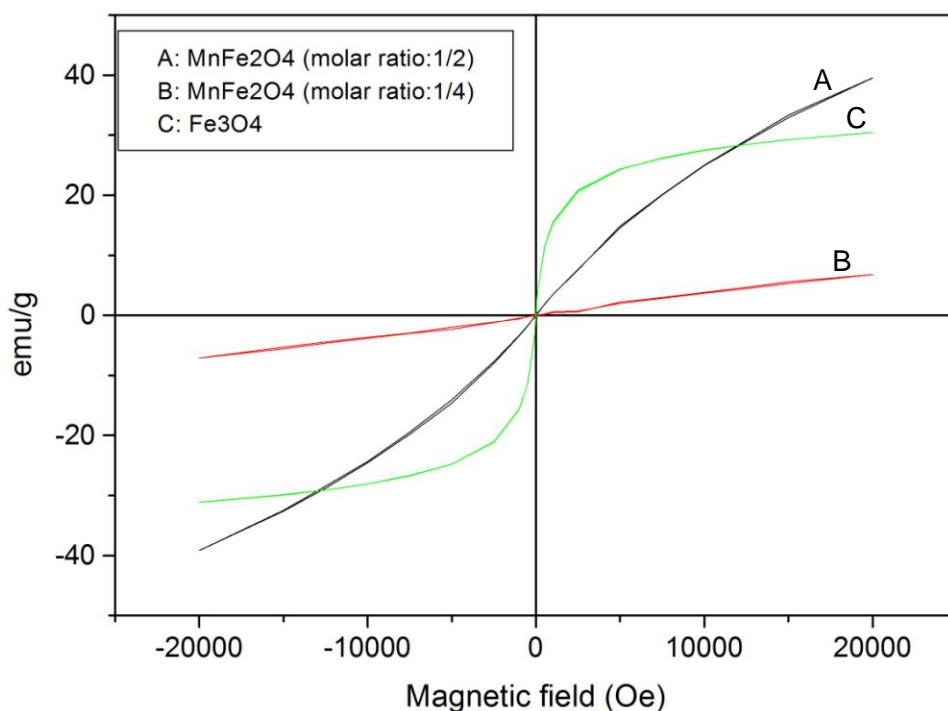


Figure 6-28: Magnetization vs. applied magnetic field for PVAm/MnFe₂O₄ with (A) 1:2 and (B) 1:4 stoichiometric ratios compared to (C) PVAm/Fe₃O₄.

This value was smaller than the reported bulk saturation magnetization value of manganese ferrite (~ 80 emu/g of manganese ferrite) but was still significantly higher than the saturation magnetization observed for PVAm/Fe₃O₄ (~30 emu/g of iron oxide) nanoparticles.^{127, 132} Studies have shown that magnetic nanoparticles with

saturation magnetization as low as 20 emu/g of iron oxide, offer potential use as MRI contrast agents.¹⁴⁵

6.4 Conclusions

In situ synthesis of manganese ferrite within polyvinylamine nanoparticles offers an alternative to ligand grafting, surfactants, or encapsulation of manganese ferrite nanoparticles to aid transfer to water.¹⁴⁶ The chelating property of primary amines in PVAm nanoparticles was utilized to hold iron and manganese ions inside the polymeric network. An *in situ* co-precipitation of stoichiometric ratios of ferric and manganese ions was then carried out followed by aging the manganese ferrite inside PVAm particles. This method yielded crystalline manganese ferrite within monodisperse nanoparticles while maintaining colloidal stability. The method reported was simple, efficient and did not require further size selection. Moreover, PVAm/MnFe₂O₄ nanoparticles possess reactive primary amines that may be modified to enable targeted delivery of this contrast enhancing agent.

Chapter 7

Conclusion and Future work

Metal chelating polymers have many applications in medicine and in industry. Physical and chemical design properties such as side chain functionality and molecular weight make polymers promising materials for use as therapeutic agents, drug delivery systems, and industrial devices.¹⁹ Metal chelating polymers have been used in tissue engineering, and as components of medical devices. Another ongoing application of chelating polymers is drug delivery of active pharmaceutical ingredients such as proteins, antibodies, plasmid DNA and siRNA. Nonetheless, there have been few reports on the application of metal chelating polymers as a drug.

The aim of this work has been to design and fabricate biologically inspired polymers to selectively bind iron or toxic metals. Iron-binding polymers can be specifically used as chelating agents in patients with iron overload diseases. The enterobactin, a potent, naturally occurring Fe (III) chelator, was used as a design model for synthesis of a siderophore-mimetic polymer. 2,3 dihydroxybenzoic acid was immobilized on polyallylamine hydrogel to mimic the structure of this naturally occurring chelator. The metal binding affinity, kinetics and selectivity of hydrogels were studied. Result suggested that the conjugate hydrogels were able to remove and accumulate ferric and ferrous ions from aqueous solutions at relatively low metal concentrations. Moreover, 2,3 DHBA conjugate hydrogel demonstrated an almost instant iron absorbance when equilibrated in ferric solution. These siderophore-mimetic hydrogels also exhibited a high affinity and selectivity for iron at different pH values.

Several ratios of PAAm:DHBA were investigated to optimize the stability constant, selectivity and binding capacity of siderophore-mimetic hydrogels. The hydrogel with ~15% DHBA exhibited the highest stability constant while maintaining selectivity and a high binding capacity for Fe (III). The high affinity and selectivity of PAAm-DHBA hydrogel for iron provides important features for this hydrogel in the treatment of iron overload disease such as hemochromatosis. Other conjugation moieties, such as TGA, were used to enhance the selectivity of PAAm toward toxic metal, i.e. Pb, Cd, and As. Conjugate polymers bearing thiol functional groups showed high affinity and selectivity for toxic metals.

Metal binding polymers were also explored as blood borne iron chelators. 2,3 DHBA was conjugated to poly-L-lysine and the binding affinity and selectivity of the conjugate polymer was studied. The Fe removal by this siderophore-mimetic polymer was almost instant. PLL/DHBA and its conjugate with Fe also showed relatively low cytotoxicity. Moreover, PLL/DHBA did not significantly rupture or perturb RBCs.

Metal binding polymeric nanoparticles were also used as a platform for MR imaging. *In situ* synthesis of manganese ferrite within polyvinylamine nanoparticles offered an alternative to ligand grafting, surfactants, or encapsulation of manganese ferrite nanoparticles. Iron and manganese were held within polymeric nanoparticles using the chelating property of primary amines of PVAm. Monodisperse PVAm nanoparticles were successfully used to template crystalline manganese ferrite. PVAm/MnFe₂O₄ nanoparticles possessed colloidal stability and offered reactive

primary amines that may be modified to enable targeted delivery of this contrast enhancing agent.

Future work with these siderophore-mimetic polymers should further examine the potential use of these polymers as therapeutic agents. This would include investigating the binding affinity, selectivity and kinetic of these polymers at several initial metal concentration and at appropriate conditions to mimic the physiological compartment. Evaluating the effect of DHBA molecules between 15%-80% graft density might help to further optimize Fe chelation. Moreover, animal studies are of interest to further investigate the performance of these polymers.

For animal studies, the initial iron concentration in blood should be measured before starting the experiment. Models should be provided with a diet containing high levels of iron. Experimental groups should then be fed ground hydrogel for 4 days to allow clearance of untreated intestinal contents. Urine and blood samples should be collected from each animal for a period of either 48 h during days 3 and 4 or 24 h during day 4 only. Whole iron levels in the blood and urine should be measured ICP-MS.

For the injectable polymer chelator (PLL-DHBA), estimating the stability constant of soluble polymer with Fe would provide important information regarding its potential use as an alternative to DFO. The flexible structure of PLL-DHBA is a likely reason for the fast complexation kinetics of this polymer toward iron. Overall, multivalent, flexible molecules may be more effective in coordinating with metal ions

than single molecules; especially when the single molecule must fold or bend to provide the necessary binding sites.

Another therapeutic use for synthetic siderophore-mimetic polymers is as antibiotics or as adjunct therapy. Siderophores and siderophore analogues can act as antibiotic agents through several different mechanisms. A biologically inactive chelator may deprive pathogenic microbes of essential iron. This iron starvation can be achieved through a decrease in local iron concentration through competitive chelation.

Iron-binding polymers may also be explored in the removal of Fe from the lung. Iron can enter the lung by inhalation (i.e. cigarette smoke or metallic dust) or by catabolism of hemoglobin after alveolar hemorrhage. Iron deposition in the lung is associated with tissue injury and fibrosis. The source of the iron that accumulates in the lung after exposure to cigarette smoke has not been identified. The metal could originate from either the cigarette or the host. Tobacco has been reported to contain 150 μg iron/g.¹⁴⁷ Only a small amount of this iron (0.1%) enters mainstream smoke, and this quantity is not considered significant.¹⁴⁸ Alternatively, host sources of iron could be bound by the particulate matter surface after its deposition in the lung. Such complexation of host iron by cigarette smoke particles is likely to alter iron homeostasis, both in the lung and systemically. Treatment with iron chelators prevents lung injury both in animal models and in human disease caused by toxic iron that has entered the lungs via smoke inhalation. Because of the detrimental effects of chelating agents on the vital organs in the human body, it is of great interest to find a new

technology to eliminate the excess iron (or other toxins) without systemic exposure to such treatments. Iron-binding polymers delivered to the lung can be used as an alternative chelator to remove Fe from the lung in smoker patients suffering from iron overload.

Waste water treatment is another significant area of interest in the application of metal-binding polymers. Future work should offer more efficient and selective toxic metal binding by polymers through the modification of functional side groups. Moreover, renewable polymers capable of selectively and effectively binding toxic metals at low concentration may find applications in the water treatment industry. Further studies should address the recycling efficiency of metal-binding polymers.

References

1. Kitagawa, S.; Kitaura, R.; Noro, S., Functional porous coordination polymers. *Angewandte Chemie International Edition* 2004, 43, (18), 2334-2375.
2. Kaliyappan, T.; Kannan, P., Co-ordination polymers. *Progress in Polymer Science* 2000, 25, (3), 343-370.
3. Flora, S.; Mittal, M.; Mehta, A., Heavy metal induced oxidative stress & its possible reversal by chelation therapy. *Indian J Med Res* 2008, 128, (4), 501-523.
4. <http://en.wikipedia.org/wiki/Plastocyanin>.
5. <http://en.wikipedia.org/wiki/Chlorophyll>.
6. <http://en.wikipedia.org/wiki/Hemoglobin>.
7. Shanmuganathan, K.; Capadona, J.; Rowan, S.; Weder, C., Biomimetic mechanically adaptive nanocomposites. *Progress in Polymer Science* 2010, 35, 212-222.
8. Mohan, D.; Pittman, C., Arsenic removal from water/wastewater using adsorbents--A critical review. *Journal of hazardous materials* 2007, 142, (1-2), 1-53.
9. Ulbricht, M., Advanced functional polymer membranes. *Polymer* 2006, 47, (7), 2217-2262.
10. Thanou, M.; Verhoef, J.; Junginger, H., Oral drug absorption enhancement by chitosan and its derivatives. *Advanced drug delivery reviews* 2001, 52, (2), 117-126.
11. Esfand, R.; Tomalia, D., Poly (amidoamine)(PAMAM) dendrimers: from biomimicry to drug delivery and biomedical applications. *Drug Discovery Today* 2001, 6, (8), 427-436.
12. Peppas, N., *Hydrogels in medicine and pharmacy*. 1986, ISBN 084935546X.
13. Jagur-Grodzinski, J., Biomedical application of functional polymers. *Reactive and Functional Polymers* 1999, 39, (2), 99-138.
14. Kestenbaum, B.; Sampson, J.; Rudser, K.; Patterson, D.; Seliger, S.; Young, B.; Sherrard, D.; Andress, D., Serum phosphate levels and mortality risk among people with chronic kidney disease. *Journal of the American Society of Nephrology* 2005, 16, (2), 520.
15. Markowitz, G.; Stokes, M.; Radhakrishnan, J.; D'Agati, V., Acute phosphate nephropathy following oral sodium phosphate bowel purgative: an underrecognized cause of chronic renal failure. *Journal of the American Society of Nephrology* 2005, 16, (11), 3389.
16. BELLASI, A.; KOOIENGA, L.; Geoffrey, A., Phosphate binders: new products and challenges. *Hemodialysis International* 2006, 10, (3), 225-234.
17. Schmidtchen, F., Reflections on the construction of anion receptors:: Is there a sign to resign from design? *Coordination Chemistry Reviews* 2006, 250, (23-24), 2918-2928.

18. Tamaru, S.; Hamachi, I., Recent progress of phosphate derivatives recognition utilizing artificial small molecular receptors in aqueous media. *Recognition of Anions* 2008, 95-125.
19. Dhal, P.; Polomoscank, S.; Avila, L.; Holmes-Farley, S.; Miller, R., Functional polymers as therapeutic agents: Concept to market place. *Advanced drug delivery reviews* 2009, 61, (13), 1121-1130.
20. Amin, N., The impact of improved phosphorus control: use of sevelamer hydrochloride in patients with chronic renal failure. *Nephrology Dialysis Transplantation* 2002, 17, (2), 340.
21. Sempos, C.; Cleeman, J.; Carroll, M.; Johnson, C.; Bachorik, P.; Gordon, D.; Burt, V.; Briefel, R.; Brown, C.; Lippel, K., Prevalence of high blood cholesterol among US adults . *The journal of the american medical association* 1993, 269, 3009-3014.
22. Kushner, J.; Porter, J.; Olivieri, N., Secondary iron overload. *Hematology* 2001, 2001, (1), 47.
23. Olivieri, N.; Brittenham, G., Iron-chelating therapy and the treatment of thalassemia. *Blood* 1997, 89, (3), 739.
24. Neilands, J., Siderophores: structure and function of microbial iron transport compounds. *Journal of Biological Chemistry* 1995, 270, (45), 26723.
25. Boelaert, J.; De Locht, M., Side-effects of desferrioxamine in dialysis patients. *Nephrology Dialysis Transplantation* 1993, 8, (suppl), 43.
27. Piga, A.; Roggero, S.; Salussolia, I.; Massano, D.; Serra, M.; Longo, F., Deferiprone. *Annals of the New York Academy of Sciences* 2010, 1202, (1), 75-78.
27. Taher, A.; Hershko, C.; Cappellini, M., Iron overload in thalassaemia intermedia: reassessment of iron chelation strategies. *British journal of haematology* 2009, 147, (5), 634-640.
28. Polomoscank, S.; Cannon, C.; Neenan, T.; Holmes-Farley, S.; Mandeville, W.; Dhal, P., Hydroxamic acid-containing hydrogels for nonabsorbed iron chelation therapy: Synthesis, characterization, and biological evaluation. *Biomacromolecules* 2005, 6, 2946-2953.
29. Dhal, P.; Holmes-Farley, S.; Huval, C.; Jozefiak, T., Polymers as drugs. *Polymer Therapeutics I* 2006, 192,9-58.
30. Qaiser, S.; Saleemi, A.; Mahmood Ahmad, M., Heavy metal uptake by agro based waste materials. *Electronic Journal of Biotechnology* 2007, 10, 409-416.
31. Demirbas, A., Heavy metal adsorption onto agro-based waste materials: a review. *Journal of hazardous materials* 2008, 157, (2-3), 220-229.
32. Valko, M.; Morris, H.; Cronin, M., Metals, toxicity and oxidative stress. *Current medicinal chemistry* 2005, 12, (10), 1161-1208.
33. Brodtkin, E.; Copes, R.; Mattman, A.; Kennedy, J.; Kling, R.; Yassi, A., Lead and mercury exposures: interpretation and action. *Canadian Medical Association Journal* 2007, 176, (1), 59.
34. Oehme, F., British anti-lewisite (BAL), the classic heavy metal antidote. *Clinical Toxicology* 1972, 5, (2), 215-222.

35. Blanusa, M.; Varnai, V.; Piasek, M.; Kostial, K., Chelators as antidotes of metal toxicity: Therapeutic and experimental aspects. *Current medicinal chemistry* 2005, 12, (23), 2771-2794.
36. Olympio, K.; Gonçalves, C.; Günther, W.; Bechara, E., Neurotoxicity and aggressiveness triggered by low-level lead in children: a review. *Revista Panamericana de Salud Pública* 2009, 26, 266-275.
37. Chisolm, J., BAL, EDTA, DMSA and DMPS in the treatment of lead poisoning in children. *Clinical Toxicology* 1992, 30, (4), 493-504.
38. Kapaj, S.; Peterson, H.; Liber, K.; Bhattacharya, P., Human health effects from chronic arsenic poisoning—a review. *Journal of Environmental Science and Health, Part A* 2006, 41, (10), 2399-2428.
39. Tunbridge, W.; Harsoulis, P.; Goolden, A., Letter: TSH level and thyroid function. *British Medical Journal* 1974, 4, (5938), 226.
40. Thunus, L.; Lejeune, R., Overview of transition metal and lanthanide complexes as diagnostic tools. *Coordination Chemistry Reviews* 1999, 184, (1), 125-155.
41. Sharma, P.; Brown, S.; Walter, G.; Santra, S.; Moudgil, B., Nanoparticles for bioimaging. *Advances in colloid and interface science* 2006, 123, 471-485.
42. Borella, P.; Bargellini, A.; Salvioli, S.; Medici, C.; Cossarizza, A., The use of non-radioactive chromium as an alternative to ⁵¹Cr in NK assay. *Journal of immunological methods* 1995, 186, (1), 101-110.
43. Tofts, P.; Shuter, B.; Pope, J., Ni-DTPA doped agarose gel--A phantom material for Gd-DTPA enhancement measurements. *Magnetic resonance imaging* 1993, 11, (1), 125-133.
44. Baraka, A.; Hall, P. J.; Heslop, M. J., Melamine–formaldehyde–NTA chelating gel resin: synthesis, characterization and application for copper (II) ion removal from synthetic wastewater. *Journal of hazardous materials* 2007, 140, (1-2), 86-94.
45. Kos, B.; Le tan, D., Influence of a biodegradable ([S, S]-EDDS) and nondegradable (EDTA) chelate and hydrogel modified soil water sorption capacity on Pb phytoextraction and leaching. *Plant and Soil* 2003, 253, (2), 403-411.
46. Davidson, M. H.; Dillon, M. A.; Gordon, B.; Jones, P.; Samuels, J.; Weiss, S.; Isaacsohn, J.; Toth, P.; Burke, S. K., Colesevelam hydrochloride (cholestigel): a new, potent bile acid sequestrant associated with a low incidence of gastrointestinal side effects. *Archives of Internal Medicine* 1999, 159, (16), 1893-1900.
47. Hwang, D. C.; Damodaran, S., Chemical modification strategies for synthesis of protein-based hydrogel. *J. Agric. Food Chem* 1996, 44, (3), 751-758.
48. Feng, M.; Van Der Does, L.; Bantjes, A., Iron (III) chelating resins II. 3-Hydroxy-4 (1H)-pyridinones-Sepharose gels. *Journal of Biomaterials Science, Polymer Edition* 1993, 4, (2), 145-154.
49. Feng, M.; Van Der Does, L.; Bantjes, A., Iron (III) chelating resins-I. Preparation and properties of Sepharose-desferrioxamine gels. *Journal of Biomaterials Science, Polymer Edition* 1993, 4, (2), 99-105.

50. Salonen, J. T.; Nyysönen, K.; Korpela, H.; Tuomilehto, J.; Seppänen, R.; Salonen, R., High stored iron levels are associated with excess risk of myocardial infarction in eastern Finnish men. *Circulation* 1992, 86, (3), 803-811.
51. Mahoney Jr, J. R.; Hallaway, P. E.; Hedlund, B. E.; Eaton, J. W., Acute iron poisoning. Rescue with macromolecular chelators. *Journal of Clinical Investigation* 1989, 84, (4), 1362-1366.
52. Ramirez, R. S.; Andrade, J. D., Polymer-Drug Grafts For Iron Chelation. *Journal of Macromolecular Science, Part A* 1976, 10, (1), 309-365.
53. Horowitz, D.; Margel, S.; Shimoni, T., Iron detoxification by haemoperfusion through deferoxamine-conjugated agarose-polyacrolein microsphere beads. *Biomaterials* 1985, 6, (1), 9-12.
54. Winston, A.; Varaprasad, D. V.; Metterville, J. J.; Rosenkrantz, H., Evaluation of polymeric hydroxamic acid iron chelators for treatment of iron overload. *Journal of Pharmacology and Experimental Therapeutics* 1985, 232, (3), 644-649.
55. Martell, A. E.; French, W.; Badman, D. G., Development of iron chelators for clinical use. Elsevier/North Holland New York 1981.
56. Harayama, S.; Sigel, H.; Sigel, A., Metal ions and biological systems. 1992, 239-328.
57. Elhabiri, M.; Carrër, C.; Marmolle, F.; Traboulsi, H., Complexation of iron (III) by catecholate-type polyphenols. *Inorganica Chimica Acta* 2007, 360, (1), 353-359.
58. Farkas, E.; Csóka, H., Solution equilibrium studies on metal complexes of 2, 3-dihydroxy-phenylalanine-hydroxamic acid (Dopaha) and models: catecholate versus hydroxamate coordination in iron (III)-, aluminium (III)-and molybdenum (VI)-Dopaha complexes. *Journal of inorganic biochemistry* 2002, 89, (3-4), 219-226.
59. Dhungana, S.; Heggemann, S.; Heinisch, L.; Mollmann, U.; Boukhalfa, H.; Crumbliss, A. L., Fe (III) Coordination Properties of Two New Saccharide-Based Enterobactin Analogues: Methyl 2, 3, 4-Tris-O-{N-[2, 3-di (hydroxy) benzoyl-glycyl]-aminopropyl}-[alpha]-d-glucopyranoside and Methyl 2, 3, 4-Tris-O-{N-[2, 3-di-(hydroxy)-benzoyl]-aminopropyl}-[alpha]-d-glucopyranoside. *Inorg. Chem* 2001, 40, (27), 7079-7086.
60. Cass, M. E.; Garrett, T. M.; Raymond, K. N., The salicylate mode of bonding in protonated ferric enterobactin analogs. *Journal of the American Chemical Society* 1989, 111, (5), 1677-1682.
61. Sela, M.; Arnon, R.; Jacobson, I., Synthesis of poly-L-lysine and poly-L-lysyl albumin via , N-trifluoroacetyl- , N-carboxy-L-lysine anhydride. *Biopolymers* 1963, 1, (6), 517-525.
62. Elving, P. J.; Markowitz, J. M.; Rosenthal, I., Preparation of buffer systems of constant ionic strength. *Analytical Chemistry* 1956, 28, (7), 1179-1180.
63. Tan, I. A. W.; Ahmad, A. L.; Hameed, B. H., Adsorption of basic dye on high-surface-area activated carbon prepared from coconut husk: Equilibrium, kinetic and thermodynamic studies. *Journal of hazardous materials* 2008, 154, (1-3), 337-346.

64. Ferruti, P.; Ranucci, E., New Functional Polymers for Medical Applications. *Polymer Journal* 1991, 23, (5), 541-550.
65. Rosenbaum, D.; Holmes-Farley, S.; Mandeville, W.; Pitruzzello, M.; Goldberg, D., Effect of RenaGel (R), a non-absorbable, cross-linked, polymeric phosphate binder, on urinary phosphorus excretion in rats. *Nephrology Dialysis Transplantation* 1997, 12, (5), 961-964.
66. Yu, Y.; Wang, F.; Shi, W. Q.; Wang, L. Y.; Wang, W. B.; Shen, J. C., Conformations and adsorption behavior of poly (allylamine hydrochloride) studied by single molecule force spectroscopy. *Chinese Science Bulletin* 2008, 53, (1), 22-26.
67. Tanaka, T., *Gels. Sci. Am.* 1981, 244, (1), 110-123.
68. Feng, M.; Van Der Does, L.; Bantjes, A., iron (III) chelating resins-IV. crosslinked copolymer beads of 1-(*fl*-acrylamidoethyl)-3-hydroxy-2-methyl-4 (1H)-pyridinone (AHMP) with 2-hydroxyethyl methacrylate (HEMA). *European Polymer Journal* 1994, 30, (8), 941-947.
69. Polomoscanik, S. C.; Cannon, C. P.; Neenan, T. X.; Holmes-Farley, S. R.; Mandeville, W. H.; Dhal, P. K., Hydroxamic acid-containing hydrogels for nonabsorbed iron chelation therapy: Synthesis, characterization, and biological evaluation. *Biomacromolecules* 2005, 6, (6), 2946-2953.
70. Dhal, P. K.; Polomoscanik, S. C.; Avila, L. Z.; Holmes-Farley, S. R.; Miller, R. J., Functional polymers as therapeutic agents: Concept to market place. *Advanced Drug Delivery Reviews* 2009, 61, (13), 1121-1130.
71. Olivieri, N. F.; Brittenham, G. M., Iron-chelating therapy and the treatment of thalassemia. *Blood* 1997, 89, (3), 739.
72. Chaston, T. B.; Richardson, D. R., Iron chelators for the treatment of iron overload disease: relationship between structure, redox activity, and toxicity. *American journal of hematology* 2003, 73, (3), 200-210.
73. Kalinowski, D. S.; Richardson, D. R., The evolution of iron chelators for the treatment of iron overload disease and cancer. *Pharmacological reviews* 2005, 57, (4), 547.
74. Crisponi, G.; Remelli, M., Iron chelating agents for the treatment of iron overload. *Coordination Chemistry Reviews* 2008, 252, (10-11), 1225-1240.
75. Boldt, D. H., New perspectives on iron: an introduction. *The American Journal of the Medical Sciences* 1999, 318, (4), 207.
76. Dhal, P. K.; Huval, C. C.; Holmes-Farley, S. R., Biologically active polymeric sequestrants: Design, synthesis, and therapeutic applications. *Pure and Applied Chemistry* 2007, 79, (9), 1521-1530.
77. Jozefiak, T. H., *Polymers as Drugs. Advanced Polymeric Science* 2006, 192, 9-58.
78. Pietrangelo, A., Hereditary hemochromatosis--a new look at an old disease. *The New England journal of medicine* 2004, 350, (23), 2383.
79. Walter, P. B.; Fung, E. B.; Killilea, D. W.; Jiang, Q.; Hudes, M.; Madden, J.; Porter, J.; Evans, P.; Vichinsky, E.; Hartz, P., Oxidative stress and

- inflammation in iron-overloaded patients with α -thalassaemia or sickle cell disease. *British journal of haematology* 2006, 135, (2), 254.
80. De Domenico, I.; Vaughn, M. B.; Li, L.; Bagley, D.; Musci, G.; Ward, D. M.; Kaplan, J., Ferroportin-mediated mobilization of ferritin iron precedes ferritin degradation by the proteasome. *The EMBO Journal* 2006, 25, (22), 5396.
 81. Dhal, P. K.; Huval, C. C.; Holmes-Farley, S. R., Polymeric sequestrants as nonabsorbed human therapeutics. *Drug discovery and development*, 383.
 82. Hadvary, P.; Lengsfeld, H.; Steffen, H., Method of treating high plasma cholesterol levels. 2006, pub. No: US 2006/0189574 A1.
 83. Oliveira, É.; Hirsch, S.; Spontak, R.; Gehrke, S., Influence of polymer conformation on the shear modulus and morphology of polyallylamine and poly (-L-lysine) hydrogels. *Macromolecules* 2003, 36, (16), 6189-6201.
 84. Evans, W. J.; McCourtney, E. J.; Shrager, R. I., Titration studies of phytic acid. *Journal of the American Oil Chemists' Society* 1982, 59, (4), 189-191.
 85. Feng, M.; Does, L. V. D.; Bantjes, A., Iron (III) chelating resins. VI. Stability constants of iron (III)-ligand complexes on insoluble polymeric matrices. *Journal of Applied Polymer Science* 1995, 56, (10), 1231-1237.
 86. Mohammadi, Z., B. C., Siderophore-mimetic Hydrogel for Iron Chelation Therapy. In progress 2010.
 87. Zhou, T.; Kong, X. L.; Liu, Z. D.; Liu, D. Y.; Hider, R. C., Synthesis and Iron (III)-Chelating Properties of Novel 3-Hydroxypyridin-4-one Hexadentate Ligand-Containing Copolymers. *Biomacromolecules* 2008, 9, (5), 1372-1380.
 88. Janus, L.; Morcellet, J.; Delporte, M.; Morcellet, M., Linear and crosslinked copolymers of vinylamine with vinyl pyrrolidone or methyl methacrylate. Chelation of copper. *European polymer journal* 1992, 28, (10), 1185-1189.
 89. Melby, L. R., Polymers for selective chelation of transition metal ions. *Journal of the American Chemical Society* 1975, 97, (14), 4044-4051.
 90. Zhou, T.; Neubert, H.; Liu, D. Y.; Liu, Z. D.; Ma, Y. M.; Kong, X. L.; Luo, W.; Mark, S.; Hider, R. C., Iron binding dendrimers: a novel approach for the treatment of haemochromatosis. *Journal of medicinal chemistry* 2006, 49, (14), 4171.
 91. Andrews, N., Molecular control of iron metabolism. *Best Practice & Research Clinical Haematology* 2005, 18, (2), 159-169.
 92. Hershko, C.; Graham, G.; Bates, G.; Rachmilewitz, E., Non Specific Serum Iron in Thalassaemia: an Abnormal Serum Iron Fraction of Potential Toxicity. *British Journal of Haematology* 1978, 40, (2), 255-263.
 93. Richardson, D., Potential of iron chelators as effective antiproliferative agents. *Canadian journal of physiology and pharmacology* 1997, 75, (10-11), 1164-1180.
 94. Richardson, D., Iron chelators as therapeutic agents for the treatment of cancer. *Critical reviews in oncology/hematology* 2002, 42, (3), 267-281.
 95. Hallaway, P.; Eaton, J.; Panter, S.; Hedlund, B., Modulation of deferoxamine toxicity and clearance by covalent attachment to biocompatible polymers.

- Proceedings of the National Academy of Sciences of the United States of America 1989, 86, (24), 10108.
96. Vana, P.; Quinn, J.; Davis, T.; Barner-Kowollik, C., Recent advances in the kinetics of reversible addition fragmentation chain-transfer polymerization. *Australian Journal of Chemistry* 55, (7), 425-431.
 97. Dart, R., *Medical toxicology*. Lippincott Williams & Wilkins: 2004.
 98. Harris, W., Kinetics of the removal of ferric ion from transferrin by aminoalkylphosphonic acids. *Journal of inorganic biochemistry* 1984, 21, (4), 263-276.
 99. Sigel, H.; Sigel, A., *Nickel and its role in biology*. CRC: 1988.
 100. Gehlbach, P.; Purple, R.; Hallaway, P.; Hedlund, B., Polymer conjugation reduces deferoxamine induced retinopathy in an albino rat model. *Investigative ophthalmology & visual science* 1993, 34, (10), 2871.
 101. Cao, H.; Luan, Z.; Wang, J.; Zhang, X., Potential ecological risk of cadmium, lead and arsenic in agricultural black soil in Jilin Province, China. *Stochastic Environmental Research and Risk Assessment* 2009, 23, (1), 57-64.
 102. Hang, X.; Wang, H.; Zhou, J.; Du, C.; Chen, X., Characteristics and accumulation of heavy metals in sediments originated from an electroplating plant. *Journal of hazardous materials* 2009, 163, (2-3), 922-930.
 103. Wang, J.; Zhang, D.; Lawson, T.; Bartsch, R., Sorption of heavy metal ions by silica gel-immobilized, proton-ionizable calix [4] arenes. *Talanta* 2009, 78, (2), 477-483.
 104. Dobson, R.; Burgess, J., Biological treatment of precious metal refinery wastewater: A review. *Minerals Engineering* 2007, 20, (6), 519-532.
 105. Sgarlata, C.; Arena, G.; Longo, E.; Zhang, D.; Yang, Y.; Bartsch, R., Heavy metal separation with polymer inclusion membranes. *Journal of Membrane Science* 2008, 323, (2), 444-451.
 106. McDonald, C.; Bajwa, R., Removal of Toxic Metal Ions from Metal-Finishing Wastewater by Solvent Extraction. *Separation Science and Technology* 1977, 12, (4), 435-445.
 107. Bartsch, R. A.; Way, J. D. In *Chemical separations with liquid membranes: an overview*, 1996; ACS Publications 1996, 1-10.
 108. Pekel, N.; Güven, O., Separation of heavy metal ions by complexation on poly (N-vinyl imidazole) hydrogels. *Polymer Bulletin* 2004, 51, (4), 307-314.
 109. Morlay, C.; Cromer, M.; Vittori, O., The removal of copper (II) and nickel (II) from dilute aqueous solution by a synthetic flocculant: a polarographic study of the complexation with a high molecular weight poly (acrylic acid) for different pH values. *Water Research* 2000, 34, (2), 455-462.
 110. Mouginot, Y.; Morlay, C.; Cromer, M.; Vittori, O., Potentiometric study of copper (II) and nickel (II) complexation by a cross-linked poly (acrylic acid) gel. *Analytica Chimica Acta* 2000, 407, (1-2), 337-345.
 111. Oliveira, E.; Hirsch, S.; Spontak, R.; Gehrke, S., Influence of Polymer Conformation on the Shear Modulus and Morphology of Polyallylamine and Poly ([alpha]-l-lysine) Hydrogels. *Macromolecules* 2003, 36, (16), 6189-6201.

112. Evans, W.; McCourtney, E.; Shrager, R., Titration studies of phytic acid. *Journal of the American Oil Chemists' Society* 1982, 59, (4), 189-191.
113. Alinnor, I., Adsorption of heavy metal ions from aqueous solution by fly ash. *Fuel* 2007, 86, (5-6), 853-857.
114. Ozay, O.; Ekici, S.; Baran, Y.; Aktas, N.; Sahiner, N., Removal of toxic metal ions with magnetic hydrogels. *Water Research* 2009, 43, (17), 4403-4411.
115. Tofan, L.; Paduraru, C., Sorption studies of Ag I, Cd II and Pb II ions on sulphhydryl hemp fibers. *Croat. Chem. Acta* 2004, 77, (4), 581-586.
116. Bresolin, I.; Souza, M.; Bueno, S., A new process of IgG purification by negative chromatography: adsorption aspects of human serum proteins onto [omega]-amiododecyl-agarose. *Journal of Chromatography B* 2010.
117. García-Zubiri, I.; González-Gaitano, G.; Isasi, J., Sorption models in cyclodextrin polymers: Langmuir, Freundlich, and a dual-mode approach. *Journal of colloid and interface science* 2009, 337, (1), 11-18.
118. Huber, D. L., Synthesis, properties, and applications of iron nanoparticles. *Small* 2005, 1, (5).
119. Torii, Y.; Tsuzuki, A.; Kato, K.; Uwamino, Y.; Choi, B. H.; Lee, M. J., Chemical processing and characterization of spinel-type thermistor powder in the Mn-Ni-Fe oxide system. *Journal of Materials Science* 1996, 31, (10), 2603-2607.
120. Albuquerque, A. S.; Ardisson, J. D.; Macedo, W. A. A.; Alves, M. C. M., Nanosized powders of NiZn ferrite: Synthesis, structure, and magnetism. *Journal of Applied Physics* 2000, 87, 4352.
121. Andreas Jordan, R. S., Peter Wust, Horst Fähling and Roland Felix, Magnetic fluid hyperthermia (MFH): Cancer treatment with AC magnetic field induced excitation of biocompatible superparamagnetic nanoparticles. *Journal of Magnetism and Magnetic Materials* 1999, 201, (1-3), 413-419.
122. Lee, J. H.; Huh, Y. M.; Jun, Y.; Seo, J.; Jang, J.; Song, H. T.; Kim, S.; Cho, E. J.; Yoon, H. G.; Suh, J. S., Artificially engineered magnetic nanoparticles for ultra-sensitive molecular imaging. *Nature medicine* 2006, 13, (1), 95-99.
123. Santra, S.; Tapeç, R.; Theodoropoulou, N.; Dobson, J.; Hebard, A.; Tan, W. H., Synthesis and characterization of silica-coated iron oxide nanoparticles in microemulsion: The effect of nonionic surfactants. *Langmuir* 2001, 17, (10), 2900-2906.
124. Yang, H. H.; Zhang, S. Q.; Chen, X. L.; Zhuang, Z. X.; Xu, J. G.; Wang, X. R., Magnetite-containing spherical silica nanoparticles for biocatalysis and bioseparations. *Anal. Chem* 2004, 76, (5), 1316-1321.
125. Gupta, A. K.; Gupta, M., Synthesis and surface engineering of iron oxide nanoparticles for biomedical applications. *Biomaterials* 2005, 26, (18), 3995-4021.
126. Chen, J. P.; Sorensen, C. M.; Klabunde, K. J.; Hadjipanayis, G. C.; Devlin, E.; Kostikas, A., Size-dependent magnetic properties of MnFe₂O₄ fine particles synthesized by coprecipitation. *Physical review. B, Condensed matter* 1996, 54, (13), 9288-9296.

127. Zhao, X.; Milton Harris, J., Novel degradable poly (ethylene glycol) hydrogels for controlled release of protein. *Journal of Pharmaceutical Sciences* 1998, 87, (11), 1450-1458.
128. Shieh, D. B.; Cheng, F. Y.; Su, C. H.; Yeh, C. S.; Wu, M. T.; Wu, Y. N.; Tsai, C. Y.; Wu, C. L.; Chen, D. H.; Chou, C. H., Aqueous dispersions of magnetite nanoparticles with NH_3^+ surfaces for magnetic manipulations of biomolecules and MRI contrast agents. *Biomaterials* 2005, 26, (34), 7183-7191.
129. Fried, T.; Shemer, G.; Markovich, G., Ordered Two-Dimensional Arrays of Ferrite Nanoparticles*. *Phys. Lett* 1998, 73, 1439.
130. Liu, C.; Zou, B.; Rondinone, A. J.; Zhang, Z. J., Reverse micelle synthesis and characterization of superparamagnetic MnFe_2O_4 spinel ferrite nanocrystallites. *J. Phys. Chem. B* 2000, 104, (6), 1141-1145.
131. Zahra Mohammadi†, A. C. a. C. J. B., In Situ Synthesis of Iron Oxide within Polyvinylamine Nanoparticle Reactors. *J. Phys. Chem. C* 2009.
132. Kang, Y. S.; Risbud, S.; Rabott, J. F., Synthesis and characterization of nanometer-size Fe_3O_4 and Fe_2O_3 particles. *Chem Mater* 1996, 8, 2.
133. Cotton FA, W. G., *Advanced inorganic chemistry*. New York, 1988.
134. Tang, Z. X.; Sorensen, C. M.; Klabunde, K. J.; Hadjipanayis, G. C., Size-dependent Curie temperature in nanoscale MnFe_2O_4 particles. *Phys Rev Lett* 1991, 67, (25), 3602-3605.
135. R. V. Upadhyay, K. J. D., S. Wells, and S. W. Charles,, *J. Magn. Magn. Mater.* 1994, (132), 249.
136. Gu, L.; Zhu, S.; Hrymak, A. N., Acidic and basic hydrolysis of poly (N-vinylformamide). *Journal of Applied Polymer Science* 2002, 86, (13), 3412-3419.
137. Mohammadi, Z.; Cole, A.; Berkland, C. J., In Situ Synthesis of Iron Oxide within Polyvinylamine Nanoparticle Reactors. *The Journal of Physical Chemistry C*, 66.
138. Kang, E.; Park, J.; Hwang, Y.; Kang, M.; Park, J. G.; Hyeon, T., Direct synthesis of highly crystalline and monodisperse manganese ferrite nanocrystals. *Journal of Physical Chemistry B-Condensed Phase* 2004, 108, (37), 13932-13935.
139. Sun, S.; Zeng, H.; Robinson, D. B.; Raoux, S.; Rice, P. M.; Wang, S. X.; Li, G., Monodisperse MFe_2O_4 (M= Fe, Co, Mn) nanoparticles. *J. Am. Chem. Soc* 2004, 126, 273-279.
140. Chen, J. P.; Sorensen, C. M.; Klabunde, K. J.; Hadjipanayis, G. C.; Devlin, E.; Kostikas, A., Size-dependent magnetic properties of MnFe_2O_4 fine particles synthesized by coprecipitation. *Physical review. B, Condensed matter* 1996, 54, (13), 9288.
141. Santra, S.; Tapeç, R.; Theodoropoulou, N.; Dobson, J.; Hebard, A.; Tan, W., Synthesis and Characterization of Silica-Coated Iron Oxide Nanoparticles in Microemulsion: The Effect of Nonionic Surfactants. *Magn. Reson. Med* 1992, 24, 75.

142. Popa, M.; Bruna, P.; Crespo, D.; Calderon Moreno, J. M., Single-Phase MnFe₂O₄ Powders Obtained by the Polymerized Complex Method. *Journal of the American Ceramic Society* 2008, 91, (8), 2488-2494.
143. Chen, J. P.; Sorensen, C. M.; Klabunde, K. J.; Hadjipanayis, G. C., Enhanced magnetization of nanoscale colloidal cobalt particles. *Physical review. B, Condensed matter* 1995, 51, (17), 11527.
144. Kamruzzaman Selim, K. M.; Ha, Y. S.; Kim, S. J.; Chang, Y.; Kim, T. J.; Ho Lee, G.; Kang, I. K., Surface modification of magnetite nanoparticles using lactobionic acid and their interaction with hepatocytes. *Biomaterials* 2007, 28, (4), 710-716.
145. Tromsdorf, U. I.; Bigall, N. C.; Kaul, M. G.; Bruns, O. T.; Nikolic, M. S.; Mollwitz, B.; Sperling, R. A.; Reimer, R.; Hohenberg, H.; Parak, W. J., Size and surface effects on the MRI relaxivity of manganese ferrite nanoparticle contrast agents. *Nano Lett* 2007, 7, (8), 2422-2427.
146. Mussalo-Rauhamaa, H.; Salmela, S. S.; Leppanen, A.; Pyysalo, H., Cigarettes as a source of some trace and heavy metals and pesticides in man. *Archives of environmental health* 1986, 41, (1), 49-55.
147. Breuer, W.; Epsztejn, S.; Cabantchik, Z. I., Iron acquired from transferrin by K562 cells is delivered into a cytoplasmic pool of chelatable iron (II). *Journal of Biological Chemistry* 1995, 270, (41), 24209.